Photocatalytic Treatment of Textile Effluent

Thesis

Submitted for the award of degree

of

Doctor of Philosophy

By

Sandeep Kumar
(Regn. no. 9050153)

Department of Chemical Engineering
Thapar University
(Formerly known as Thapar Institute of Engineering & Technology)
Patiala-147004, Punjab, India. URL: www.thapar.edu

October 2012

CERTIFICATE

This is to certify that the thesis entitled "**Photocatalytic treatment of textile effluent**" being submitted by Mr. Sandeep Kumar to the Department of chemical Engineering, Thapar University, Patiala for the award of degree of **Doctor of Philosophy**, is a record of bonafide research work carried out by him. Mr. Sandeep Kumar has worked under my guidance and supervision and has fulfilled the requirements for the submission of this thesis, which to my knowledge has reached the requisite standard.

The results embodied in the thesis have not been submitted in part or full to any other University or Institute for award of any degree or diploma.

I wish him success for his future endeavors.

1/10/2012

(Haripada Bhunia)
Associate Professor
Department of Chemical Engineering
Thapar University, Patiala

ACKNOWLEDGEMENT

I am highly grateful to the authorities of Thapar University, Patiala for providing this opportunity to carry out the present research work. I got the opportunity to associate myself with Dr. Haripada Bhunia, Associate Professor (Department of Chemical Engineering, Thapar University, Patiala) as my supervisor. As an outstanding scientist, he has given me the benefit of his guidance throughout the course work.

I am also thankful to Dr. Pramod Kumar Bajpai, Distinguished Professor, Department of Chemical Engineering and Dean, Research and Sponsored Projects, Thapar University, Patiala for his valuable comments and suggestions during research work.

I am grateful to both for showing me all the angles of research life. Their deep insight into the problem and ability to provide constructive suggestions have been of immense value in improving the quality of my research work at all stages.

Heartiest thanks to Dr. Abhijit Mukherjee, Director, Thapar University, Patiala, Dr. K. K. Raina, Dy. Director, Thapar University, Patiala, and Dr. Rajeev Mehta, Professor and Head, Department of Chemical Engineering, Thapar University, Patiala, Dr. D. Gangacharyulu for their encouragement and support during this research work. I am also thankful to all the authors whose research work has been referred to by me. I am grateful to Dr. Satnam Singh, Head, School of Chemistry and Biochemistry for providing valuable suggestions during the research work.

I am also thankful to some of the fellow researchers for the valuable support extended during research work. These include Dr. Priyabrata Pal, Dr. Gursewak Singh, Mr. Ranpreet Singh and Mr. Gaurav Madhu.

I express my gratitude to my wife Neeru Sharma, son Daanish, and daughter, Chetna and other family members for their patience, sacrifice, and support throughout the research work. My firm faith in almighty has led me to face all the problems with smile and helped me to cross all the hurdles which came in my way during the journey to success. I would like to thank "The God" for not letting me down during the crisis and showing me the silver lining in the dark clouds.

Last but not the least my parents deserve special thanks for their love affection and blessings showered on me to undertake and successfully complete this research work leading to Ph. D degree.

Date: 1/10/2012

Place: Patiala

(Sandeep Kumar)

ABSTRACT

Textile industry, which meets the demand of ever growing human population, is one of the sources of non-biodegradable toxic effluents. The origin of toxicity in such effluents is mainly from the complex aromatic dye compounds. Various types of dyes have different environmental aspects. Reactive azo dyes are one of the most extensively and commonly used dyes and belong to one of the most polluting dye class. Most of the conventionally used techniques for such waste water have been found to be either ineffective in treatment or merely resulting in transfer of pollutants from one phase to the other. Recently, a great amount of research effort is being made in development and understanding of alternative methods of waste treatment. Advance oxidation processes (AOPs) are being widely studied for this purpose. In this thesis, the degradation and kinetic studies of Reactive Red 120 dye (RR120), Reactive black 5 dye (RB5) and simulated effluent containing dye mixture and salts respectively have been studied.

In case of RB5 dye, RR120 dyes, the degradation characteristics have been investigated in the presence of UV light using Degussa P25 TiO_2. Preliminary investigations were made to determine the effect of hydrolysis, solar photolysis, and UV chamber photolysis on dye decolorization kinetics. The equilibrium adsorption of dye on TiO_2 was studied at various pH values. The effect of various parameters like pH, catalyst load, initial dye concentration, area to volume ratio of the reactor, and dye salts were also studied. The adsorption of dye on the semiconductor showed a strong dependence on the pH and followed a Langmuir adsorption model. Finally, the mineralization characteristics of dye were studied simultaneously with dye decolorization. The degradation studies of simulated textile effluent were made in shallow pond slurry reactor. The equilibrium adsorption studies of two dyes RB5 and RR120 were compared as single dyes with their mixture solution. The degradation characteristics of dyes were also compared with their single dye solutions.

Contents

List of Symbols

Symbol	Description	Units
λ_X	Absorbance at X nanometer wavelength	-
K_c	Adsorption equilibrium constant of dye	L/mg
K_i	Adsorption equilibrium constant of intermediate i	L/mg
q_e	Amount of dye adsorbed per gram of catalyst at equilibrium	mg/g
K_C	Combined adsorption equilibrium constant of dye and intermediates	L/mg
C_i	Concentration of intermediate i	mg/L
C	Dye concentration at instant t	mg/L
C_0	Dye concentration at t = 0	mg/L
e^-	Electron	-
C_e	Equilibrium dye concentration	mg/L
h^+_{vb}	Hole in valance band	-
•OH	Hydroxyl radical	-
b	Langmuir adsorption equilibrium constant	L/mg
q_m	Maximum amount of dye adsorbed per gram of catalyst	mg/g
k_{app}	Pseudo-first-order rate constant	per minute
O_2^{-}•	Superperoxide radical	-
t	Time of reaction	minute

List of Abbreviations

Abbreviation	Description
AOP	Advanced oxidation processes
BET	Branauer-Emmett-Teller
BOD	Biochemical oxygen demand
CB	Conduction band
CCD	Central composite design
CFFP	Cascade falling film photoreactor
COD	Chemical oxygen demand
CPC	Compound parabolic collector
DOE	Design of experiment
IC	Inorganic carbon
NDIR	Non dispersive infrared
pH_{pzc}	Point of zero charge pH
ppm	Parts per million
RB5	Reactive Black 5
RR120	Reactive red 120
RSM	Response surface methodology
TC	Total carbon
TOC	Total organic carbon

List of Figures

List of Tables

CHAPTER – 1

INTRODUCTION

Introduction

It is no accident that Earth is often referred to as ‘the water planet’ or ‘blue planet’. Earth is unique amongst the planets of our solar system largely because of its abundant water - in oceans, in the atmosphere, in glaciers and as fresh water on land. Without water, life as we know, could not exist.

Despite abundant availability of water, the amount of potable fresh water available is a tiny fraction of the total amount of water in the world. Most of the world's water is in the oceans, but because of the salts in ocean water it is largely unsuitable for use. The supply of fresh water is limited, vulnerable to human abuse and not evenly distributed in both time and space. Fresh water resources around the world are overused, polluted, fought over and squandered with little regard for human health and ecological consequences. Industrial development is pervasively connected with the disposal of a large number of various toxic pollutants that are harmful to the environment, hazardous to human health, and difficult to degrade by natural means.

It is difficult to imagine any type of industry in which water is not used. Water is used for cleaning, heating and cooling; for generating steam; for transporting dissolved substances or particulates; as a raw material; as a solvent; and as a constituent part of products (as in the beverage industry). The volume of water used by industry is low, constituting less than 10% of total water withdrawals but industry creates marked pressure on water resources from the impacts of wastewater discharges and their pollution potential than by the quantity used in actual production [1]. At the same time, Industry is an essential engine of economic growth and therefore is key to economic and social progress.

The textile industry has been condemned as being one of the world’s worst offenders in terms of pollution because it requires a great amount of two components namely chemicals and water. The amount and variety of chemicals used in textile industry is quite large. As per international textile auxiliaries buyers guide prepared by Association of producers of textile, paper, leather and fur auxiliaries and colorants, surfactants, complexing agents, antimicrobial agents, polymeric flocculants, cosmetic raw materials, pharmaceutical excipients and allied products, as many as 5,500 different chemicals are available based on 400-600 active compounds used in the textile industry [2, 3].

Water is used at every step of the process both to convey the chemicals used during that step and to wash them out before beginning of the next step. The water becomes full of chemical additives and thus wastewaters from textile units are highly polluted.

1.1 Textile plant effluent characteristics

Effluent streams from textile plants, dyeing units, dye and dye intermediates manufacturing units generate toxic pollutants. Typical values of various parameters for composite textile effluent as reported in literature [4] are shown in Table 1.1.

Table 1.1 Textile industry wastewater characteristics

Sr. No.	Parameter	Value
1	pH	7.0– 9.0
2	Biochemical Oxygen Demand (mg/L)	80 – 6,000
3	Chemical Oxygen Demand (mg/L)	150 – 12,000
4	Total Suspended Solids (mg/L)	15 – 8,000
5	Total Dissolved Solids (mg/L)	2,900 -3,100
6	Chloride (mg/L)	1000 – 1600
7	Total Kjeldahl Nitrogen (mg/L)	70 – 80
8	Color (Pt-Co)	50-2500

Effluent streams from dye house are colored and contribute significantly to the pollution load. Most of the dyes used for dying purpose are stable chemical structures which resist degradation under diverse conditions [5]. Among the dyes, reactive azo dyes are well-known for their toxicity and recalcitrant nature. It is reported that more than 15 % of the dye remains unfixed at the end of the dying process [6]. This results in huge amount of toxic effluents discharge to water bodies. In some countries, there is a ban over the use of this class of dyes but these continue to be used for the required properties; which are best met by this class of dyes. In addition to the pollution load by dyes, various dye bath additives like Glauber's salt ($Na_2SO_4 \cdot 10H_2O$), sodium chloride, etc. also contribute to the pollution. This altogether results in highly recalcitrant mixture, resistant to most of the convention treatment processes. Dye house effluents are found to be strongly colored, and have high COD values, low BOD to COD ratios, high pH values, high temperature, high values of TDS, low values of suspended solids, heavy metal loaded.

Apart from a few exceptions, most of the emissions originating from the dyeing process are emissions to water. Water-polluting substances can originate from the dyes themselves (e.g. aquatic toxicity, metals, color), auxiliaries contained in the dye formulation , basic chemicals and auxiliaries used in dyeing processes (e.g. alkali, salts, reducing and oxidising agents, etc.) and residual contaminants present on the fiber (e.g. residues of pesticides on wool, spin finishes on

synthetic fibers). Consumption and emission levels are strongly related to the type of fiber, the dyeing technique and the machinery employed.

In batch dyeing, the concentration levels vary greatly in the dyeing sequence. Generally, spent dye baths have the highest concentration levels (values of COD well above 5000 mg /L are common). The contribution of dyeing additives to the COD load is quite high.

Rinsing baths show concentrations 10 - 100 times lower than the exhausted dyeing bath and water consumption 2 to 5 times higher than for the dyeing process itself. In continuous and semi-continuous dyeing, the water consumption is lower than in batch dyeing processes, but the discharge of highly concentrated residual dyeing-liquors can result in higher pollution load when short runs of material are processed (COD attributable to the dyestuffs may be in the order of 2 - 200 g/L).

1.2 Type of dyes and envioronmental aspects

The process of dyeing can be defined as imparting color to textile, fiber or leather. Generally, dyes can be classified on the basis of structure, function or both. Dyes are frequently used in textile industries to color cotton, woolen and polyamide fibers. Dyes may be classified in a number of ways like type of chemical structure, use, etc. Few of the most commonly used dyes, their properties, chemical characteristics, environmental aspects are discussed in next sections [3].

1.2.1 Acid dyes

Acid dyes are mainly applied to polyamide (80–85%) and wool (10–15%). These are also used for silk and some modified acrylic fibers. Acid dyes exhibit little affinity for cellulose and polyester fiber.

Properties: Colors are generally bright and fastness to light and washing range from poor to excellent depending on the chemical structure of the dyestuff.

Chemical characteristics and general application conditions: Acid dyes are azo (the largest group), anthraquinone, triphenylmethane chromophoric systems, which are made water-soluble by the introduction in the molecule of up to three sulphonate groups. Their interaction with the fiber is based partly on ionic bonds between sulphonate anions and the ammonium groups of the fiber. Degree of fixation varies from 85-93%.

Parameters of environmental concern: Bio-eliminability, organic halogens, eco-toxicity, heavy metals, aromatic amines, unfixed dye, dye bath additives.

1.2.2 Basic dyes

Applicability

Basic dyes were initially used to dye silk and wool (using a mordant), but they exhibited poor fastness properties. Nowadays these dyestuffs are almost exclusively used on polyacrylic fibers.

Properties

On polyacrylonitrile fibers fastness performances are excellent. In addition, they have unlimited color range.

Chemical characteristics and general application conditions

Cationic dyes contain a quaternary amino group which can be an integral part (more common) or not of the conjugated system. Sometimes a positively-charged atom of oxygen or sulphur can be found instead of nitrogen. Ionic bonds are formed between the cation in the dye and the anionic site on the fiber.

Environmental issues

Many basic dyes exhibit high aquatic toxicity but, when applied properly, they show fixation degrees close to 100 %. Problems are more often attributable to improper handling procedures, spill clean-up and other upsets.

1.2.3 Direct (substantive) dyes

Applicability

Direct dyes are used for dyeing cotton, rayon, linen, jute, silk and polyamide fibers.

Properties

Colors are bright and deep, but light-fastness can vary greatly depending on the dyestuff. Wash-fastness properties are also limited unless the textile is after-treated. Only occasionally are direct dyes used in direct printing processes.

Chemical characteristics and general application conditions

Direct dyes (also called substantive dyes) can be azo compounds, stilbenes, oxazines, phtalocyanines. They always contain solubilising groups (mainly sulphonic acid groups, but carboxylic and hydroxyl groups can also be found) that ionise in aqueous solution. Direct dyes are characterised by long planar molecular structures that allow these molecules to align with the flat cellulose macromolecules, the dye molecules being held in place mainly through Van der Waals forces and hydrogen bonds.

Environmental issues

The ecological properties of direct dyes are assessed under the various parameters. Parameters of environment concern mentioned below do not consider the environmental issues related to chemicals and auxiliaries employed in the dyeing process.

Parameters of environmental concern

Bio-eliminability, organic halogens, eco-toxicity, heavy metals, aromatic amines, unfixed dye, dye bath additives.

Degree of fixation in batch dying process varies from 70 to 96% as per Environmental Protection Agency (USA). Benzidine component of certain dyes is specifically carcinogenic.

1.2.4 Naphtol dyes

Applicability

Azoic dyes, also known as naphtol dyes, are used for cellulosic fibers (particularly cotton), but may also be applied to rayon, cellulose acetate, linen and sometimes polyester. These are developed on the fiber.

Properties

Azoic dyes have excellent wet fastness properties. Also good is light, chlorine and alkali fastness, while rubbing fastness is poor.

Chemical characteristics and general application conditions

From a chemical point of view naphtol dyes are very similar to azo dyes, the main difference being the absence of sulphonic solubilising groups. They are made up of two chemically reactive compounds that are applied to the fabric in a two stage process. The insoluble dye is synthetised directly in the fiber as the result of the coupling reaction between a diazotized base (developing agent) and a coupling component. The coupling components are usually derivatives of the anilides of the 2-hydroxy-3-naphtoic acid (also called naphtol AS). These naphtols are available in powder form or in liquid form (in this case the solution also contains caustic soda, the naphtol concentration ranges between 30 % and 60 %).

Parameters of environmental concern

Bio-eliminability, organic halogens, eco-toxicity, heavy metals, aromatic amines, unfixed dye, dye bath additives.

1.2.5 Reactive dyes

Applicability

Reactive dyes are mainly used for dyeing cellulose fibers such as cotton and rayon, but are also sometimes used for wool, silk and polyamide.

Properties

They provide high wet fastness (better than the less expensive direct dyes). Chlorine fastness is slightly poorer than that of vat dyes, as is light fastness under severe conditions. The range of available reactive dyes is wide and enables a large number of dyeing techniques to be used.

Chemical characteristics

Reactive dyes are unique in that they contain specific chemical groups capable of forming covalent links with the textile substrate. The energy required to break this bond is similar to that required to degrade the substrate itself, thus accounting for the high wet fastness of these dyes. Chemical structure of reactive dyes can be schematically represented by the following formula:

Col-B-R

where Col is the chromophore that is in general constituted by monoazoic, anthraquinone, phtalocianine and metal-complex compounds.

B is the linking group between the chromophore and the reactive group (-NH- group is the most common)

R represents the reactive group.

The reactive groups of the colorant react with the amino groups of the fiber in the case of protein and polyamide fibers, and with the hydroxyl groups in the case of cellulose. In both cases, depending on the anchor system, two reaction mechanisms are possible: a nucleophilic substitution mechanism or a nucleophilic addition mechanism. Furthermore, anchor systems are characterized by their reactivity. Based on this, they are classified as hot, warm and cold dyers.

An important issue to consider when dealing with reactive dyes is the fact that two competing reactions are always involved in the coloring process:

1. Hydrolysis: Dye + water ⟶ hydrolysed dye washed away after dyeing
2. Alcoholysis: Dye + fiber ⟶ dye fixed on the fiber

This fact has important consequences, especially in the case of cellulose fibers. In fact, the alkaline conditions in which reactive dyes react with cellulose fibers increase the rate of the hydrolysis reaction (undesired reaction). As a result, a certain amount of unfixed hydrolised dye is always present at the end of the process.

Poor dye fixation has been a long-standing problem with reactive dyes in particular in batch dyeing, where a significant amount of salt is normally added to improve dye exhaustion (and therefore also dye fixation).

Dyeing cellulose fibers with reactive dyes may imply the use of the following chemicals and auxiliaries:

- alkali (sodium carbonate, bicarbonate and caustic soda)
- salt (mainly sodium chloride and sulphate)
- urea (usually added to the padding liquor in continuous processes).

Reactive dyes are applied to wool or polyamide fibers under different conditions. In the case of wool and polyamide fibers, reactivity of the amino groups is considerably higher than that of hydroxyl groups in cellulose.

Leveling properties are often achieved with the use of specialty amphoteric leveling agents, which form complexes with the dye at low dye-bath temperatures. These complexes are absorbed onto the fiber surface in a more even manner than that of the dyestuff itself. They then break down as the dyeing temperature increases, allowing the dye to penetrate and react with the substrate.

Reactive dyes are generally applied at pH values of between 5 and 6, depending on depth of shade, in the presence of ammonium sulphate and the specialized levelling agents.

Environmental issues

The ecological properties of reactive dyes are assessed under various parameters. Table 1.2 shows the environmental aspects of reactive dyes.

Table 1.2 The environmental aspects of reactive dyes

Sr. No.	Parameters of concern	Comments
1	Bio-eliminability	Unfixed reactive dye and its hydrolysate are readily soluble so they are difficult to eliminate in biological treatment plants.
2	Organic halogen	Many organic dyes contain organic halogen.
3	Eco-toxicity	Acts as eco-toxin.
4	Heavy metals	Heavy metals may be present as impurities in dyes and heavy metals may also be the integral part of chemical structure of dye.
5	Aromatic amines	Are hazard to health.
6	Unfixed colors	Generally dye exhaustion for reactive dyes is poor. Research efforts are directed to increase the level of fixation. The fixation degree varies from - 50-80% for cotton batch dying - 90- 97% for wool batch dying - 60% in printing (general)

1.2.6 Sulphur dyes

Applicability

Sulphur dyes are mainly used for cotton and rayon substrates. They may also be used for dyeing blends of cellulose and synthetic fibers, including polyamides and polyesters. They are occasionally used for dyeing silk. Apart from black shades, sulphur dyes play almost no part in textile printing.

Properties

Bleach and wash fastness properties are very good, while light fastness varies from moderate to good. Although they encompass a broad shade range, sulphur dyes are mostly used for dark shades because lighter shades have poor resistance to light and laundering. Sulphur dyes tend to be dull compared with other dye classes.

Environmental issues

The ecological properties of sulphur dyes are assessed under the following parameters. Table 1.3 shows the various environmental aspects of sulphur dyes.

Table 1.3 Environmental aspects of sulphur dyes

Sr. No.	Parameters of concern	Comments
1	Bio-eliminability	Resistant to biological degradation.
2	Organic halogen	Possible contaminant from halogen containing oxidizing agent used.
3	Eco-toxicity	Acts as eco-toxin.
4	Heavy metals	Heavy metals may be present as impurities in dyes and heavy metals may also be the integral part of chemical structure of dye.
5	Unfixed colors	Degree of fixation varies from 60-90% in case of dyeing and 65-95% in case of printing.
6	Pollution load of dye bath additives.	Poorly degradable dispersant are used.

1.2.7 Vat dyes

Applicability

Vat dyes are used most often in dyeing and printing of cotton and cellulose fibers. They can also be applied for dyeing polyamide and polyester blends with cellulose fibers.

Properties

Vat dyes have excellent fastness properties when properly selected and are often used for fabrics that will be subjected to severe washing and bleaching conditions (toweling, industrial and military uniforms, etc.). The range of colors is wide, but shades are generally dull.

Chemical characteristics and general application conditions

From a chemical point of view vat dyes can be distinguished into two groups: indigoid vat dyes and anthraquinoid dyes. Indigo dyes are almost exclusively used for dyeing warp yarn in the production of blue denim.

Like sulphur dyes, vat dyes are normally insoluble in water, but they become water-soluble and substantive for the fiber after reduction in alkaline conditions (vatting). They are then converted again to the original insoluble form by oxidation and in this way they remain fixed into the fiber.

1.3 Occupational health problems caused by dyes

There is a risk of exposure to chemicals because dye manufacturing is generally as frequent manual handling is involved. Thus there is an interaction between chemicals and man which leads to occupational health problems.

1.3.1 Irritation, sensitization and pigmentary disorder

These effects are related to skin disorders. These skin disorders are reffered to as “Dermattits”. Dye chemicals generate skin irritations which may prolong and generate secondary problems [7, 8]. These effects are generated due to combination of dye chemical with skin proteins. These conditions also lead persensitivity of skin. Sensitization of skin means that there are no changes at the first contact of the chemical but they occur after 7-10 days on the site of contact or elsewhere. For certain group of chemical the skin pigment is affected thus causing change of skin color. These changes are caused by prolonged skin exposure to the chemical. The adverse effects are worsened by exposure to sunlight.

1.3.2 Effects on blood and hemopoietic system

Dye chemicals and intermediates contain benzene which may produce changes in blood on both short term and long term exposure. The effects observed after prolonged exposure include reduction in number of red blood cells and haemoglobin content of blood, causing anaemia. The toxic effect may cause bone-marrow depression, resulting in the reduction in the number of all types of cells of the blood [9]. This condition is called aplastic anemia. The reduction of platelets will cause hemorrhagic disease of various organs. The prolonged absorption of benzene can produce leukemia in few cases.

1.3.3 Nephrotoxic and hepatotoxic effects

These are serious effects related to dyestuff chemicals. Nephrotoxic refers to the chemical which act as toxins to the kidney. These effects may be temporary or irreversible depending upon the level

of exposure. Irreversible damage may be caused by prolonged exposure while temporary effect may result from acute short time exposure. The toxic effect can be detected by regular urine examination. The urine picture will show the presence of albumin, RBC and WBC. The injury to liver cells occurs following the absorption of certain chemicals [9]. The offending chemical causes the disturbance of the liver function. The symptoms may be mild loss of appetite to severe jaundice.

1.3.4 Cyanosis

Cynosis is the deprivation of oxygen availability to tissues. This effect results in peculiar blue discoloration of skin and mucous membrane [9]. Dyestuff chemicals cause "methaemoglobinaemia" by conversion of hemoglobin to methaemoglobin. The condition is also called anilism. This name itself is derived from aniline, which is a well-known cyanosing agent. The affected person feels weakness, headache and giddiness after a mild exposure. Serious poisoning may lead to collapse, loss of consciousness and even death. The cyanosing compounds mainly enter the body through the skin.

1.3.5 Pulmonary effect

Pulmonary effects are commonly seen in the dyestuff industry following exposure to the noxious gases. Chemical fumes may result in direct irritant effect on the lungs or systematic toxic effect after their absorption in the lungs [10]. HCN and H_2S have systemic effects, which may cause fatality if not treated in time. The dust like nature of dye may cause asthma like condition arising due to its exposure.

1.3.6 Carcinogenicity

The greatest hazard of dyestuff industry has been the occurrence of occupation tumors of urinary bladder (papilloma) [7, 11]. They are usually malignant. There is a long dormant period (20 to 25 years) between the first exposure and ultimate development of tumor.

1.4 Methods for removal of dyes and other organic compounds from wastewater

The most common treatment method for any industrial effluent is use of aerobic degradation process at secondary stage of effluent treatment. However, this process mostly remains a failure as far as degradation of toxic dyes is concerned. The sludge generated in this process contains untreated toxic dyes and treatment efficiency is also reduced. Another possibility is the use of anaerobic treatment methods which again result in generation of decolorized toxic end products and has been also found to be not quite effective [12].

To counter these drawbacks various physical, chemical, and combination of these techniques have been developed over the last three decades. Sorption of dye as pretreatment step over some medium like activated carbon, peat, silica gel etc has been tried. These methods simply transfer the pollutants from one medium to another. Membrane filtration has been tried but fails to meet practical issues of large scale industrial application and too results in toxic sludge. Electro-coagulation results in removal of dye but again generates high amount of sludge. Table 1.4 shows the benefits and limitations of various dye removal techniques [12].

Most of the processes, discussed so far, are either ineffective in treating these toxic effluents and/or are merely resulting in transfer of toxicity from effluent to huge amount of solid waste. On the other hand, various AOPs offer the possibility of complete destruction of these toxic compounds without generating solid waste. These methods rely on the formation of highly reactive chemical species that degrade more number of recalcitrant molecules into biodegradable compounds and are called advanced oxidation processes (AOPs).

Advanced oxidation processes (AOPs) such as fenton and photo-fenton catalytic reactions [13, 14], H_2O_2/UV processes, and TiO_2 photocatalysis [15-19] have been found to be useful.

However all AOP methods are not fully environment friendly as they use material and energy resources. The best possible configuration in this context may result from the method which may use renewable source of energy and no chemical should be consumed in the process. TiO_2 based photocatalysis in presence of solar radiation provides such configuration. The various advantages and limitations of its use are discussed in next chapter.

Table 1.4 Advantages and disadvantages of the current methods of dye removal from industrial effluents

Sr. No.	Physical/chemical methods	Advantages	Disadvantages
1	Activated carbon	Good removal of wide variety of dyes	Very expensive
2	Peat	Good adsorbent due to cellular structure	Specific surface areas for adsorption are lower than activated carbon
3	Wood chips	Good sorption capacity for acid dyes	Requires long retention times
4	Silica gel	Effective for basic dye removal	Side reactions prevent commercial application
5	Membrane filtration	Removes all dye types	Concentrated sludge production

6	Electrokinetic coagulation	Economically feasible	High sludge production
7	Electrochemical destruction	Breakdown compounds are non-hazardous	High cost of electricity
8	Fentons reagent	Effective decolorization of both soluble and insoluble dyes	Sludge generation
9	Ion exchange	Regeneration: no adsorbent loss	Not effective for all dyes
10	Ozonation	Applied in gaseous state no alteration of volume	Short half-life time of reactive species.

CHAPTER – 2

LITERATURE REVIEW

Literature Review

2.1 Advance oxidation processes

Advanced oxidation processes (AOPs) are an attractive alternative for the treatment of toxic and recalcitrant laden waste waters as well as for the purification and disinfection of drinking water. Although various AOPs use different reacting systems, all are characterized by the same chemical feature: production of hydroxyl radicals. This radicals is extraordinary reactive species Hydroxyl radicals are also characterized by a low selectivity of attack which is a useful attribute for an oxidant used in wastewater treatment and to solve pollution problems [20]. Advanced oxidation processes involve the generation of hydroxyl ($^{\bullet}OH$) radicals which oxidize the pollutants. After fluorine, the hydroxyl radical is the second strongest known oxidant having an oxidation potential of 2.8 eV. It is able to oxidize and mineralize almost every organic molecule, yielding CO_2 and inorganic ions.

The versatility of AOPs is also enhanced by the fact that they offer different possible ways for OH radical's production thus allowing a better compliance with the specific treatment requirements. Various combinations of AOPs are used in waste water treatment as shown in Figure 2.1.

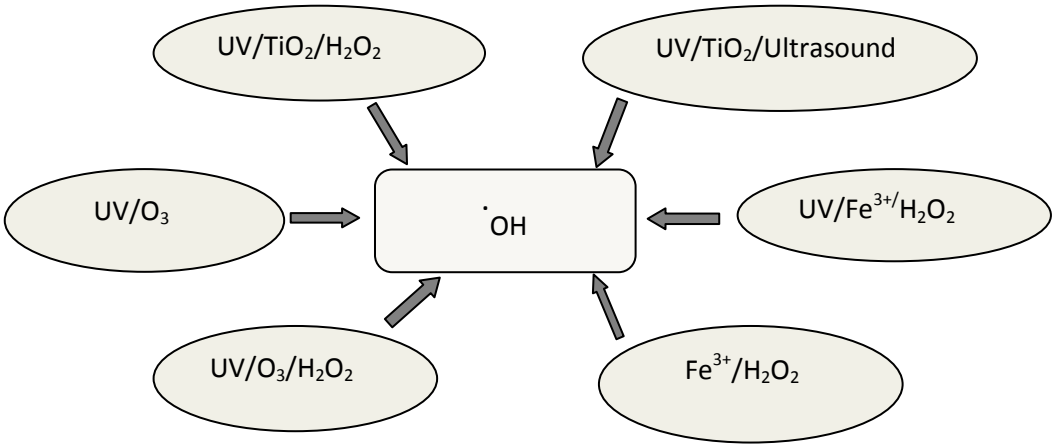

Figure 2.1 Various combined advanced oxidation processes

Ozone gas plays an important role in number of AOPs. Ozone is a powerful oxidizing agent for water and wastewater. Photolysis effect by UV radiations provides synergistic effect to the action of ozone. Once dissolved in water, ozone reacts with a great number of organic compounds in two different ways: by direct oxidation as molecular ozone or by indirect reaction through formation of secondary oxidants like hydroxyl radical [21]. The conventional fine bubble contactor is the most widely ozone generator used because of the high ozone transfer efficiency (90%) and high performance [22].

Photocatalysis based AOPs mostly use titanium dioxide as photocatalyst. UV-radiations are required for photocatalytic action. Sonolysis refers to the use of ultrasound radiation for degrading pollutants. Sonolysis on combination with photocatalytic processes creates synergistic effect [23]. This process is usually referred to as sonophotocatalysis.

All these processes have been successfully used to decompose many toxic and bio-resistant organic pollutants in aqueous solution to acceptable levels, without producing additional hazardous by-products or sludge which requires further handling [24-32].

Advanced oxidation processes based upon photocatalysis can be broadly classified into the two groups based upon existing phases, i.e. homogenous photocatalysis and heterogeneous photocatalysis.

2.2 Homogeneous photocatalysis

The applications of homogeneous photodegradation (single-phase system) to treat contaminated water, involves the use of an oxidant to generate radicals, which attack the organic pollutants to initiate oxidation. The major oxidants used are:

- Hydrogen peroxide (UV /H_2O_2)
- Photo-Fenton reagent (UV/H_2O_2/Fe)

Table 2.1 summarizes the features of various homogeneous AOPs.

Table 2.1 Hydroxyl radical generation in different AOPs (homogeneous)

Type	Major reaction	Drawbacks
UV/H_2O_2	$H_2O_2 + h\nu \rightarrow 2HO^{\cdot}$	- Low molar extinction co-efficient. - Absorbs $\lambda < 300$nm, a lesser component in solar radiation.
UV/H_2O_2/Fe (Photo-Fenton)	$H_2O_2 + Fe^{3+} \rightarrow Fe^{2+} + {\cdot}OH + OH^-$ $Fe^{2+} + H_2O + h\nu \rightarrow Fe^{3+} + {\cdot}OH + H^+$	- Process is expensive. - Sludge disposal problem - Continuous supply of feed chemicals is required.

AOPs listed in Table 2.1 utilize the chemical, hydrogen peroxide. The oxidising strength of hydrogen peroxide alone is relatively weak, but the addition of UV light enhances the rate and strength of oxidation through production of increased amounts of hydroxyl radicals. Hydrogen peroxide may also be used to enhance other AOPs if added in low concentrations, as the molecule easily splits into two hydroxyl radicals.

2.3 Heterogeneous photocatalysis

Heterogeneous photocatalysis refers to the photocatalytic process when the catalyst form is different in phase than the medium in which it is placed to act as photocatalyst. Heterogeneous photocatalysis, is a discipline that include a large variety of reactions like mild or total oxidation, dehydrogenation, hydrogen transfer, metal deposition, gaseous pollutant removal, bactericidal action, and water detoxification etc [33] .

Heterogeneously dispersed semiconductor surface provides both a fixed environment to influence the chemical reactivity of a large range of adsorbates and a means to initiate light induced redox reactivity in these weakly associated molecoules. The photoexitation process results in simultaneous oxidation and reduction reactions. Figure 2.2 shows various reaction occurring over the titanium dioxide [33].

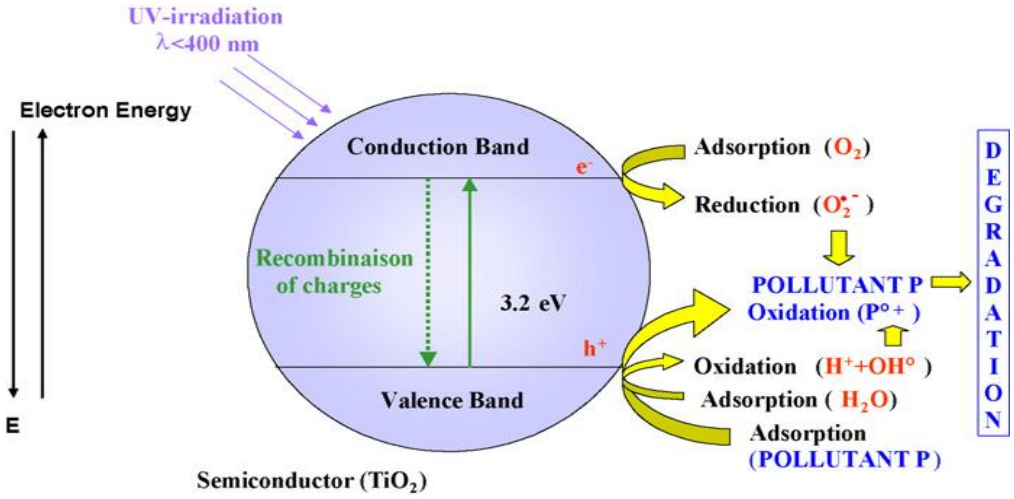

Figure 2.2 Photocatalysis process on TiO_2 surface [33]

A number of excellent reviews are available in literature regarding heterogeneous photocatalysis with comprehensive discussions on all relevant aspects [34-39].

A review by Herrmann suggests that the photocatalytic process can be decomposed to five independent steps [33].

1. Transfer of reactant in fluid phase to the surface
2. Adsorption of at least one of the reactant
3. Reaction in the adsorbed phase
4. Desorption of products
5. Removal of product from interface region

Steps 1, 2, 4 and 5 of photocatalysis are common to conventional catalysis reactions. However, the step 3 contains all the photo-electronic processes and can be subdivided in to following steps.

3.1 Absorption of a photon by solid and not by reactant. There is no photochemistry in adsorbed phase.

3.2 Creation of electron hole pairs which dissociate in to photoelectron and positive holes.

3.3 Electron transfer reactions such as ionosorption, charge neutralization, surface reactions, etc.

When TiO_2 surface is irradiated with UV radiation, the valance band electrons of TiO_2 are excited and jump to conduction band. This results in generation of an electron-hole pair. Minimum energy required for generation of an electron–hole pair is 3.2eV. This electron-hole pair results in different oxidation and reduction reactions unless recombination of electron-hole pair occurs. Major reaction during photocatalytic degradation of dyes can be expressed as follows [40].

$$TiO_2 + h\nu(UV) \leftrightarrow TiO_2(e^-_{CB} + h^+_{VB}) \quad (1)$$

$$TiO_2(h^+_{VB}) + H_2O \rightarrow TiO_2 + H^+ + {}^\bullet OH \quad (2)$$

$$TiO_2(h^+_{VB}) + OH^- \rightarrow TiO_2 + {}^\bullet OH \quad (3)$$

$$TiO_2(e^-_{CB}) + O_2 \rightarrow TiO_2 + O_2^{\bullet -} \quad (4)$$

$$O_2^{\bullet -} + H^+ \rightarrow HO_2^\bullet \quad (5)$$

$$Dye + {}^\bullet OH \rightarrow \textit{degradation products} \quad (6)$$

$$Dye + h^+_{VB} \rightarrow \textit{oxidation products} \quad (7)$$

$$Dye + e^-_{CB} \rightarrow \textit{reduction products} \quad (8)$$

In the above equations OH^-, ${}^\bullet OH$ and $O_2^{\bullet -}$ represent hydroxyl ion, hydroxyl radical and superoxide anion respectively. Various AOPs depend upon application of hydroxyl radical for oxidizing the pollutant. In case of TiO_2 based photocatalytic degradation, oxidation and reduction reactions based upon equations (7) and (8) are important since cationic dyes get adsorbed over catalyst surface in acidic pH conditions.

There are certain reactions in which adsorbed phase plays a role by taking part in photoelectronic processes during photocatalysis. The adsorbed phase in certain cases of dyes receives energy from photon in visible range of wavelength. Excitation of an electron in the dye molecule occurs to either the singlet or triplet excited state of the molecule (Eq. (9)). If the oxidative energy level of the excited state of the dye molecule with respect to the conduction band energy level of the semiconductor is favorable (i.e. more negative), the dye molecule can transfer the electron to the

conduction band of the semiconductor (Eq. (10)). The surface acts as a quencher accepting an electron from the excited dye molecule. The electron in turn can be transferred to reduce an adsorbed organic acceptor molecule or adsorbed oxygen on the surface (Eq. (11)) whereas the dye is converted to the cationic dye radicals (Dye•+) that undergoes degradation (Eq. (12)). This is called surface sensitization. Surface sensitization of a wide bandgap semiconductor photocatalyst (TiO_2) via chemisorbed or physisorbed dyes can increase the efficiency of the excitation process. Thus photosensitization process can also expand the wavelength range of excitation for the photocatalyst through excitation of the sensitizer followed by charge transfer to the semiconductor [41].

$$Dye + h\nu\,(Vis) \rightarrow {}^{1}Dye^{*} \text{ or } {}^{3}Dye^{*} \quad (9)$$

$${}^{1}Dye^{*} \text{ or } {}^{3}Dye^{*} + TiO_2 \rightarrow Dye + TiO_2\,(e^{*}_{CB}) \quad (10)$$

$$TiO_2\,(e^{*}_{CB}) + O_2 \rightarrow O_2^{\cdot -} + TiO_2 \quad (11)$$

$$Dye^{\cdot +} \rightarrow degradation\ products \quad (12)$$

Some common dyes which are used as sensitizers include erythrosin B [42], thionine [43]. Advanced oxidation processes like photochemical processes, Fenton, Photo–Fenton, ozonation, and heterogeneous photocalysis are being applied with better results [24-32]. Heterogeneous photocatalysis is wiser option among these because it results in least secondary pollution both onsite and offsite. Only required chemical is catalyst, which can be recovered. Solar radiation can be utilized as source of energy. Additionally, this technology is emerging due to lack of limitations in mass transfer, the ability to be carried out at ambient conditions, and its ability to completely mineralize the pollutants [44].

Heterogeneous photocatalytic process consists of utilizing the near UV radiation to photo-excite a semiconductor catalyst in the presence of oxygen. Under these circumstances oxidizing species, either bound hydroxyl radicals or free holes, are generated as shown in Fig. 2.2. Using photocatalysis, organic pollutants can be completely mineralized reacting with the oxidizers to form CO_2, water and dilute concentration of simple mineral acids. The process is heterogeneous because there are two active phases, solid and liquid. Also a number of studies related to photocatalytic degradation air born pollutants have been made successfully [45-48]. This process can also be carried out utilizing the part of solar spectrum (λ < 380nm) what transforms it into a good option to be used [49].

TiO_2/ UV process is known to have many advantages:

- A large number of organic compounds dissolved or dispersed in water can be completely mineralized.
- The rate of reaction is relatively high if large surface area of the catalyst can be used.
- TiO_2 is available at a relatively modest price and can be recycled on a technical scale.
- UV lamps emitting in the spectral region required to initiate the photocatalytic oxidation are well-known and are produced in various sizes.
- Absorption cross-section of TiO_2 can be improved by its surface modifications, e.g. by transition metal ion doping.

However, the only drawback in this method is that the liquid-solid separation is expensive, due to the formation of milky dispersions after mixing the powder catalyst in water. To solve this separation problem, fixed TiO_2 is prepared by coating a substrate with a TiO_2 solution and in most cases the catalyst shows a higher photocatalytic activity than the TiO_2 in slurry mode. However, in general, the adherence of TiO_2 to support is not by a chemical bond and the heavier catalyst can be worn off easily.

The various combined methods for $^{\bullet}OH$ radical production mentioned above for the decomposition of a wide variety of organic contaminants have been reported by several authors and are of special interest since some of them can also use solar energy. A common problem of all the AOPs is their high cost, mainly due to high demand of electrical energy for ozonizers and/or UV lamps. Application of solar irradiation to the photochemical process reduces cost but it is possible only for catalyzed homogeneous and heterogeneous reactions using iron ions and titanium dioxide respectively.

2.4 Photocatalysts - Recent developments

TiO_2 has many advantages as photocatalyst; some of those are listed below:

- Chemical stability of TiO_2 in aquous medium and in large range of pH (0-14)
- No additives requirement.
- System applicable at low concentration also.
- Absence of inhibtion or low inhibtion by ions generally present in water.
- Total mineralization achievable for organic pollutants.
- Efficient application in case of halogenated compound which are sometimes very toxic to biological water treatment.
- Possible combination with other decontamination methods.

However, to further improve the suitability of TiO_2, it has been modified by different means. Few of the recent such studies are summarized in Table 2.2.

Table 2.2 Various studies based on TiO_2 and modified TiO_2

Sr. No.	About catalyst	Study details	Ref. No.
Studies on pure TiO_2 catalyst			
1	Nano-TiO_2 crystals synthesized by hydrothermal reaction in an ethanol-water mixture	4-7 nm range particles showing visible light driven photocatalysis.	[50]
2	Porous TiO_2 microspheres synthesized by facile hydrothermal method	Enhanced degradation rate of gaseous benzene as compared to Degussa P25 titanium dioxide	[51]
3	Mesoporous TiO_2 microparticles prepared through the micelle hydrothermal method	Enhanced degradation rate of reactive black 5 dye as compared to Degussa P25 titanium dioxide	[52]
4	TiO_2 nanoparticles synthesized by microwave hydrothermal process in the temperature range of 140-180 °C for 1 h	Enhanced degradation rate of methylene blue dye as compared to Degussa P25 titanium dioxide	[53]
Studies on doped catalysts			
5	Nitrogen-doped TiO_2 nanopowders	Enhanced degradation of Rhodamine B due to shift in absorption spectrum of catalyst.	[54]
6	Nitrogen doped TiO_2 particles characterized by TEM, XRD	Enhanced degradation rates of acid orange 7 dye in solar radiations.	[55]
7	Fe-doped TiO_2	More active than P25 TiO_2 under solar light irradiation. Better recoverability due to faster precipitation after treatment.	[56]
Studies on titanium dioxide nanotubes			
8	TiO_2 nanotubes synthesis confirmed by XRD,TEM,ESR	Atrazine is completely degraded in 5 min and the mineralization efficiency is 98.5% using microwave assisted photocatalytic degradation	[57]
9	Au/TiO_2 heterojunction composite nanotube arrays	Enhanced degradation rate of acid orange 7 (AO7) and reduction rate of Cr(VI)	[58]
10	ZnTe modified TiO_2 nanotube (NT) array prepared by pulse potential electrodeposition	Enhanced photocatalytic activity towards 9-AnCOOH under simulated solar light	[59]
11	Ag-doped TiO_2 nanotubes	Enhanced photocatalytic degradation of toluene	[60]
12	Pt/N-codoped TiO_2nanotubes	Enhanced photodegradation of Rhodamine B (RB)	[61]

2.5 Parameters affecting photocatalytic degradation

The various operational parameters have been studied like pH, temperature, effluent concentration, type compounds under degradation, adsorption characteristics of catalyst, amount of catalyst used, type of catalyst used, type of light source used, type of reactor used. Intensive reviews have been also made on research work done in this regard.

2.5.1 Effect of pH

This parameter is one of the most critical parameter in determining the efficiency of photocatalytic degradation. Understanding the effect of pH in determining photocatalytic degradation is very difficult task due to its multiple roles [40]. It is also difficult to generalize in most of the cases.

The most important role is played in many cases by the ionization state of surface according to following reactions [62].

$$TiOH + H^+ \leftrightarrow TiOH_2^+ \qquad (13)$$

$$TiOH + OH^- \leftrightarrow TiO^- + H_2O \qquad (14)$$

The ionization state of reactant dyes, other chemicals and intermediates generated during degradation is also equally important. Adsorption which is an important step in photocatalytic degradation is thus influenced due to surface charge interaction and dye and chemical to be degraded. The effect of acid base properties of metal oxide surfaces on photocatalytic properties has been well reviewed [40, 63]. The point of zero charge pH (pH_{pzc}) for Degussa P25 TiO_2 have been found out to be 6.8 [64]. Thus, TiO_2 surface is positively charged in acidic medium (pH<6.8) and is negatively charged in alkaline conditions (pH>6.8).

It has been reported that degradation rate of azo dyes increases with decrease in pH [65]. At lower values of pH (i.e. $pH<pH_{pzc}$) the negatively charged dye can easily get adsorbed over catalyst surface. However, under alkaline condition similar charges exist over catalyst surface and dye. Thus there is scarcely any adsorption [66, 67].

Another factor is formation of hydroxide ions and hydroxyl radical. Both of these are involved in degradation reactions. Hydroxyl radical can be formed by reaction between hydroxide ion and positive holes. The positive holes are considered as major oxidation species in acidic conditions while hydroxyl radical are considered to be dominant species in case of alkaline or neutral conditions [68]. It has been reported that in alkaline condition the hydroxyl ions can be easily generated as more hydroxide ions are available on TiO_2 surface [69].

Also it has been reported that TiO_2 particles tend to agglomerate under acidic conditions resulting in lower surface adsorption of dye and photon absorption. This results in reduced degradation as pH decreases [70].

2.5.2 Effect of temperature

It has been reported that photocatalytic degradation is not affected much by temperature. This is due to the fact that amount of activation energy (a few kJ/mole) available at room temperature is not sufficient to affect wide band semiconductor like TiO_2. However, this much orders of activation energy is favorable in generation of hydroxyl radical formation. The effect of temperature might influence the rate of interfacial electron transfer to oxygen. Secondly more rapid desorption of dye and intermediates of degradation may occur at higher temperature. At lower temperature desorption may be the rate limiting step. Additionally the initial adsorption of dye may also get affected at higher temperature.

2.5.3 Influence of catalyst load

Catalyst load plays an important role in determining the rate of degradation of various pollutants. A number of studies have been reported in literature [70-76]. It has been reported that with initial increase in catalyst load the degradation rates increase. The reason generally advanced for this is that the increase in the amount of catalyst increases the number of active sites on the photocatalyst surface, which in turn increase the number of oxidizing radicals. This increasing trend continues till an optimum value is reached beyond which the degradation starts reducing [75]. It has been assumed that this decrease in degradation rate is attributable to increased opacity resulting from increased amount of catalyst particles. It has been also reported that optimum value of catalyst load increases with increase in intensity of radiation. This results from ability of high intensity light to remain effective under high opacity conditions also [74]. Furthermore, the increase of catalyst concentration beyond the optimum may result in the agglomeration of catalyst particles [76, 77], hence the part of the catalyst surface becomes unavailable for photon absorption, and degradation rate decreases.

2.5.4 Influence of dye concentration

The concentration dye also plays an active role in the degradation rate by photocatalysis. It is generally noted that the degradation rates increase with increase in dye concentration from very low values. However, the rate of degradation starts decreasing beyond a certain value of dye concentration. The degradation rates are affected by summation of the probability of •OH formation and further the probability of effective reactions resulting from theses radicals on dye and other dye

degradation intermediates. So the degradation rates are the result of series process of •OH formation and its subsequent effective utilization. So the initial trend of increasing rate might be due to enhanced probability of •OH formation as sufficient required adsorption upon catalyst surface is attained with increasing dye concentration. The importance of initial adsorption of dye upon catalyst surface has been confirmed by number of studies. It has been reported that dye degradation follows the Langmuir-Hinshewood (LH) kinetics [78-81] which implies that degradation steps are influenced by adsorbed species on catalyst surface.

At higher concentrations of dyes, the dye screening effect also comes in to play. Dye screening refers to the absorption of UV radiation by dye molecules rather than getting used effectively in generation of electron hole pair [73, 77, 82, 83]. The screening by dye reduces the intensity and shields the catalyst.

2.5.5 Influence of ultraviolet radiations

Review studies made by Ollis et al. [84] reported that at low intensity (0-20 mW/cm^2) the rate of degradation increases linearly with light intensity [70, 77, 85, 86]. At intermediate higher light intensities (approximately 25 mW/cm^2) rate would depend upon square root of light intensity. At still higher light intensities, rate was found to be independent of light intensity. At low intensity range the rate of electron-hole pair generation is expected to be the reason of increasing degradation rate. However, as the light intensity increases to higher ranges the electron-hole pair recombination competes with electron-hole pair generation. This causes lower effect in degradation rate enhancement in higher range of light intensity. However, the reason for rate of degradation being independent from light intensity may be due to saturation factor of number of active sites being excited by radiations.

2.6 Design of experiment (DOE) based study of Parameters affecting photocatalytic degradation

Most of the studies related to photocatalytic degradation characteristics are made by variation of one factor at a time. However, the factors may have interactions among themselves. These interactions sometimes are very high. This may result in wrong conclusion about the optimum conditions.

To explore the interactions and to meet the objective of optimization one needs to vary more than one factor at a time. Some research efforts by different groups have been in this regard also. However the end result is related to optimization conditions which are valid for a particular type of reactor system set up and may not be best condition for scaled up system. At the same time, this

optimization process shows the vital interactions which are also intrinsically valid on all types of reactor systems but may be up to different extent.

By using DOE, one may also optimize more than one response, depending upon the desirability of each response.

Various studies using multiple factors at a time are made based upon design of experiment approach (DOE). DOE approach is also useful in case one wants to find out the variables influencing the response out of a large number of variables. This type of study is called screening study based upon design of experiment (DOE). This method helps by reducing the experimental work to meet the objective of screening. Screening test is most appropriate experimental procedure to discover suitable independent variables and to screen out insignificant variables. The well-known Packet-Burman or full factorial design are usually employed for screening test [87].

The path of steepest assent approach is used when the range of variables to be studied is quite large and there is no idea about how far one is from optimum condition. This involves step by step approach which decides the next set of experimental study. To determine the optimum condition in a narrow range of variable one may use response surface methodology (RSM). RSM approach again uses DOE based methodology. A number of informative article related to RSM have been published [88-95]. Depending upon the design of experiment matrix chosen the RSM studies generate the response surface. The level of precision and prediction possibilities based upon RSM generated model equations depend upon the DOE design matrix chosen. Although there are many options to make RSM study, but a few DOE matrix like full factorial with two level design, central composite design, box-behnken design are commonly used.

Three level full factorial design matrix consists of 3^k number experiment. The k refers to the number of independent variables under study. However, three level factorial design results in large number of experiments, so these are used rarely. On the other hand, design matrix with two levels is used quite often.

Central composite design is another most often used design matrix for RSM. This design consists of cube corner points that come from factorial design, axial points and centre point. Therefore, total number of experiments (N) can be determined by:

$$N = 2^k + 2k + C_0 \qquad (15)$$

where k is the number of variables. Fig. 2.3 shows the central composite design matrix with three variables. C_0 is the number of runs at centre point. Centre point is used to determine experimental error.

Box-behnken design is for three variables. The design matrix consists of relative equally spaced points. The numbers of experiments are given by

$$N = 2k\,(k-1) + C_0 \qquad (16)$$

where k is the number of variables, C_0 is the number of runs at centre point. Ferreira et al. [90] has discussed use of Box-behnken design in detail.

The experimental results based upon various design matrixes are used to generate response surface as well as equation representing that surface. In order to develop a proper response resurface one has to move through a sequence of steps. This sequence of steps based methodology is called sequential mathematical model fitting. Generally one moves from lower order equations to higher order equation while simultaneously exploring the quality of fitting of experimental results. The quality of fitting has to be checked by a number of mathematical tools like normal plots, residual plots, analysis of variance, t-test, F-test, R square value, adjusted R square value and lack of fit etc. Table 2.3 shows the literature available on DOE based optimization in photocatalytic process

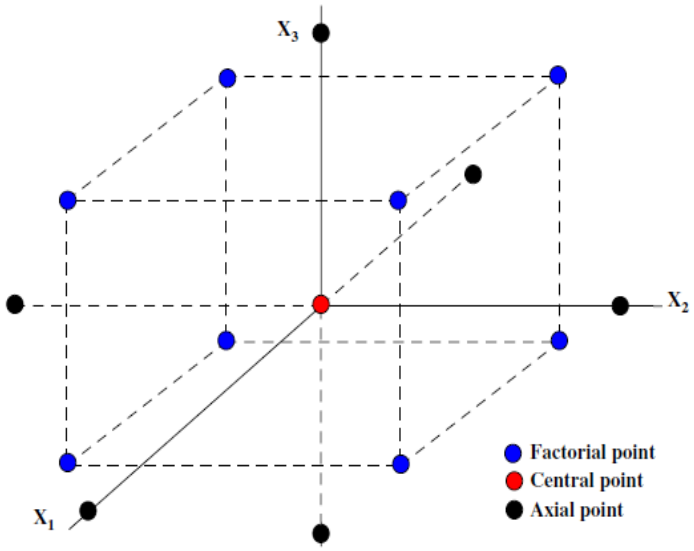

Figure 2.3 A typical schematic diagram of experimental points based upon central composite design (CCD) as a function of X1 (TiO_2 concentration), X2 (dye concentration), and X3 (pH)

Table 2.3: Optimization of conditions for photocatalytic degradation of dyes based upon design of experiment approach

Sr. No.	Compound	Photocatalytic Process	Selected variables	DOE optimization technique	Analytical instrument	Ref. No.
1	Acid blue 7	Nano TiO_2/UV	pH, Light intensity, TiO_2 concentration	Box-benkhen design	UV- visible spectrophotometer	[96]
2	Reactive blue 19	TiO_2/ZnO/UV	pH, TiO_2 concentration, Dye concentration	Factorial design	UV- visible spectrophotometer	[97]
3	Metanil yellow	TiO_2/UV	pH, TiO_2 concentration, Dye concentration, Light intensity	Central composite design with face centres	UV- visible spectrophotometer	[79]
4	Acid red 14	UV/FeZSMS/H_2O_2	pH, TiO_2 concentration, Dye concentration, H_2O_2 concentration	Box benkhen design	TOC and UV- visible spectrophotometer	[98]
5	Basic Red 2 (BR2)	H_2O_2/UV	pH, Dye concentration, H_2O_2 concentration	D-optimal design	UV- visible spectrophotometer	[99]
6	Carmine (C.I. natural red 4)	H_2O_2/UV	pH, H_2O_2 concentration, Dye concentration	D-optimal design	UV- visible spectrophotometer	[100]
7	Dyeing wastewater	TiO_2/ H_2O_2/UV	TiO_2 dosage, H_2O_2 concentration	Central composite design	UV- visible spectrophotometer	[101]
8	Orange II	TiO_2/ H_2O_2/UV	Solution initial pH, Oxidizing agent (H_2O_2), Initial concentration, UV-A irradiation time	Central composite design	UV- visible spectrophotometer	[102]
9	Direct red 28	Fe(II)/H_2O_2/UV	Effects of the dyestuff and the reagent concentration (H_2O_2 and Fe (II)) on oxidation of the azo dye	Box benkhen design	UV- visible spectrophotometer	[103]
10	Reactive red 120	TiO_2/UV	Dye concentration, TiO_2 concentration, UV intensity	Central composite design	TOC and UV- visible spectrophotometer.	[104]

2.7 Studies on photocatalytic degradation of dyes

Research and development work related photocatalystic degradation of many toxic compounds has been under taken by many researchers. A large number of studies are available on the photocatalytic degradation of various dyes. Since the present work is regarding the photocatalytic degradation of reactive red 120 (RR120) and Reactive black 5 (RB5), a detailed discussion on the various studies made so far is discussed.

Poulios et al. studied photocatalytic degaradation of RB 5 under UV black light [64]. The studies showed that optimum pH for photocatalytic degradation was 6. Strong dye adsorption was observed at lower pH values. It was concluded that high adsorption hinders the photocatalytic action. Mineralization studies were made based upon evolution of CO_2 and sulphate.

Tang et al. studied photocatalytic degaradation of RB 5 in an annular photoreactor [105]. Studies showed that pH of effluent have not much effect on degradation. The important parameters identified were catalyst loading, initial dye concentration, dissolved oxygen concentration. The Langmuir Hinsehlwood kinetics applicability was confirmed.

Yu et al. studied the comparative degradation of RB5 by UV/TiO_2, UV/TiO_2/oxidant, UV/oxidant [106]. It was concluded that direct oxidation holes was major factor in UV/TiO_2 based system.

Sahel et al. studied photocatalytic degradation of RB 5 and MX-5B [107]. The TOC studies showed that the percentage of TOC removal at total decoloriozation was lesser for high initial dye concentration. The adsorption characteristics of two dyes were also found to be significantly different.

Studies related to Reactive red 120 dyes degradation has been done by different authors [104, 108, 109]. Cho et al. tried to determine optimum values of pH, catalyst load, dye concentration and UV intensity in circular type phocatalytic reactor system [104]. The optimum value of pH as per their study was 5. They used design of experiment approach. Kusvuran et al. compared several AOPs for degradation of RR120 dye [108]. Park et al. explored the application of solar radiation for RR120 dye degradation [109].

It has been observed, in general, that various photocatalytic studies have been done on different types of photo reactors, with different operating conditions like source of UV, UV intensity, area to volume ratio of reactor, dye purity, etc. However, the parameters under investigations have been invariably adsorption, pH, catalyst loading, dye concentration mainly. Various parameters determining dye degradation have been found to be interdependent. Also, it has been observed that effect of area to volume ratio (A/V) of reactor has not been studied much which is a very important

parameter, in case we want to harvest solar radiations for effluent treatment purposes. Taking into consideration the prevailing facts, further research is required to develop deeper insight.

There are a number of factors which result in variation in conclusion of various studies on same dye. These include type and source of catalyst used, type of reactor used for study, type of light source, reactor volume, purity of dye, etc. Variation in these combinations makes it difficult to generalize the conclusions regarding photocatalytic processes of specific compound. Table 2.4 shows the name of compound studied, type of reactor system and type of light source used in study along with reference to the study.

Table 2.4 List of dye degradation studies with various types of photoreactors and light sources

Sr. No.	Compound under degradation study	Characteristics of photoeactor used	Irradiation source	Ref. No.
1	Reactive orange 4 dye	Reflecting light	Medium pressure mercury vapor lamp 254 nm	[24]
2	Methylene blue, Reactive red 195, Reactive yellow 145	Supported catalyst on stainless steel	Solar light	[110]
3	Reactive yellow 14	Reflecting light, Slurry reactor	Medium pressure mercury vapor lamp	[111]
4	Methyl orange	Non immersed direct light slurry photoreactor	UV lamp 365nm	[112]
5	RR198	Direct lighting non immersed slurry reactor	Medium pressure mercury vapor lamp 254nm	[113]
6	RO16	Immersion type slurry reactor	Low pressure mercury vapor lamp	[114]
7	Basic dyes HF6 and coral pink	Immersion type slurry reactor	UV black tubes 365 nm	[115]
8	Reactive red 239 (RR239)	Direct lighting non immersed slurry reactor	Black light mercury vapor lamp	[116]
9	Metanil yellow	Direct lighting non immersed slurry reactor	UV black tubes 365 nm	[79]
10	Methyl orange II	Solar radiation focused by using Fresnel lens on slurry type reactor	Solar radiations	[117]
11	Reactive yellow 17, Reactive red 239, Reactive black 5	Direct lighting non immersed slurry reactor	Shell removed medium pressure mercury vapor lamp more than 254 nm	[118]
12	Reactive black 5, Procion MX-5B	Immersion type slurry reactor	High pressure mercury vapor lamp	[119]
13	Reactive red 120	Non concentrating recirculation photoreactor	Solar radiations	[104]
14	Direct yellow 12	Direct lighting non immersed slurry reactor	UV black tubes 365 nm	[120]

2.8 Phtocatalytic reactors

The performance of photocatalytic degradation process depends upon a number of factors. The objectives of photocatalytic treatment are:

- Ability to treat the toxic compound in overall environment friendly method.
- Ability to treat at the least cost and effort.

The ability to treat has been testified on large number of compounds but the ability to treat with lower effort and cost remains elusive. To meet the second objective research effort is being made both in term of development of suitable reactor system as well as in developing better understanding to the operating mechanisms under diverse conditions.

The choice of photocatalytic reactor system is one of them. The choice of photocatalytic reactor system depends upon the requirement to be met. There are a number of factors that are to be considered like:

- Volume of effluent to be treated.
- Effluent characteristics.
- Objective of the treatment i.e. whether photocatalytic treatment steps is to be followed by other treatment method or it has to be the last step in treatment.
- Availability of solar radiations.
- Cost of power in case artificial light has to be used.
- Amount of space available.
- Cost of land available for the purpose.
- Cost of photocatalytic reactors.
- Life of photocatalytic reactors.
- Maintenance requirements of photocatalytic reactors.

In fact, the requirements from practical considerations are immense but this technology is immature at this time to meet all these. However, depending upon the availability of resources and the urgency to meet the standards, the photocatalytic reactor developments are taking place all over the world.

Photocatalytic reactors can be broadly classified as of two types depending upon the type of radiation source.

1 Photocatalytic reactor based upon solar radiations.

2 Photocatalytic reactor based upon artificial radiations generated by using power.

The objectives of environmental consideration are best met by use of photocatalytic reactors based upon solar radiations rather than other sources of power. Photocatalytic reactors based upon artificial radiations may result in secondary pollution as the source of power may not be renewable.

Solar radiation based photocatalytic reactors can be further classified in to two types depending upon way the solar radiation is used. The solar radiation may be focused or may be used without any focusing by using either reflected surface or lens.

1. Non concentrating solar radiation photocatalytic reactors.
2. Concentrating photocatalytic reactors.

Artificial light radiation based photocatalytic reactors may have many configurations. Some of the popular configurations in use are described below depending upon the position of irradiation source are:

1. Reactors with immersed light source.
2. Reactors with light source outside the effluent.
3. Reactors with distributed light source.

First two types of reactors are quite common. Reactors with distributed light sources comprise of transfer of radiation through set of reflectors or other methods.

Further, both solar radiation based reactor and artificial light based reactors can be of two types depending upon the state of photocatalyst. These are:

1. Slurry reactors.
2. Photocatalytic reactors with catalyst on some support (immobilized photocatalyst reactors).

Slurry reactors are photocatalytic reactors with catalyst in the form of suspension. However, immobilized photocatalyst reactors comprise of photocatalyst supported on some material like paper, glass, fiber, etc.

Immobilized catalyst photoreactors have advantage of elimination of catalyst recovery effort. However, there are many other points which are to be considered. Table 2.5 shows the relative comparison of two types of reactor systems.

Table 2.5 Comparison of slurry reactors and immobilized catalyst reactor

Slurry reactors	Immobilized catalyst reactors
Advantages - Fairly uniform catalyst distribution. - High catalyst surface are per unit reactor volume. - Well mixed particle suspension. - Lesser limitations of mass transfer, - Low pressure drop.	**Advantages** - Continuous removal possible. - No need of additional catalyst.
Disadvantages - Post treatment removal of catalyst is required. - Light scattering by particles.	**Disadvantages** - Higher pressure drops in case of fixed bed use. - Low efficiency of photon utilization. - Possible catalyst deactivation. - Catalyst wash out**.**

Fig. 2.4 and 2.5 show two schematic digrams of two typical reactor configurations. Fig 2.4 shows a solar radiation based compound parabolic collector (CPC) photoreactor used at Platforma Solar de Almiria in Spain [33]. Although actual reactor configuration appears to be that of plug flow reactor but the recirculation of effluents makes it batch reactor type configuration. Fig 2.5 solar photoreactor with catalyst supported on paper [33]. This reactor system has been named as cascade falling film photoreactor. The catalyst is supported on Ahlstorm special paper. These two reactor systems have shown almost similar performance based upon per unit area and TOC removal of 50 ppm solution containing 4-chlorophenol [33].

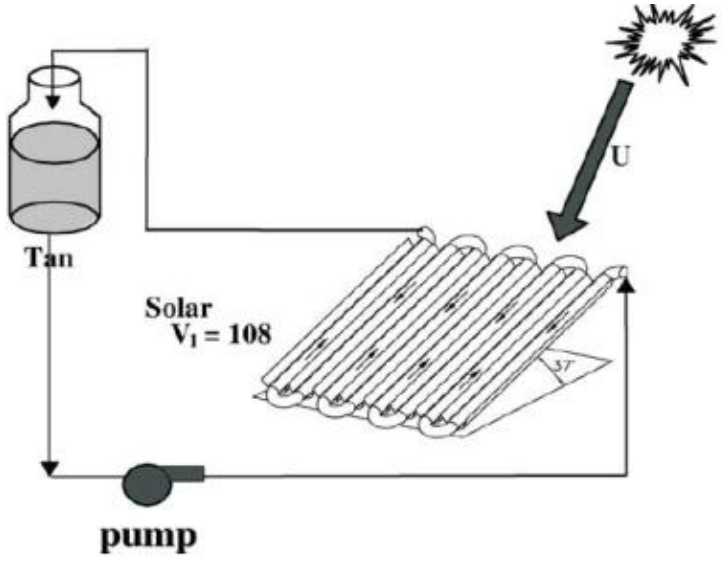

Figure 2.4 Scheme of compound parabolic collector (CPC) photoreactor

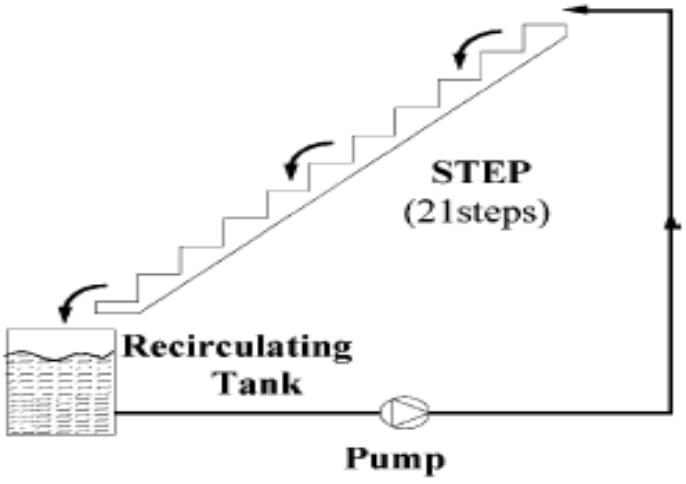

Figure 2.5 Scheme of cascade falling film photoreactor (CFFP)

2.9 Scope and objectives of present work

It has been observed, in general, that various photocatalytic studies have been done on different types of photoreactors, with different operating conditions like source of UV, UV intensity, area to volume ratio of reactor, dye purity, etc. and hence their results cannot be comparable. It has been observed that there is considerable variation in the results reported by different authors for the same dyes. Thus, studies based upon simple reactor configurations and suitable materials are required. Mineralization of dyes has not been investigated extensively as compared to studies based on decolorization. Also, it has been observed that effect of area to volume ratio (A/V) of reactor and UV-intensity have not been studied much which are very important parameters, in case we want to harvest solar radiations for effluent treatment purposes. Taking into consideration the prevailing facts, further research is required to develop deeper insight. Also, it has been observed that photocatalytic degradation of various types of single dyes has been reported largely. However, the literature of photocatlytic degradation of a mixture of dyes is very little. This is relevant because industrial effluents contain a mixture of dyes.

Present work intends to fulfill the above gaps. Studies are based upon the adsorption and subsequent decolorization kinetics of reactive azo dyes; RR120 and RB5 in single dye solution as well as in their mixture. The objective of the study is to compare the adsorption and subsequent photodegradation behavior of the two dyes in their single solution to that of their mixture. These two dyes have been chosen because they have:

- widely varying molecular weight, and
- different number of sulphonate groups.

The studies have been made to fill in the gaps in literature and meeting the set objectives. Following objectives were outlined in the research proposal:

1. To study the kinetics of photocatalytic degradation of simulated effluent containing azo dyes.
2. To study the effect of various parameters affecting performance.
3. To study the catalyst deactivation.

CHAPTER – 3

MATERIALS AND METHODS

Materials and Methods

This chapter describes the materials used and methods adopted for carrying out the experimental work.

3.1 Materials

3.1.1 Dyes

The following dyes were used for preparing synthetic wastewater:

Reactive Red 120 dye (RR 120) and Reactive Black 5 (RB5) were purchased from Sigma Aldrich and was used as such without any purification. The chemical structures of the dyes are shown in Fig 3.1 and 3.2.

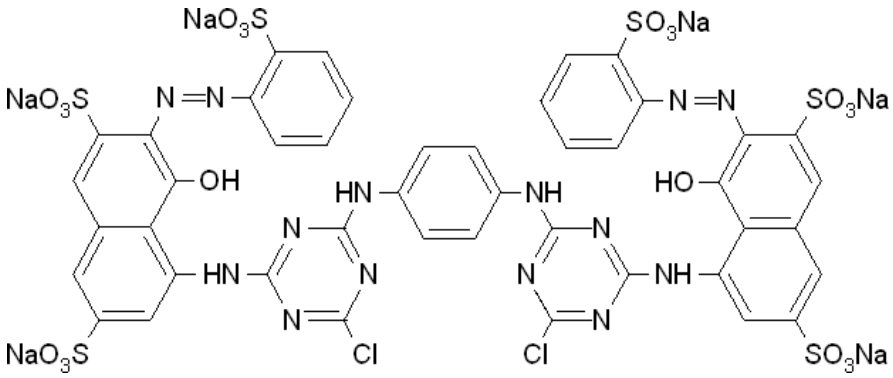

Figure 3.1: Molecular structure of reactive red 120 (RR120).

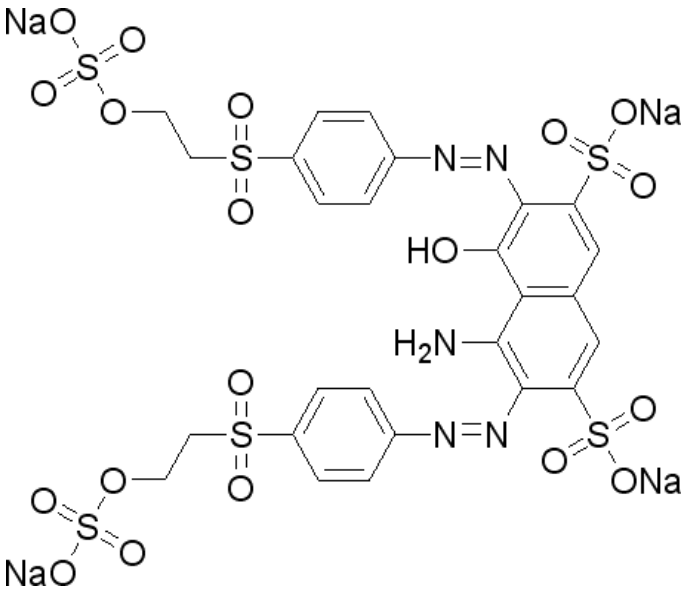

Figure 3.2: Molecular structure of reactive black 5 (RB5).

3.1.2 Catalysts used

Degussa P25 TiO_2 was procured from Evonik Industry AG, Germany. It has a BET surface area of 50 ± 15 m_2/g and is 70% in anatase crystal form with average particle size of 30 nm. Table 3.1 below shows some physicochemical properties of TiO_2.

Table 3.1 Physicochemical properties of Degussa P25 TiO_2. (Source: Evonik Industry AG, Germany)

Property	Unit	Typical Value / Description
Appearance	-	Fluffy White Powder
Specific Surface Area (BET)	m^2/g	50 ± 15
Average Particle size	Nm	30
Behavior towards H_20	-	Hydrophilic
Crystalline polymorphs	-	70% anatase and 30% rutile
Tamped Density	g/L	130
pH in 4% dispersion	-	3.5-4.5
Titanium Dioxide Content	wt%	≥ 99.5
HCl Content	wt%	≤ 0.3
Al_2O_3 Content	wt%	≤ 0.3
Fe_2O_3 Content	wt%	≤ 0.01
SiO_2 Content	wt%	≤ 0.2
Application	-	Photocatalytic reaction, raw material, adsorption and thermal stability

3.1.3 Reagents and chemicals

All chemicals used for analysis were of analytical grade and were obtained from Ranbaxy Laboratories, India. All chemicals were used as received. In all the experiments, double distilled water was used.

3.2 Equipment and instruments

3.2.1 Photoreactor

A batch type bench scale photocatalytic reactor system was fabricated for conducting experiments. The set up consisted of a batch reactor placed on a platform under UV tubes housed in a box. The

tube box (1.219m x 0.762m x 0.762m) used was made up of galvanized aluminum sheet and fitted with 8 UV black tubes of 36 W each, fitted in parallel on the top of the reactor as shown in Fig. 3.3 and 3.4. The UV lamps emit radiation in the range of 300-400 nm, with the peak intensity at 350 nm. An exhaust fan is fitted on the sidewall of the setup to maintain a constant temperature by air circulation**.** Energy distribution in Philips UV black tube spectra is shown in Fig 3.5.

Figure 3.3 Photoreactor with UV lamps and magnetic stirrer

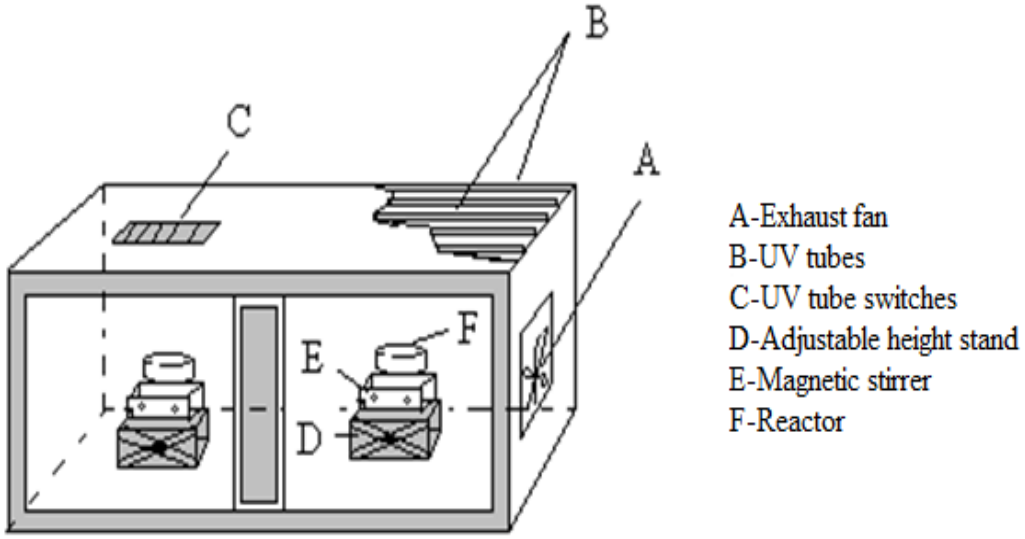

Figure 3.4 Schematic and labeled diagram of photoreactor

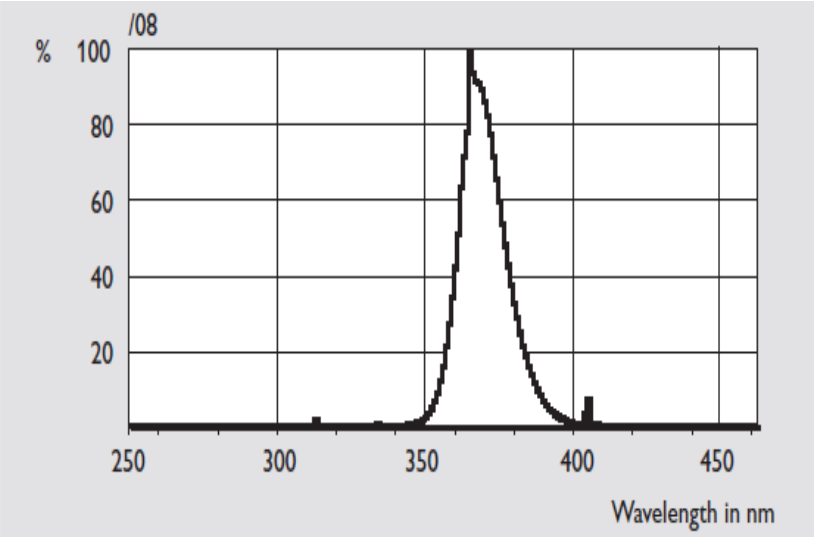

Figure 3.5 Energy distribution in Philips UV black tube spectra.

3.2.2 Radiometer

The UV radiation intensity was measured by using an Eppley Laboratries, USA make Total UV radiometer. The radiometer consists of a UV sensor unit connected to an instantaneous readout. The total UV radiometer is shown in Fig. 3.6

Figure 3.6 Eppley make Total UV radiometer

3.2.3 pH meter

pH value of solution prepared were determined by Orion 5-Star pH/DO/Conductivity Portable Multiparameter. The instrument specifications are as given in Table 3.2.

Table 3.2 Specification and features of Orion 5-star pH meter

Range	-2.000 to +19.999
pH Resolution	0.1/0.01/0.001
pH Relative Accuracy	±0.002
Meter calibration points	Points 1 to 5
Other functions	calibration alarm ,automatic buffer recognition of USA, NIST and DIN buffers

3.2.4 Centrifuge

Catalyst particles were separated from solution by making use of a Hitachi make centrifuge model no. CF15RXII. The instrument is equipped with temperature control arrangement. Other specifications of the instrument used are given in Table 3.3.

Table 3.3 Specification and features of centrifuge used

Type of centrifuge	High speed micro
Maximum speed	15000 rpm
Maximum RCF (Xg)	21900 (using rotor T14A31)
Rotation control range	300- 15000
Timer	5-55 sec/1-99 min., with HOLD function
Temperature setting range	-9°C to +40°C

In addition to this, another centrifuge machine was used to recover the entire amount of catalyst used for reuse purpose. It was Remi make centrifuge (Model: R-8C BL). This machine can accommodate four tubes of 100 ml each.

3.2.5 UV- Visible Spectrophotometer

Absorbance measurements were made by using a double beam UV-Visible spectrophotometer of Perkin Elmer make (Model: Lambda 35). The spectrophotometer was connected to a personal computer. The instrument specifications are given in Table 3.4.

Table 3.4 Specifications and features of UV-Visible spectrophotometer

Range	190 - 1100 nm
Bandwidth	0.5 - 4 nm (variable)
Modes Of Operation	scanning, wavelength program, time-drive, rate, quant, scanning quant

3.2.6 TOC analyzer

Shimadzu make TOC analyzer (Model - TOC-V_{CPH}) was used for measuring total organic carbon (TOC) of samples. TOC was measured as the difference of total carbon (TC) and inorganic carbon (IC) content of the samples.

Two types of carbon are present in water: organic carbon and inorganic carbon. Organic carbon (TOC) bonds with hydrogen or oxygen to form organic compounds. Inorganic carbon (IC or TIC) is the structural basis for inorganic compounds such as gas carbonates and carbonate ions. Collectively the two forms of carbon are referred to as total carbon (TC) and the relationship between them is expressed TOC = TC + IC.

Sample is introduced into the TC combustion tube, which is filled with an oxidation catalyst and heated to 680°C. The sample is burned in the combustion tube and, as a result, the TC components in the sample are converted to carbon dioxide. Carrier gas, which flows at a rate of 150 mL/min to the combustion tube, carries the sample combustion products from the combustion tube to an electronic dehumidifier, where the gas is cooled and dehydrated. The gas then carries the sample combustion products through a halogen scrubber to remove chlorine and other halogens. Finally, the carrier gas delivers the sample combustion products to the cell of a non-dispersive infrared (NDIR) gas analyzer, where the carbon dioxide is detected. The NDIR outputs an analog detection signal that forms a peak; the peak area is measured by the TOC-Control V software.

The peak area is proportional to the TC concentration of the sample. A calibration curve equation that mathematically expresses the relationship between peak area and TC concentration can be generated by analyzing various concentrations of a TC standard solution. The TC concentration in a sample can be determined by analyzing the sample to obtain the peak area and then using the peak area in the calibration curve equation.

Table 3.5 Specifications and features of TOC analyzer

S. No.	Description	Specifications
1.	Analyte	TC, IC, TOC (TC-IC), NPOC
2.	Measurement principle	680°C catalytically-aided combustion oxidation/non-dispersive infrared detection (NDIR)
3.	Carrier gas	High purity air (from cylinder)
4.	Carrier gas flow rate	230mL/min when performing in-syringe sparging
5.	Sample introduction	Auto injection using syringe pump/slider
6.	Repeatability	CV within 1.5%

7.	Measuring range	TC: 0 - 25000mg/L IC: 0 - 30000mg/L
8.	Sample dilution function	Dilution within syringe, dilution factor 2 - 50 times
9.	Pretreatment for IC	Automatic acid addition and sparging
10.	Measurement time TC	Approx. 3min
11.	Measurement time IC	Approx. 3min
12.	Detection limits TC	4µg/L
13.	Detection limits IC	4µg/L
14.	Carrier gas flow rate	150mL/min
15.	Carrier gas pressure	Approx. 300 - 600kPa
16.	Ambient temperature	5 - 35°C
17.	Approximate dimensions	(W) 440 x (D) 560 x (H) 460mm (excluding projections)

3.2 Methods

3.3.1 Preparation of stock solution of single dyes

Stock solution of various dyes under study were made by mixing 100 mg/L of dyes to double distilled water. The dyes were used without further purification. The dyes were mixed by stirring manually. The prepared stock solution was used for further studies. Fresh solutions were made after every five days of storage.

3.3.2 Calibration curve for single dyes

Prepared stock solution was scanned by using UV-visible spectrophotometer between 190-700 nm. Each dye solution exhibits a peak in visible region of wavelength (400-700 nm). This helped us to determine the characteristic wavelength (λ_{max}) of each dye. Further, the concentrations of dye solution were made by serial dilution of prepared stock solution. The absorbance values for dye solution at various concentrations were measured at their corresponding λ_{max} values.

3.3.3 Preparation of stock solution of dyes mixture

Stock solution for dye mixture was prepared by making two single dye solutions of 100 mg/L of each dye as per section 3.3.1. These solutions were mixed in equal ratios to make 100 mg/L total dye concentration. The initial dye concentration of each dye in dye mixture thus becomes 50 mg/L.

3.3.4 Quantification of dyes in dyes mixture

The solutions of dye mixture were made from single dye solutions having concentration as per Table 3.6. The initial dye concentrations of both dyes are also shown in table. Absorbance values

at 524 nm and 597 nm for dye mixture were taken and multiple regression method was employed by using 'Origin pro 8' software to develop equations for measuring concentrations of individual dyes. Statistical analysis of the multiple regression model equation was done by using 'Origin pro 8 software' to validate the calibration.

Table 3.6 Composition of dye mixture taken to develop calibration curves for dye mixture

Sr. No.	Total RR120 and RB5 concentration in dye mixture (mg/L)	RR120 concentration (mg/L)	RB5 concentration (mg/L)
1	100	50	50
2	75	50	25
3	75	25	50
4	50	50	0
5	50	0	50
6	0	0	0

3.3.5 Preliminary experiments

Preliminary experiments were performed to explore the extent of photolysis, adsorption and photocatalysis on decolorization at natural pH of dyes. Decolorization of dye was studied under following conditions:

(i) Hydrolysis
(ii) UV-A photolysis
(iii) Solar photolysis
(iv) Adsorption
(v) Photocatalysis

Hydrolysis of dye at natural pH of dye was determined by stirring the dye solution in dark. The absorbance values at λ_{max} were taken. The change in absorbance if any may be due to hydrolysis.

UV-A photolysis refers to the dye degradation under UV-A radiation in the absence of photocatalyst. This was done by exposing the dye solution to UV-A radiation inside the photoreactor. The absorbance values at λ_{max} were taken at an interval of 10 minutes for 90 minutes. The change in absorbance if any may be due to UV-A photolysis.

Solar photolysis refers to the photolytic degradation under natural solar radiation. The dye solution was exposed to solar radiation. The absorbance values at λ_{max} were taken after 60 minutes. The change in absorbance if any may be due to solar photolysis.

Adsorption study at natural pH of dye was made by exposing 250 ml of 100 mg/L dye solution to known amount of TiO_2. The solution was allowed to equilibrate under constant stirring and dark conditions. Dark condition was kept to avoid any photolytic degradation. The absorbance values at λ_{max} were taken after 60 minutes. The change in absorbance if any may be due to adsorption.

Photocatalytic degradation of dye at natural pH was explored by using dye solution obtained after adsorption. The dye solution was exposed to UV-A radiation in photoreactor. The absorbance values at λ_{max} were taken at an interval of ten minutes up to 60 minutes. The change in absorbance helps to determine photocatalytic degradation.

3.3.6 Adsorption on TiO_2 suspension

The adsorption characteristics of dye solutions on to TiO_2 surface were studied by exposing 100 mg/L of dye solution (250 ml volume) to different amounts of catalyst (0.5-2.0 g/L) in dark to make sure that no photocatalytic reaction takes place. The dye solution was mixed vigorously in a stirrer with catalyst for 30 minutes. Thirty minute of time was found sufficient to attain adsorption-desorption equilibrium. The samples were withdrawn and centrifuged to determine the absorbance at the respective λ_{max} values to determine the dye concentration in the supernatant.

3.3.7 Photocatalytic degradation measurement by TOC

A Borosil glass beaker of 500 mL capacity was used as the photocatalytic reactor. The area to volume ratio (A/V) of the reactor was kept 0.201 cm^2/mL for all experiments or otherwise stated. A magnetic stirrer was used to keep the reactor contents well mixed, so that the TiO_2 stayed suspended. The samples were withdrawn from reactor and centrifuged at 14,500 rpm for 15 minutes to separate suspended catalyst particles. Two milliliter volume was withdrawn from centrifuge tubes by using fixed volume pipette to determine absorbance.

TOC was determined by Shimadzu make TOC analyzer (Model-TOC-V_{CPH}) as the difference of total carbon (TC) and inorganic carbon(IC).

3.3.7.1 Calibration for TC measurement

Sample is introduced into the TC combustion tube, which is filled with an oxidation catalyst and heated to 680°C. The sample is burned in the combustion tube and, as a result, the TC components in the sample are converted to carbon dioxide. Carrier gas, which flows at a rate of 150mL/min to the combustion tube, carries the sample combustion products from the combustion tube to an electronic dehumidifier, where the gas is cooled and dehydrated. The gas then carries the sample combustion products through a halogen scrubber to remove chlorine and other halogens. Finally, the carrier gas delivers the sample combustion products to the cell of a non-dispersive infrared

(NDIR) gas analyzer, where the carbon dioxide is detected. The NDIR outputs an analog detection signal that forms a peak; the peak area is measured by the TOC-Control V software. The peak area is proportional to the TC concentration of the sample. A calibration curve equation that mathematically expresses the relationship between peak area and TC concentration can be generated by analyzing various concentrations of a TC standard solution. The TC concentration in a sample can be determined by analyzing the sample to obtain the peak area and then using the peak area in the calibration curve equation (Fig. 3.7).

TC calibration was done by taking 2.125 g/L of potassium hydrogen phthalate solution. TC content of this solution was taken as 1000 mg/L.

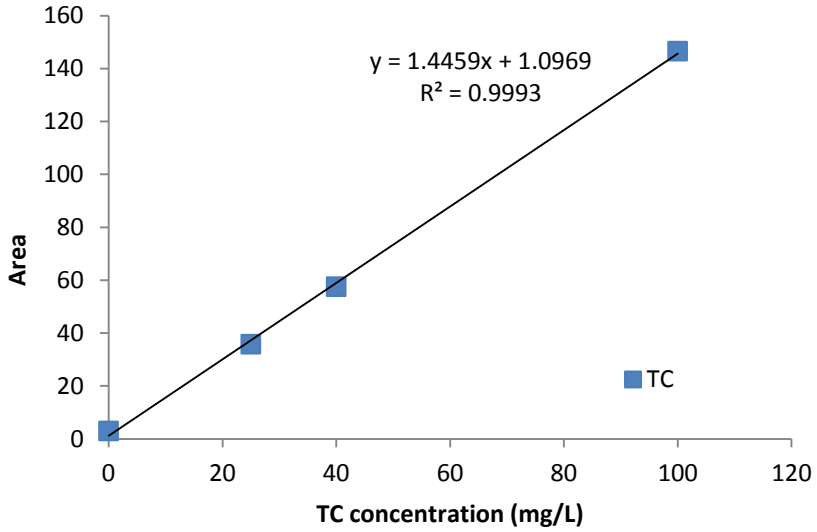

Figure 3.7 Calibration curve for TC measurement by TOC analyzer

3.3.7.2 Calibration for IC measurement

Two methods for measuring IC using the TOC-V are available: analysis within the injection syringe and analysis using the optional IC reactor. In both methods, the measured IC consists of carbon derived from carbonates, hydrogen carbonates and dissolved carbon dioxide.

The IC measured by TOC analysis consists of the carbon contained in carbonates and in carbon dioxide dissolved in water. By acidifying the sample with a small amount of hydrochloric acid to obtain a pH less than 3, all carbonates are converted to carbon dioxide (CO_2) by the following reactions:

$$Me_2CO_3 + 2HCl \longrightarrow CO_2 + 2MeCl + H_2O$$

$$MeHCO_3 + HCl \longrightarrow CO_2 + MeCl + H_2O$$

Me refers to any metallic element. Other symbols have their usual meanings. Carbon dioxide and

dissolved carbon dioxide in the sample are volatilized by bubbling (sparging) air or nitrogen gas that does not contain carbon dioxide through the sample.

The TOC-V IC reactor kit is used to sparge the IC reaction solution (acidified reaction liquid) with carrier gas. Sample is injected into the IC reaction vessel and the IC in the sample is converted to carbon dioxide, which is volatilized by the sparging process and detected by the NDIR

IC calibration was done by using 3.5 g/L of sodium hydrogen carbonate. IC content of this solution was taken as 1000 mg/L (Fig. 3.8).

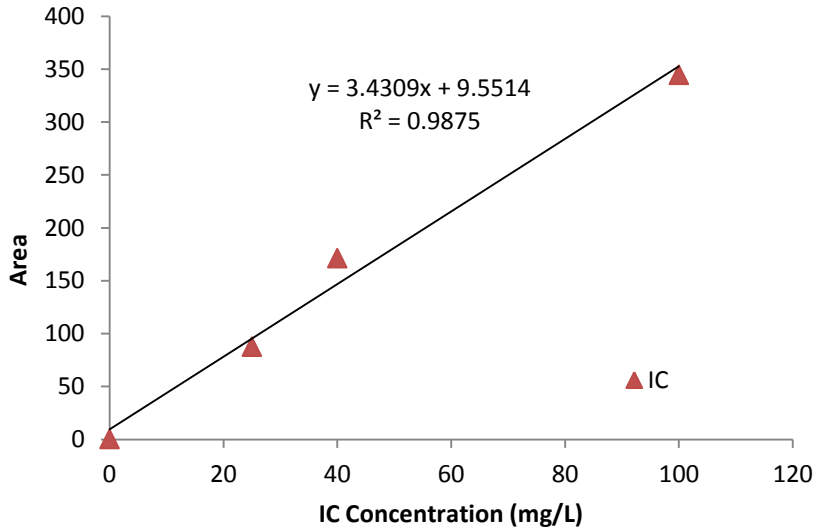

Figure 3.8 Calibration curve for IC measurement by TOC analyzer.

3.3.8 Catalyst recovery for reuse and analysis

The catalyst recovery was done by centrifuging the entire solution using Remi make centrifuge at 6000 rpm for 30 minutes. The catalyst recovered was washed four times with hot distilled water. Each time catalyst was recovered by using centrifuge. The recovered catalyst was kept in an oven for 6 hours at 150 ^{0}C. Finally, the catalyst was pulverized by using pestle mortar (made of Granite stone). Recovered catalyst was analyzed for carbon content by using TOC analyzer.

CHAPTER – 4

PHOTOCATALYTIC DEGRADATION OF REACTIVE BLACK 5 DYE

Photocatalytic Degradation of Reactive Black 5 Dye

4.1 Introduction

Present study is about the photocatalytic degradation of RB5 dye ($C_{26}H_{21}N_5Na_4O_{19}S_6$, Molecular Weight= 991.82) by using TiO_2 as photo-catalyst in a lab scale shallow pond batch reactor. Effect of parameters such as adsorption, initial pH, dye concentration, UV intensity, area to volume ratio of reactor, and catalyst load have been studied. The variation in total organic carbon (TOC) values along with dye decolorization has been also studied in order to study mineralization.

4.2 Calibration curve

RB5 dye solution of 100 mg/L concentration was prepared as per section 3.3.1. The dye solution thus made was scanned in 200-700 nm wavelength for absorbance. The wavelength of maximum absorbance in visible region was found to be 597 nm. Further RB5 calibration curves were made by making solutions of 20, 40, 60, 80 mg/L from 100 mg/L solution by serial dilution. Absorbance values were measured at λ_{max} (597 nm) wavelength. The calibration curve thus obtained is shown in Figure 4.1.

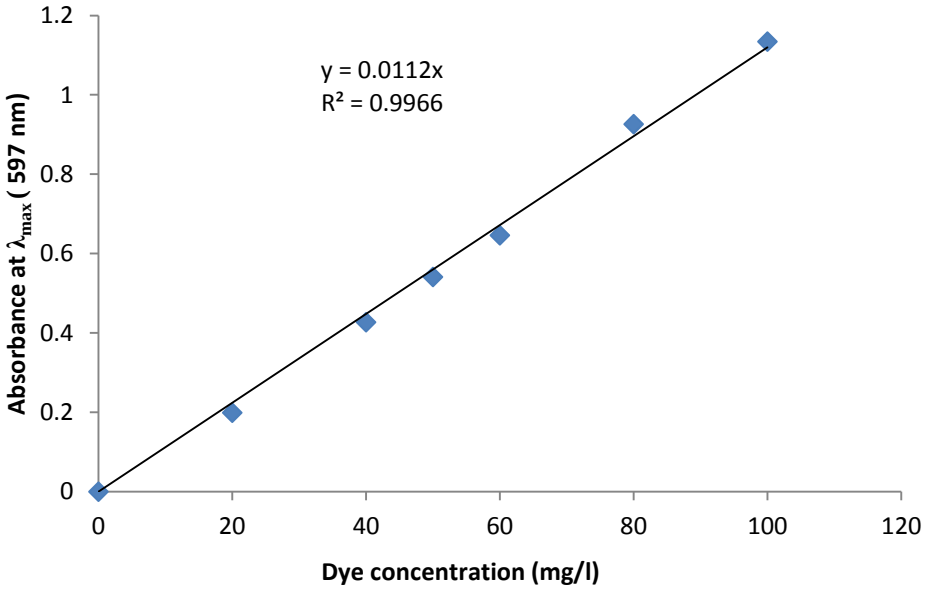

Figure 4.1 Calibration curve for reactive black 5 dye concentration

4.3 Preliminary studies

Preliminary experiments were performed to explore the extent of photolysis, adsorption and photocatalysis on decolorization at natural pH of dyes. Decolorization of dye was studied under following conditions as per procedure mentioned in section 3.3.5.

(i) Hydrolysis

(ii) UV-A photolysis

(iii) Solar photolysis

(iv) Adsorption

(v) Photocatalysis

Adsorption study at natural pH of dye was made by exposing 250 mL of 100 mg/L dye solution to 1 gram of TiO_2. The solution was allowed to equilibrate under constant stirring and dark conditions. Dark condition was kept to avoid any photolytic degradation. The absorbance values at λ_{max} were taken after 30 minutes. The change in absorbance if any may be due to adsorption.

Photocatalytic degradation of dye at pH 3 was explored by using dye solution obtained after adsorption. The dye solution was exposed to UV-A radiation in photoreactor. The absorbance values at λ_{max} were taken at an interval of ten minutes up to 60 minutes. The change in absorbance helps to determine photocatalytic degradation.

Figure 4.2 shows the experimental results. It can be observed clearly that hydrolysis as well UV photolysis effect does not result in any appreciable change in dye concentration. Solar photolysis studies were also made separately which showed similar results. On the other hand, there is appreciable change due to adsorption as well as photocatalysis.

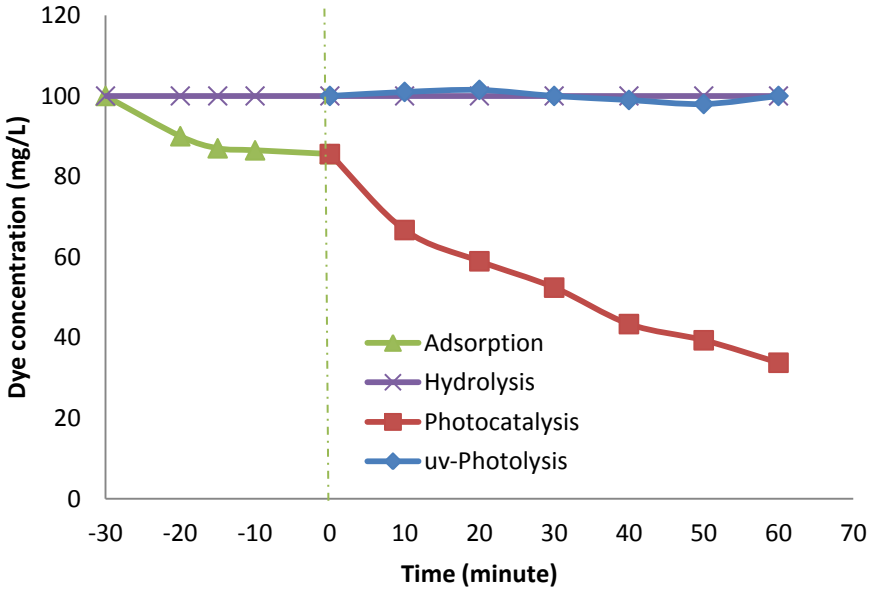

Figure 4.2 Decolorization of RB5 dye versus time due to adsorption, hydrolysis, photocatalysis, and UV-photolysis

4.4 Equilibrium adsorption

Adsorption test in absence of light were done in order to study the adsorption of RB5 dye on to TiO_2 surface. The adsorption experiments at pH 3, 5, 7, 9, and 11 were conducted with different amounts of catalyst. The adsorption of dye at pH 7, 9, and 11was found to be nil. The maximum value of adsorption at pH 3 was 25 mg/g and at pH 5 was 7 mg/g. This implies that adsorption occurs only in acidic conditions and is higher at lower pH values. The adsorption is governed by charge status of TiO_2 surface. Details related to TiO_2 surface charge conditions are discussed in section 4.5.1. Fig. 4.3 gives the adsorption isotherm at pH 3. The equilibrium constants were determined by fitting the experimental data to the Langmuir equation (Eq. (1)) to describe the adsorption of dye.

$$q_e = (q_m.b.C_e)/(1+b.C_e) \qquad (1)$$

where q_m is the maximum amount of dye adsorbed on forming a complete monolayer (mg dye adsorbed per gram of catalyst), b the equilibrium constant, C_e the concentration of dye in the aqueous solution after adsorption, q_e is the amount of dye adsorbed per unit weight of catalyst.

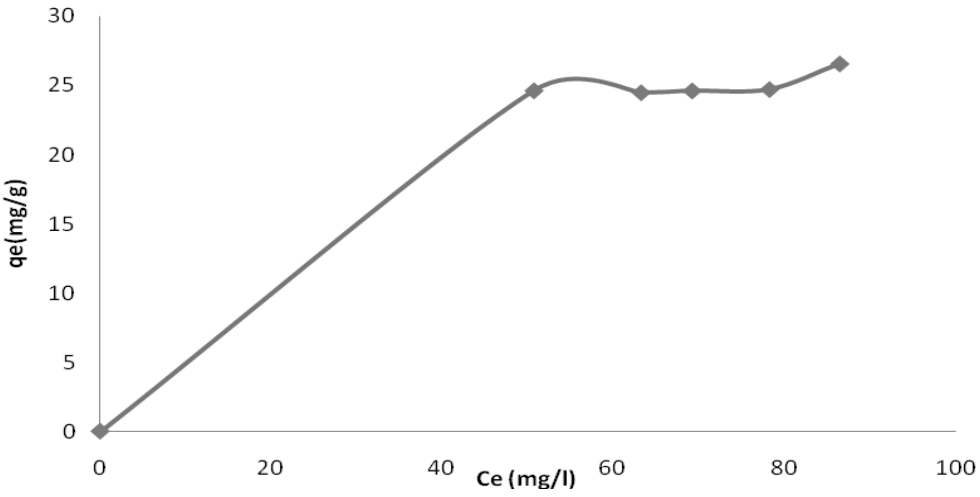

Figure 4.3: Adsorption isotherm of RB5 dye on TiO_2 surface at pH 3

(**Note**: Raw data are shown in Appendix A)

The data at pH 3 has been found to fit well in linearized form of Langmuir equation (Eq. (2)).

$$C_e/q_e = 1/b.q_m + C_e/q_m \qquad (2)$$

A plot between C_e/q_e and C_e has shown a good fit with R square value of 0.97 (Fig. 4.4) and the value of b comes out as 0.09451 L/mg. The value of dimensionless separation (R_L) (Eq. (3)) is 0.095.

$$R_L = 1/(1+b.C_0) \qquad (3)$$

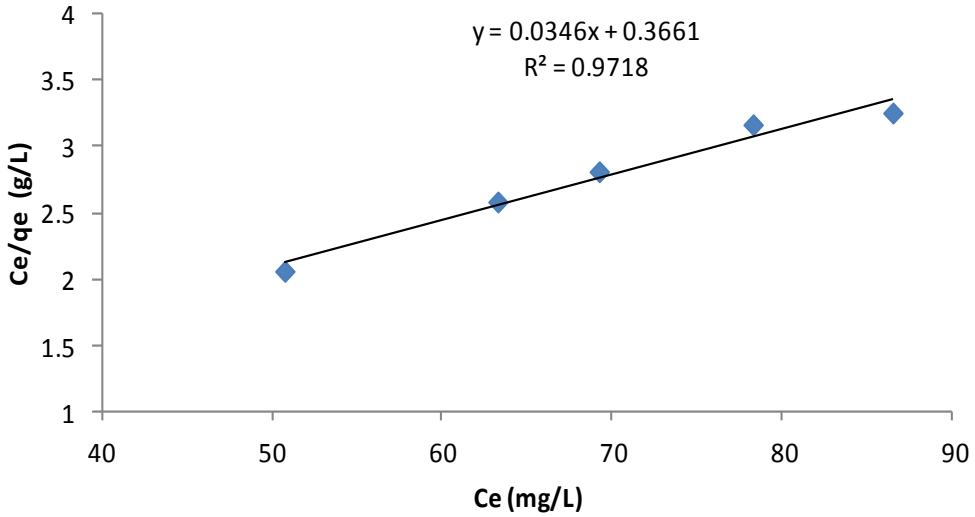

Figure 4.4: Langmuir adsorption fitting of RB5 data

(**Note**: Data values are shown in Appendix A)

where C_0 is the initial dye concentration. The value of R_L between zero and one indicates the favorable shape of Langmuir isotherm [24].

4.5 Decolorization studies

4.5.1. Effect of pH on RB5 dye

Effect of pH is most important parameter for photocatalytic process. Experiments were performed at various pH values (3, 5, 7, 9 and 11) to observe the effect of pH on decolorization kinetics. The samples were allowed to equilibrate for adsorption process for 30 minutes in absence of light and later kept in photoreactor for photocatalytic degradation. After that, the samples were taken at different intervals of time. Fig. 4.5 shows the spectral changes during decolorization. When the kinetics of the photocatalytic decolorization reactions were studied, it was found that the correlation between $\ln(C/C_0)$ and the irradiation time was linear. This is a typical first-order reaction plot. The slopes of the lines give the apparent rate constant (k_{app}). The kinetic expression can be presented as follows:

$$\ln\left(C/C_0\right) = k_{app}t \qquad (4)$$

C: dye concentration at instant t (mg/L)

C_0: dye concentration at t=0 (mg/L)

k_{app}: pseudo-first-order rate constant (L/min)

t: time of reaction in minutes

The variation of rate constant (k_{app}) with pH is shown in Fig. 4.6. The effect of pH as observed above, clearly favors the low pH over high pH. The catalyst surface states vary with pH. In acidic conditions the TiO_2 surface is positivily charged (Eq. 5) and in the basic conditions the TiO_2 surface is negatively charged (Eq. 6)

$$TiOH + H^+ \leftrightarrow TiOH_2^+ \quad (5)$$

$$TiOH + OH^- \leftrightarrow TiO^- + H_2O \quad (6)$$

The point of zero charge pH (pH_{pzc}) of TiO_2 is 6.8 [64]. Thus, TiO_2 surface is positively charged in acidic conditions (pH<6.8), and negatively charged in basic conditions (pH>6.8). There exists a strong electrostatic attraction between positively charged TiO_2 surface and negatively charged sulphonic and ethyl sulphonic groups in RB5 structure [64]. This results in higher adsorption of dye in acidic conditions. .

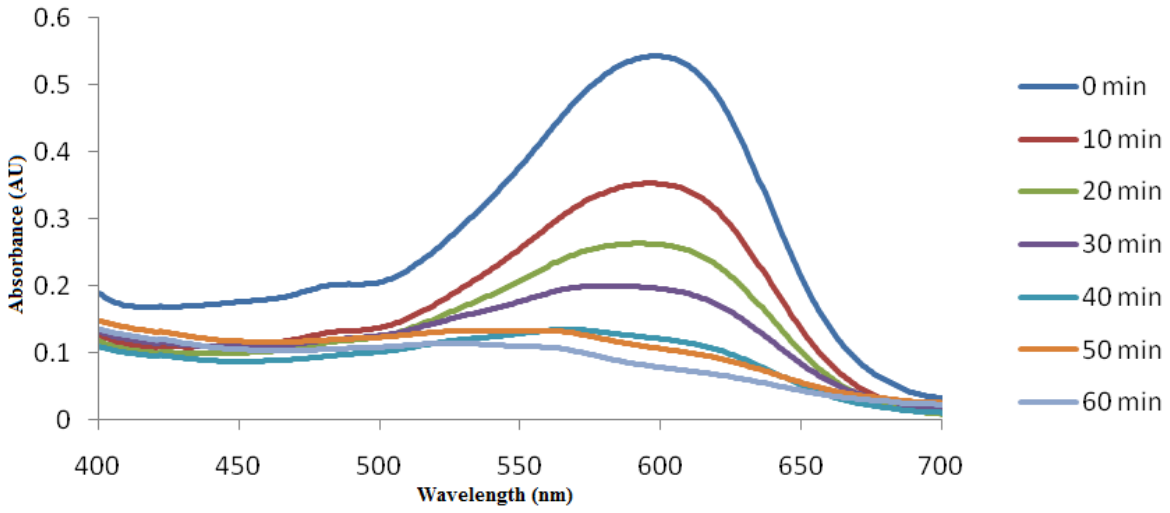

Figure 4.5 Spectral changes of RB5 dye during photocatalytic exposure

Similar to adsorption, the rate of decolorization is also found high at low pH values. At lower values of pH i.e., pH less than pH_{pzc}, the surface of TiO_2 is positively charged, thus increasing the adsorption and further degradation of RB5 dye [62]. Incident UV radiation results in generation of electron hole pair. The positive holes become major source of oxidation at low pH. Decolorization in such conditions may take place by direct reduction mechanism i.e. the electron in the conduction band of TiO_2 causes reduction of azo linkage of adsorbed dye on catalyst surface [26, 121, 122].

This causes high value of rate constant at low pH values. The hydroxyl radicals can be generated by reaction between hydroxide ion and positive holes.

Due to poor adsorption at pH higher than 3, the photocatalysis gets affected largely and hence the lower values of rate constants. This reduced decolorization rate thus might be due to absence of reductive decolorization of dye at higher pH values. However, slight improvement in rate constant is seen at pH 11. The increased value of rate constant may be due to change in degradation mechanism. The decolorization may be resulting from hydroxyl ions. It is assumed that in alkaline conditions, generation of hydroxyl ions may be easier by oxidizing more hydroxide ions available on TiO_2 surface [68, 123]. Another reason for lower decolorization rate constant at basic and neutral pH values may be due to lower photo-activated resulting from difference in degree of suspension of catalyst. The catalyst gets agglomerated in acidic pH conditions. However, with basic and neutral pH conditions, the agglomeration does not take place and suspension is very stable. The photo activated volume of reactor is reduced with high amount of suspended catalyst as discrete particles. Agglomeration reduces the available catalyst surface area but helps by reduced negative effect to UV light penetration in the solution. Due to difference in degree of suspension at different pH values, the optimum amount of catalyst load is also expected to be different.

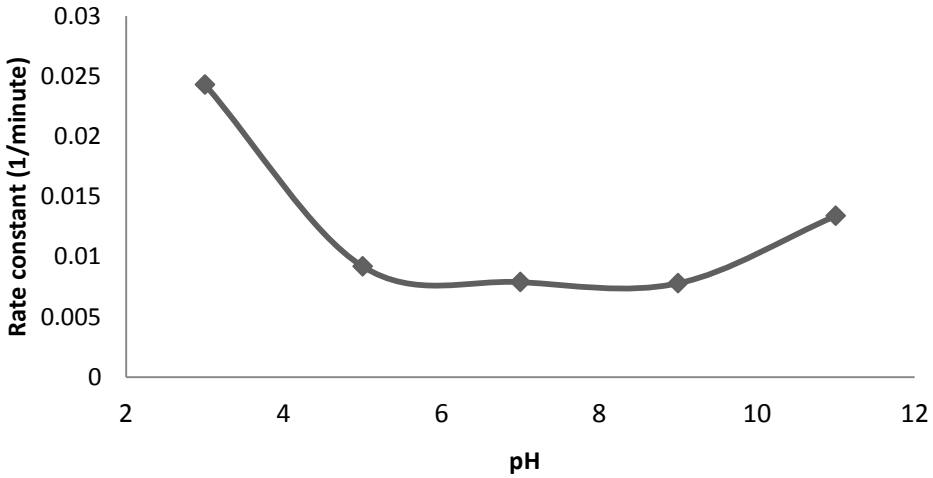

Figure 4.6 Effect of pH on decolorization rate constant at various pH values and 1 g/L of TiO_2

(**Note**: Data values are shown in Appendix A)

4.5.2 Effect of dye concentration

To observe the effect of dye concentration on decolorization of RB5, various initial concentrations of dye were exposed to UV radiation with 1 g/L catalyst load. The initial pH was fixed at 3 because the highest rate constant value was observed at this pH. Different initial concentrations (100, 80, 60, 40, 20 mg/L) of dye solutions were exposed to UV radiation.

Dye decolorization at various initial concentrations of dye is presented in the form of C/C_o vs. time in Fig. 4.7., where C_o is the initial concentration of dye and C is the residual dye concentration at any time 't'. Typical wavy nature of curves is obtained (Fig. 4.7) specifically for 100 and 80 mg/L dye concentration. This can be attributed to the fact that there is substantial formation of degradation intermediates during degradation. These intermediates may be supposed to have no color. Decolorization rate during such conditions is affected. This may be due to preferential further degradation of intermediates.

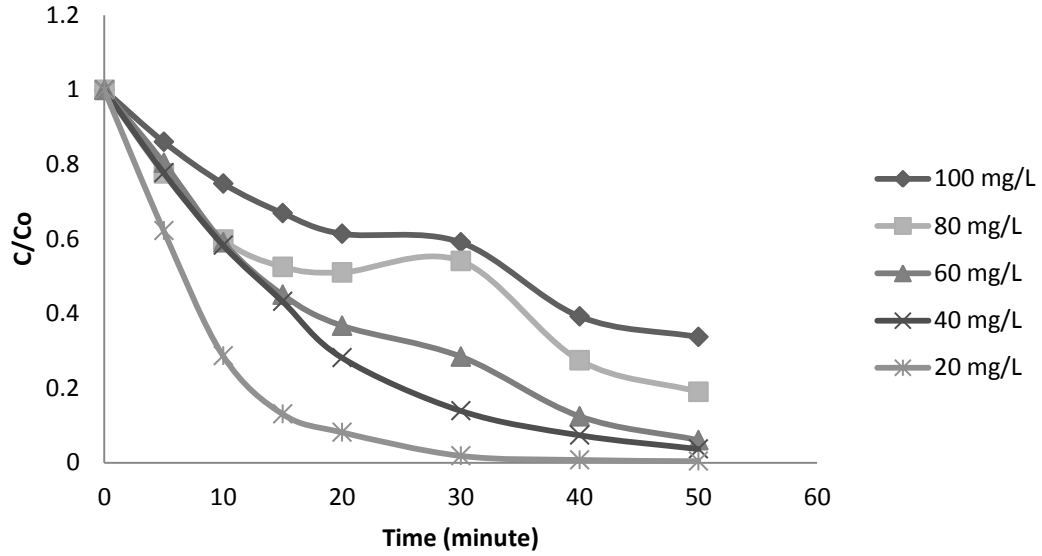

Figure. 4.7 Effect of RB5 dye initial concentration on decolorization characteristics at pH = 3, TiO_2 = 1.0 g/L

Furthermore, the overlap of C/Co data in 80, 60, and 40 mg/L dye concentration unto 10 minute (Fig. 4.7) suggests that these dye concentration screening effect to UV radiation is not affecting decolorization; but the decolorization rate is affected subsequently due to formation of intermediates. Further amount of such formed intermediates is different depending upon the initial dye concentration, resulting in difference in decolorization rate constants (k_{app}) depending upon the dye concentration as shown in Fig.4.8.

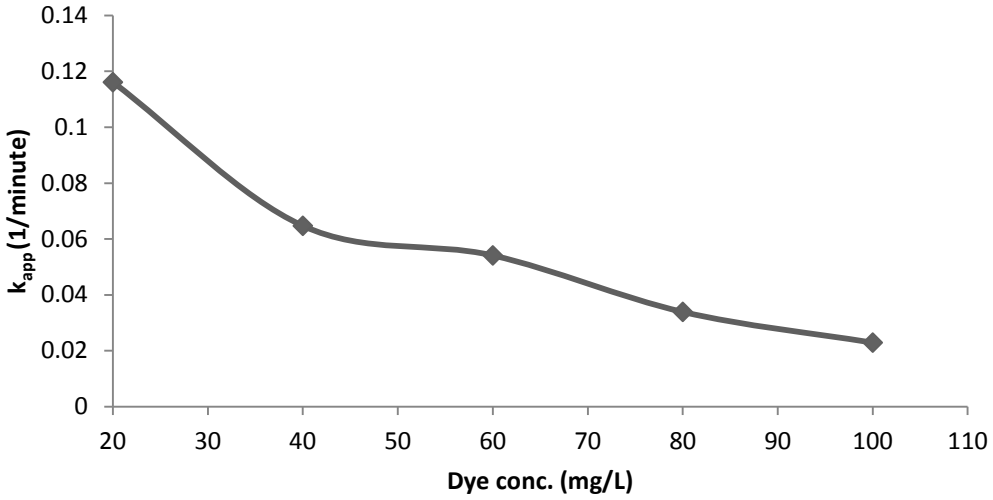

Figure 4.8 Effect of RB5 initial dye concentration on decolorization rate constant at pH = 3, TiO_2=1.0 g/L

(**Note**: Data points are presented in tabulated form in Appendix A)

Additionally, there exists screening effect to UV radiation by increased dye concentration in general also; as it decreases the depth of UV radiation entering the reactor. Since the rate of decolorization is proportional to the photoexitation of TiO_2 particles and subsequent reduction of azo bond of adsorbed dye. The influence of initial concentration of dye on decolorization over illuminated TiO_2 surface can be observed in term of Langmuir-Hinshelwood model equation, modified for reactions occurring over the liquid-solid interface [124]. Rate of reaction during photocatalysis can be expressed as

$$R = -dC/dt = (k_c K_c C)/(1 + K_c C + \sum K_i C_i) \qquad (7)$$

Where C and C_i are the concentrations of substrate and intermediate compound i, respectively, at time t, t is the reaction time, k_c is the Langmuir reaction rate constant. K_c and K_i are adsorption equilibrium constants for dye and intermediate compound i, respectively. Since as decolorization kinetics of dye follows the pseudo first order kinetics with respect to concentration in bulk solution

$$R = -dC/dt = -\ln\left(C/C_0\right) = k_{app} C \qquad (8)$$

Further, if it is assumed that adsorption equilibrium constants for all organic molecules present in the reacting mixture are effectively equal, following assumption can be made

$$K_c C + \sum K_i C_i = K_C C_0 \qquad (9)$$

Combing above equation,

$$1/k_{app} = 1/k_c K_c + C_0/k_c \qquad (10)$$

A plot of $1/k_{app}$ vs. Co yields a slope of $1/k_c$ and intercept $1/(k_c K_C)$ as shown in Fig. 4.9. It was found that the dye decolorization follows the above equation up to 80 mg/L concentration. Thus in light of the above, Langmuir reaction rate constant (k_c) value is 3.078 per minute and adsorption equilibrium constant (K_C) on illuminated TiO_2 surface equal to 0.2039 L/mg.

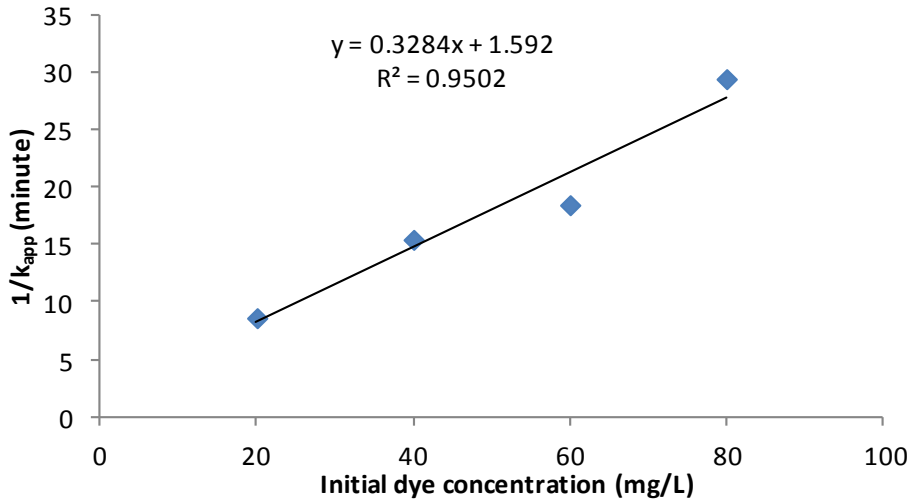

Figure 4.9 Linear transform ($1/k_{app}$= f(C_o)) of modified Langmuir-Hinshelwood model for RB5 decolorization on TiO_2 Degussa P25

4.5.3 Effect of catalyst loading

Further experiments were performed to determine the optimum catalyst loading by varying the catalyst concentration from 0.5 g/L to 3.0 g/L. Initial dye concentration was kept as 100 mg/L. Percentage decolorization at the end of 30 minutes of photocatalytic reaction was measured. Fig. 4.10 shows the variation in percentage decolorization with catalyst load. The optimum catalyst load under experimental conditions for RB5 was found to be 1.5 g/L. Catalyst loading beyond 1.5 g/L contributes to additional opacity in liquid and light scattering by TiO_2 particles which cause a decrease in photocatalytic active volume of reactor. Also, aggregation of TiO_2 particles is enhanced at high concentration of catalyst.

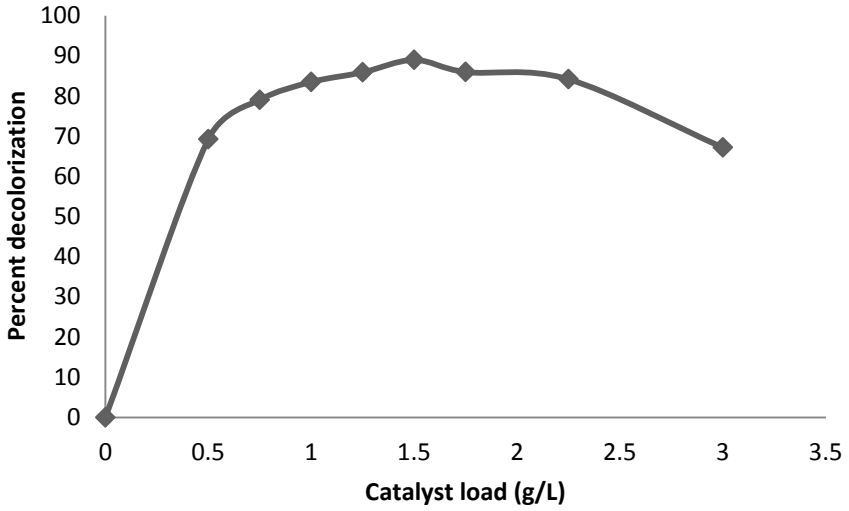

Figure 4.10 Percentage decolorization of RB5 dye at the end of 30 minute of photocatalyis

4.5.4 Effect of UV intensity

The effect of UV intensity was studied for one hour by varying the intensity from 4.6 to 15 W/m^2, with 1 g/L of catalyst load and 100 mg/L of dye concentration at pH 3. The decolorization was studied for 1 h. At an intensity of 4.6 W/m^2, the decolorization of RB5 was 56.94% in 1 h whereas with increase in intensity to 14.7 W/m^2, the decolorization was up to 92.19 % in 1 h. This shows that at higher intensity, more decolorization of dye takes place as shown in Fig. 4.11. The rate constant increases linearly with increase in intensity of UV radiations (Eq. (11)). The R square value of this linear relation is 0.976; which implies a good linear relation between rate constant and UV intensity.

Rate constant (k_{app}) = 0.0029 (UV intensity) - 0.0085 (11)

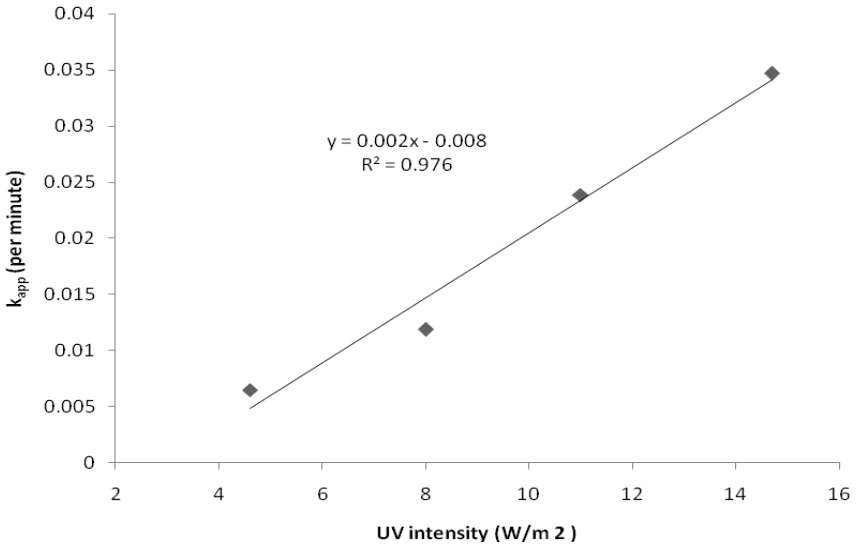

Figure 4.11 Effect of UV intensity on decolorization rate constant (k_{app}) at pH = 3, TiO_2=1 g/L, and C_0 = 100 mg/L

4.5.5. Effect of A/V ratio of reactor

The ratio of area to volume (A/V) is critical for the shallow pond reactor as the photocatalytic oxidation reaction depends on area available for the irradiation of light. More area and less depth enhance the rate of decolorization as the penetration of UV rays into the solution increases. Hence, the reaction rate increases with increasing aperture to volume ratio of the shallow pond type reactor as shown in Fig. 4.12. As A/V ratio is increased from 0.1005 to 0.502727 cm^2/mL, the decolorization increased from 75% to 88.94 % in 1 h for 100 mg/L of initial concentration of RB5. The linear relation between rate constant and area to volume ratio was found (Eq. (12)) with R square value of 0.942 (Fig. 4.12).

Rate constant (k_{app}) = 0.0591 (A/V) + 0.0086 (12)

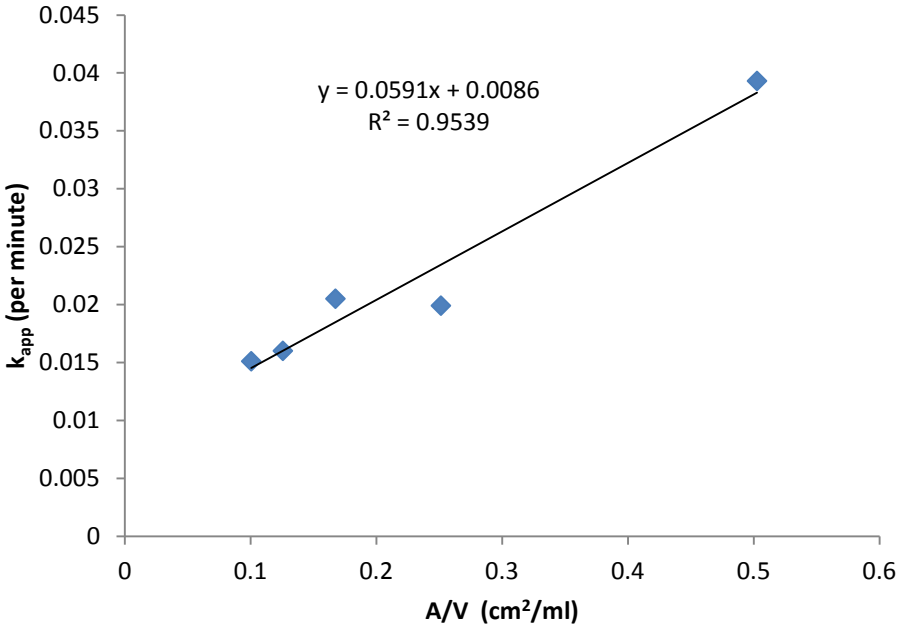

Figure 4.12 Effect of A/V ratio of reactor on decolorization rate constant (k_{app}) at pH = 3, TiO_2=1.5 g/L, and C_0 = 100 mg/L

(**Note**: Data points are presented in tabulated form in Appendix A)

4.6 Total organic carbon variation vs. decolorization

In order to determine the degree of mineralization during photocatalysis, the TOC of different samples was determined along with dye concentration measurement. Area to volume ratio was kept constant at 0.10054 cm^2/mL to ensure that reactor volume should not vary appreciably due to increase in number of samples withdrawn. Further, UV intensity was maintained at 14.7 W/m^2. TOC variation along with dye concentration is shown in Fig. 4.13.

Table: 4.1 Changes in TOC and dye color of RB5 due to adsorption

Parameter	Initial value	After adsorption	Percent change due to adsorption
Color	100	89.8	10.2
TOC	20.19	12.83	36.75

The RB5 dye under experimental conditions shows almost complete decolorization by the end of 5 hours. However, the decrease in TOC starts only after 6 hours of photocatalysis. TOC variation up to 5 hours shows first a decrease up to three hours and later an increase in value.

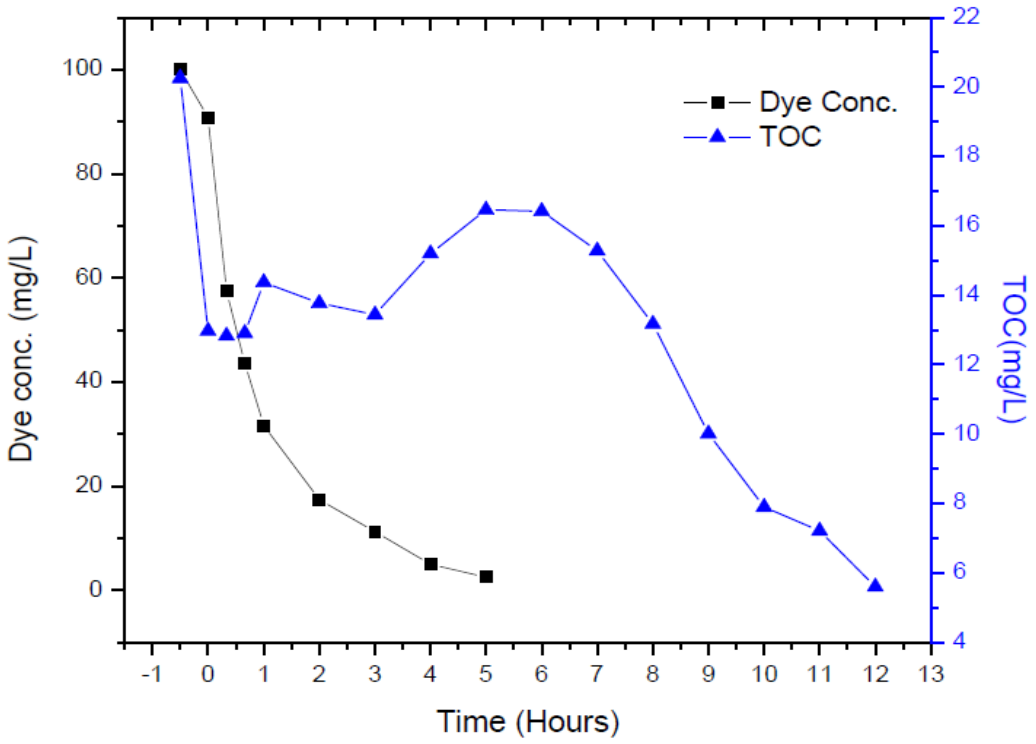

Figure 4.13 Variation of dye concentration and TOC during photocatalysis at pH = 3, TiO_2 = 1.5 g/L, C_0 = 100 mg/L, (Area to volume ratio of reactor = 0.10054 cm^2/mL)

(**Note**: Data points are presented in tabulated form in Appendix A)

This trend is similar to that observed for change in COD values while studying photocatalytic decolorization of Reactive orange 16 [114]. Initial decrease in TOC is due to adsorption of dye and impurities present in dye. It is worthwhile to note that there is large difference in percent changes in TOC and dye concentration resulting from adsorption (Table 4.1). Further changes might be resulting from adsorption and desorption of intermediates formed during decolorization and due to photocatalytic reactions taking place simultanously. Subsequent increase in TOC values might be due to release of more dye intermediates to the solution from the surface of catalyst which might not be getting further adsorbed over catalyst surface due to non-availability of more active sites.

Another reason for such increase can be the formation of different intermediates, which may not have any tendency to get adsorbed over catalyst surface. From TOC and dye concentration measurements, it may conclude that during decolorization dye gets decomposed to intermediates which have lesser adsorptivity on catalyst surface. It has been observed that 70 % mineralization of the RB 5 dye in 100 mg/L dye at 12 h.

4.7 Conclusions

The reactive black 5 dye can be degraded by TiO_2-P25 assisted photocatalysis in aqueous dispersion under irradiation by UV-A light. The dye shows good adsorption at low pH due to catalyst surface charge interactions with dye. The adsorption data fits well with Langmuir isotherm. The optimum catalyst load is 1.5 g/L at pH 3.The decolorization rate increases with decrease in initial dye concentration. Dye decolorization follows modified Langmuir-Hinshelwood kinetics between 20 mg/L and 80 mg/L dye concentration. Rate constant of decolorization varies linearly with area to volume ratio between 0.1 cm^2/mL and 0.5 cm^2/mL.

The mineralization of the dye was investigated by total organic carbon (TOC) measurements that showed 70 % mineralization of 100 mg/L dye in 12 h. The rate of mineralization observed in our studies is much lower than previously reported in literature [12, 14, 17]. The slow mineralization rates have implications on post photocatalytic treatment requirements based upon BOD/COD ratios, and toxicity of effluent at various stages of treatment. Thus, photocatalytic treatment of colored effluent under low UV intensity, and Low A/V ratio may result in completely decolorized effluent but still having high COD.

Appendix A

A1: Raw data related to equilibrium adsorption studies of reactive black 5 (RB5)

Table AT1: Data related to equilibrium adsorption studies of RB5 dye at pH 3

Sr. No.	W	C_o	C_e	V	q	Ce	q_e	C_e	C_e/q_e
1	0.127	100	86.50265	250	26.56958	86.5	26.56	86.5	3.256777
2	0.25	100	75.28448	250	24.71552	78.28	24.71	78.28	3.167948
3	0.3125	100	69.23718	250	24.61026	69.23	24.61	69.23	2.813084
4	0.375	100	63.27752	250	24.48165	63.27	24.48	63.27	2.584559
5	0.5	100	50.74472	250	24.62764	50.74	24.62	50.74	2.060926
6	0	100	0	250	0	0	0		0

where W = Weight of catalyst used (g)

C_0 = Initial dye concentration (mg/L)

C_e = Dye concentration at equilibrium after adsorption (mg/L)

V = Volume gram of dye used (ml)

q_e = Amount of dye adsorbed in mg per gram of catalyst (mg/g)

A2: Effect of pH on RB5 photocatalytic decolorization

Table AT2.1: Apparent decolorization rate constant of RB5 dye at various pH values

Sr. No.	pH	k_{app}	R square
1	3	0.0243	0.9946
2	5	0.0092	0.9819
3	7	0.0079	0.9614
4	9	0.0078	0.9702
5	11	0.0134	0.9905

Table AT2.2: Raw data for determination of rate constant at pH 3

Sr. No.	Time (minute)	Dye conc. (mg/L)	Ln (C_t/C_0)
1	0	96.2692	0.038022
2	10	73.47338	0.308247
3	20	62.72029	0.466485
4	30	48.49788	0.72365
5	40	35.8739	1.02516
6	50	29.33486	1.226394
7	60	21.3427	1.54446

A3: Effect of UV intensity on RB5 photocatalysis

Table AT3: Apparent decolorization rate constant of RB5 dye with UV intensity

Sr. No.	UV intensity (W/m^2)	k_{app} (per minute)	R square
1	4.6	0.0065	0.9815
2	8	0.0119	0.9639
3	11	0.0239	0.9786
4	14.7	0.0347	0.9820

A4: Effect of A/V ratio on RB5 photocatalysis

Table AT4: Apparent decolorization rate constant of RB5 dye with A/V ratios

Sr. No.	A/V (cm^2/ml)	k_{app} (per minute)	R square
1	0.5027	0.0393	0.9562
2	0.25136	0.0199	0.9834
3	0.1675	0.0205	0.9947
4	0.12568	0.016	0.9671
5	0.100544	0.0151	0.9621

A5: Effect of dye concentration on RB5 photocatalysis.

Table AT5: Apparent decolorization rate constant of RB5 dye at various dye concentration

Sr. No.	Dye conc. (mg/L)	k_{app} (per minute)	R square	$1/C_0$
1	100	0.0229	0.9865	0.01
2	80	0.0339	0.9693	0.0125
3	60	0.0541	0.9958	0.0167
4	40	0.0647	0.9957	0.025
5	20	0.1161	0.9888	0.05

A6: Decolorization and mineralization of RB5 dye

Table AT6: Data related to variation of dye concentration and TOC of RB5 photocatalysis

Sr. No.	Time (Hours)	TOC	Dye color
1	-0.5	20.25	100
2	0	12.97	90.81984
3	0.33	12.83	57.4592
4	0.66	12.904	43.65184
5	1	14.37	31.64544
6	2	13.77	17.40928
7	3	13.44	11.23456
8	4	15.2	4.97408
9	5	16.46	2.48704
10	6	16.42	-
11	7	15.28	-
12	8	13.17	-
13	9	10.01	-
14	10	7.895	-
15	11	7.21	-
16	12	5.597	-

CHAPTER – 5

PHOTOCATALYTIC DEGRADATION OF REACTIVE RED 120 DYE

Photocatalytic Degradation of Reactive Red 120 Dye

5.1 Introduction

Present study is about the effect of operational parameters like pH, catalyst load, initial dye concentration, area to volume ratio (A/V) of reactor, and UV intensity in a UV chamber on photocatalytic degradation of Reactive Red 120 (RR120). Mineralization study has been done along with decolorization studies to evaluate reduction in total organic carbon content (TOC) during photocatalysis.

5.2 Calibration curve

RR120 dye solution of 100 mg/L concentration was prepared as per section 3.3.1. The dye solution thus made was scanned in 200-700 nm wavelength for absorbance. The wavelength of maximum absorbance in visible region was found to be 524 nm. Further RR120 calibration curves were made by making solutions of 20, 40, 60, 80 mg/L from 100 mg/L solution by serial dilution. Absorbance values were measured at the value at λ_{max} (524 nm) wavelength. The calibration curve thus obtained is shown in Figure 5.1.

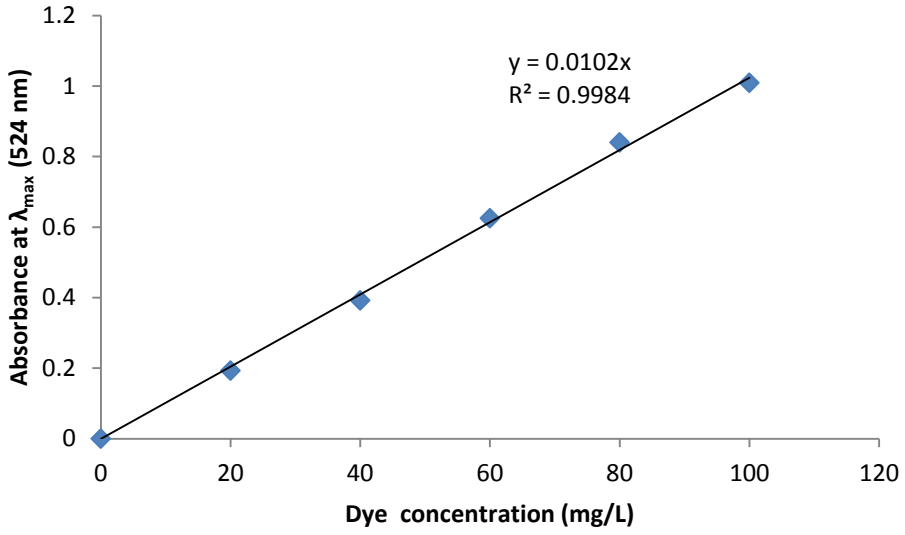

Figure 5.1 Calibration curve for reactive red 120 dye concentration

5.3 Preliminary studies

Preliminary experiments were performed to explore the extent of photolysis, adsorption and photocatalysis on decolorization at natural pH of dyes. Decolorization of dye was studied under following conditions as per procedure mentioned in section 3.3.5.

(i) Hydrolysis

(ii) UV-A photolysis

(iii) Solar photolysis

(iv) Adsorption

(v) Photocatalysis

Adsorption study at natural pH of dye was made by exposing 250 mL of 100 mg/L dye solution to 1 gram of TiO_2. The solution was allowed to equilibrate under constant stirring and dark conditions. Dark condition was kept to avoid any photolytic degradation. The absorbance values at λ_{max} were taken after 30 minutes. The change in absorbance if any may be due to adsorption.

Photocatalytic degradation of dye at pH 3 was explored by using dye solution obtained after adsorption. The dye solution was exposed to UV-A radiation in photoreactor. The absorbance values at λ_{max} were taken at an interval of ten minutes up to 60 minutes. The change in absorbance helps to determine photocatalytic degradation.

Fig. 5.2 shows the experimental results. It can be observed clearly that hydrolysis as well as UV photolysis effect does not result in any appreciable change in dye concentration. Solar photolysis studies were also made separately which showed similar results. On the other hand there is appreciable change due to adsorption as well as photocatalysis.

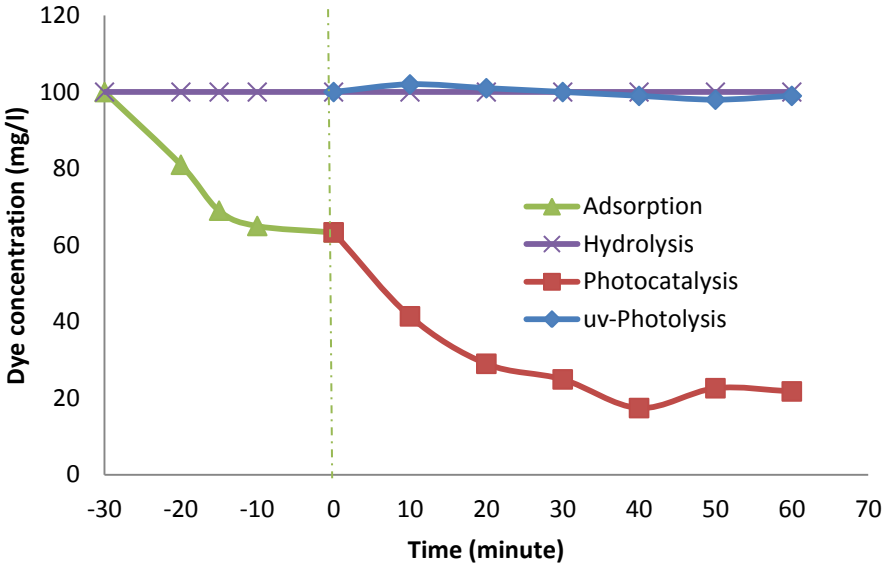

Figure 5.2 Decolorization of RR120 versus time due to adsorption, hydrolysis, photocatalysis, and UV-photolysis.

5.4 Equilibrium adsorption

Adsorption tests in absence of light were performed in order to study the adsorption of RR120 dye on to TiO_2 surface. The value of adsorption was noted at pH 3, 5, 7, 9, and 11 with various amounts of catalyst. The maximum value of adsorption at pH 3 was 49 mg/g and at pH 5 was 6 mg/g. The adsorption of dye at pH 7, 9, and 11was found to be nil. The specific adsorption at pH 7 might be too small if any to be determinable accurately within experimental accuracy (~3-4 mg/L). However, adsorption at pH 9, and 11 is as per expectation. The adsorption is governed by charge status of TiO_2 surface. Details related to TiO_2 surface charge conditions are discussed in section 5.5.1. Fig. 5.3 gives the adsorption isotherm at pH 3. The equilibrium constants were determined by fitting the experimental data to the Langmuir equation (Eq. (1)) to describe the adsorption of dye.

$$q_e = (q_m . b . Ce)/(1 + b . C_e) \qquad (1)$$

where q_m is the maximum amount of dye adsorbed on forming a complete monolayer (mg dye adsorbed per gram of catalyst), b the equilibrium constant, C_e the concentration of dye in the aqueous solution after adsorption, q_e is the amount of dye adsorbed per unit weight of catalyst.

The data at pH 3 has been found to fit well with linearized form of Langmuir equation (Eq. (2)).

$$C_e / q_e = 1 / bq_m + C_e / q_m \qquad (2)$$

The graph between C_e/q_e and C_e is shown as a good fit with R square value of 0.9924 (Fig 5.4) and the value of b comes out as 1.626 L/mg.

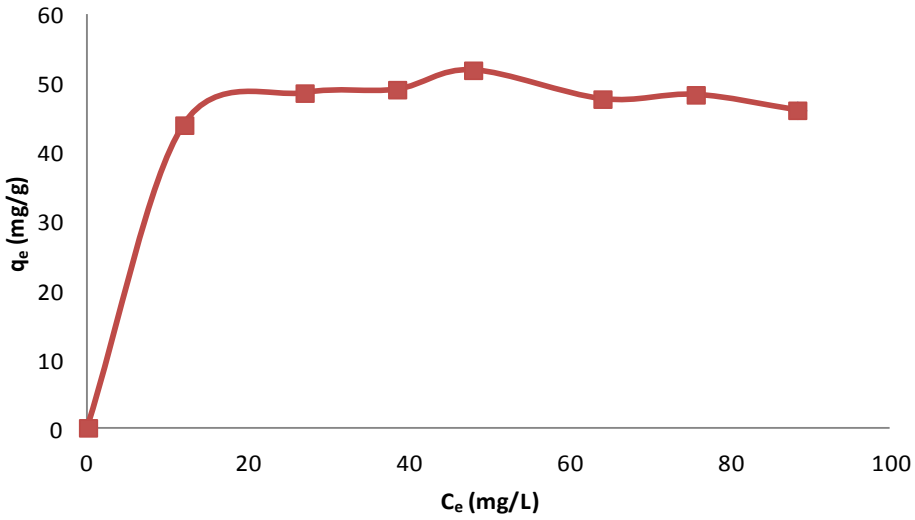

Figure 5.3 Adsorption isotherm of RR120 dye at pH 3.

(**Note**: Raw data are shown in Appendix B)

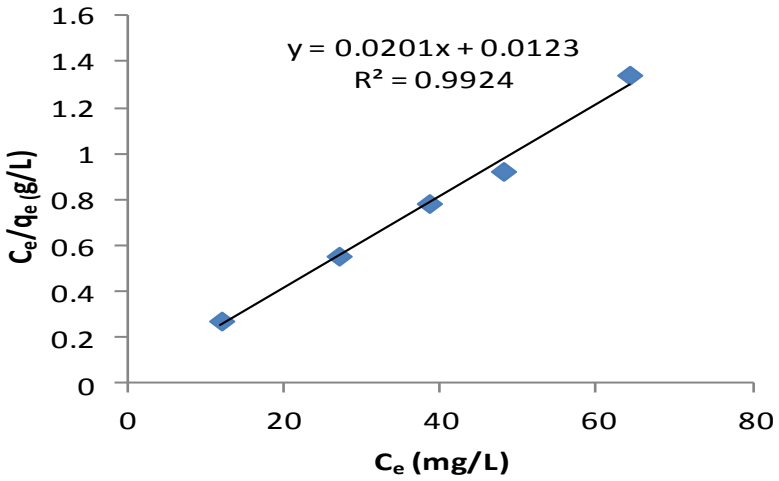

Figure 5.4 Langmuir adsorption fitting of RR120 data at pH 3

(**Note**: Raw data are shown in Appendix B)

5.5 Decolorization studies

5.5.1 Effect of pH on RR120 dye

pH effect is an important parameter for photocatalytic process. Experiments were performed at various pH values (3, 5, 7, 9 and 11) to observe the effect of pH on decolorization kinetics. The reactor contents were allowed to equilibrate for adsorption process for 30 minutes in absence of light and then kept in photoreactor for photocatalytic degradation. Later the samples were withdrawn at regular intervals.

When the kinetics of the photocatalytic decolorization reactions were studied, it was found that the correlation between ln (C/C_0) and the irradiation time was linear. This is a typical first-order reaction plot. The slopes of the lines give the apparent rate constant (k_{app}). The kinetic expression can be presented as follows:

$$\ln\left(C/C_0\right) = k_{app}t \qquad (3)$$

C: dye concentration at instant t (mg/L);

C_0: dye concentration at t = 0 (mg/L);

k_{app}: pseudo-first-order rate constant (L/min);

t: time of reaction in minutes.

The data fits well with pseudo first order kinetics (Fig. 5.5). The variation of rate constant with pH is shown in Fig. 5.6.

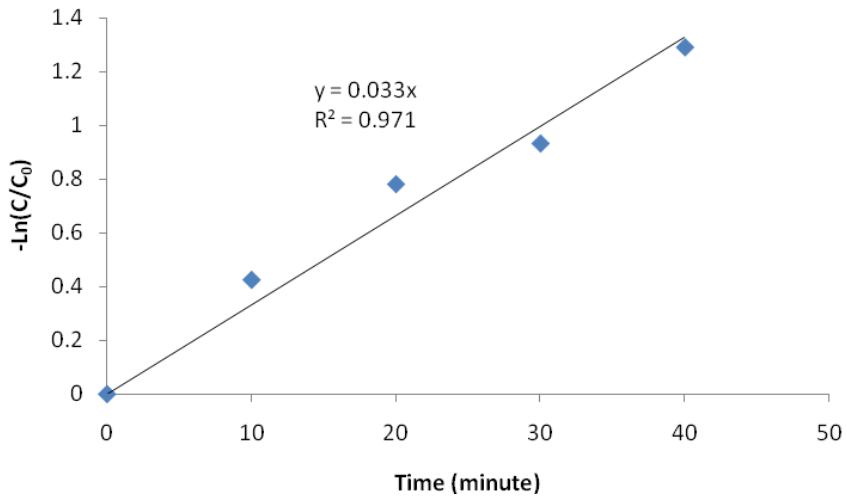

Figure 5.5 Photocatalytic decolorization kinetics of RR120 with TiO_2 = 1 g/L, pH = 3, and C_0 = 100 mg/L

The effect of pH as observed above, clearly favors the low pH over high pH. The catalyst surface states vary with pH. The reactions below show the surface charge conditions in acidic and basic conditions.

$$TiOH + H^+ \leftrightarrow TiOH_2^+ \quad (4)$$

$$TiOH + OH^- \leftrightarrow TiO^- + H_2O \quad (5)$$

The point of zero charge pH (pH_{pzc}) of TiO_2 is 6.8 [64]. Thus, TiO_2 surface is positively charged in acidic conditions (pH<6.8), and negatively charged in basic conditions (pH>6.8). Thus, there exists a strong electrostatic attraction between positively charged TiO_2 surface and negatively charged sulphonic groups in RR120 structure [64] .

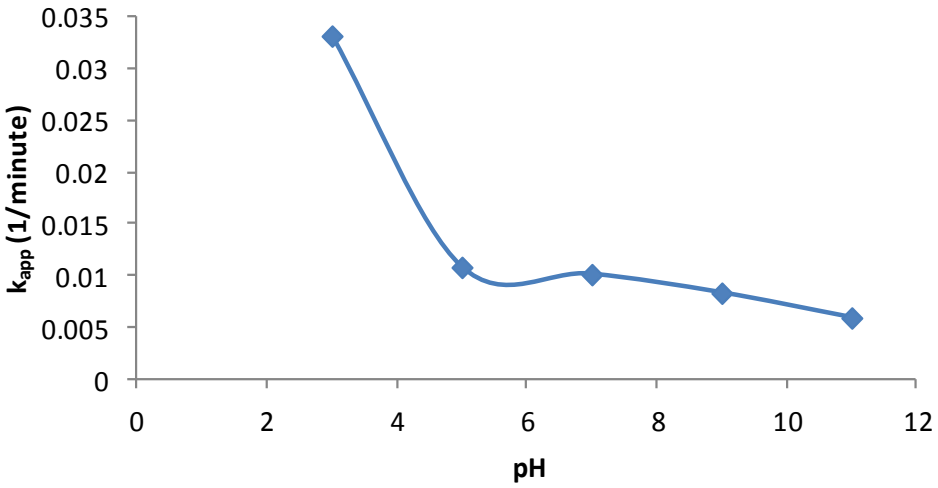

Figure 5.6 Effect of pH on decolorization rate constant of RR120 dye at TiO_2 = 1 g/L, C_0 = 100 mg/L

The positive holes become major source of oxidation at low pH. Decolorization in such conditions may take place by direct reduction mechanism i.e. the electron in the conduction band of TiO_2 causes reduction of azo linkage [26, 121, 122] of adsorbed dye on catalyst surface. This causes high value of rate constant at low pH values. Additionally, hydroxyl radicals can be generated by reaction between hydroxide ion and positive holes.

Similar to adsorption, the rate of decolorization is also found high at low pH values. At lower values of pH (pH less than pH_{pzc}), the surface of TiO_2 is positively charged, thus increasing the adsorption and further degradation of RR120 dye [62].

Due to poor adsorption at pH higher than 3, the photocatalytic decolorization gets affected largely and hence the lower values of rate constants. This reduced decolorization rate thus can be due to absence of reductive decolorization of dye at higher pH. The decolorization rate constant (k_{app}) decreases sharply at higher pH due to reduced adsorption.

It is assumed that in alkaline conditions generation of hydroxyl ions may be easier by oxidizing more hydroxide ions available on TiO_2 surface [68, 123]. However, the results do not show any increase but decrease in degradation rate from neutral to highly basic pH. Another reason for lower decolorization rate constant at basic and neutral pH values may be due to lower photo-activated resulting from difference in degree of suspension of catalyst. The catalyst gets agglomerated in acidic pH conditions. However, with basic and neutral pH conditions, the agglomeration does not take place and suspension is very stable. The photo activated volume of reactor is reduced with high amount of suspended catalyst as discrete particles. Agglomeration reduces the available catalyst surface area but helps by reduced negative effect to UV light penetration in the solution. Due to difference in degree of suspension at different pH values, the optimum amount of catalyst load is also expected to be different.

From the sharp variations in rate constant (k_{app}), q_{max} values at various pH, it may be concluded that dye decolorization may be mainly occurring over catalyst surface after adsorption.

5.5.2 Effect of dye concentration

To observe the effect of dye concentration on decolorization of RR120, various initial concentrations of dye were exposed to UV radiation with 0.5 g/L as catalyst load. The initial pH was fixed at 3 as the highest decolorization rate was observed at this pH. Various initial dye concentrations i.e. 100, 80, 60, 40 mg/L dye solutions were exposed to UV radiation.

The effect of initial dye concentration on decolorization rate constant (k_{app}) is presented in Fig. 5.7. It has been observed that dye shows maximum decolorization rate constant with lowest initial dye

concentration (i.e. 40 mg/L). As the dye concentration is increased; a significant amount of UV radiation entering the reactor is absorbed by dye molecules rather than TiO_2. This causes reduction in photocatalytic efficiency. It may be concluded from Fig. 5.7 that the decrease in rate constant with increase in dye concentration is not directly proportional to increase in concentration. This can be due to difference in UV screening effect by dye, relatively different amount of intermediates formed, and type of intermediate existing at any time.

In previous studies it was found that decolorization rate constant increases with increasing dye concentration to a certain level and further increase in dye concentration leads to decrease in degradation rate of dyes [40, 107]. Reactive black 5 studies under experimental condition only show decrease in rate constant with increasing dye concentration.

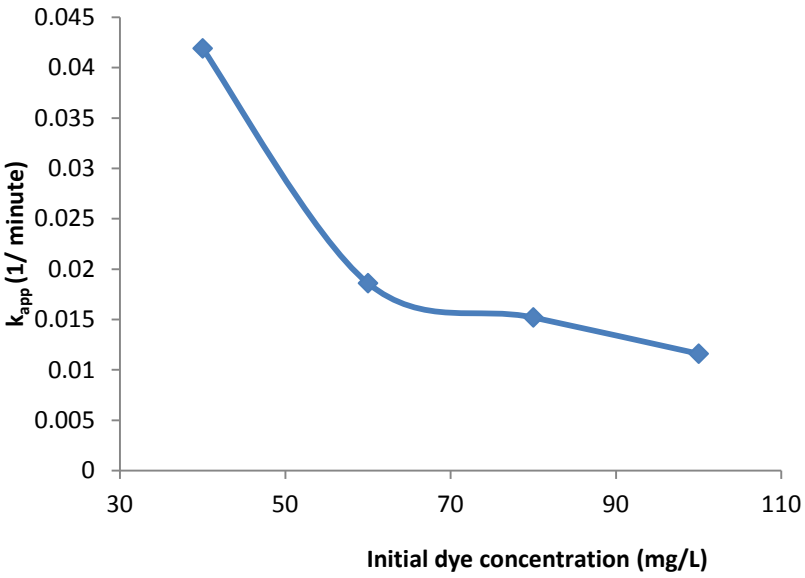

Figure 5.7 Effect of initial dye concentration on decolorization rate constant at pH = 3, and TiO_2=1 g/L. (**Note**: Raw data are shown in Appendix B)

5.5.3 Effect of catalyst loading

Catalyst load plays an important role in determining total color removal from dye solution. The residual dye content at any time represents the remaining dye content in the solution irrespective of adsorbed quantity of dye. The adsorption of dye over catalyst surface reaches 95.67 % when catalyst load is increased up to 3 g/L. It was also observed that with higher values of catalyst load, desorption of dye from catalyst occurs during photocatalytic degradation. Fluctuations in residual dye content are observed due to desorption and degradation occurring simultaneously. This results in loss of pseudo first order decolorization nature. So, dye decolorization studies based upon decolorization kinetics (k_{app}) cannot be made at higher catalyst loading.

Therefore, for catalyst load optimization, objective was set to achieve maximum photocatalytic decolorization in 30 minutes of photocatalytic exposure. To determine optimum catalyst load, dye solution with various amounts of catalyst were subjected to 30 minutes of adsorption and further 30 minutes of photocatalysis. Dye concentration was determined from absorbance values after adsorption and after photocatalysis. Initial concentration of dye solution in all the cases was 100 mg/L.

To understand further this optimization issue, Fig. 5.8 shows the details of experimental investigation related to catalyst load optimization. Series 1 curve shows the color removed from a dye solution after 30 minutes of adsorption, starting with initial concentration of 100 mg/L. Series 2 curve shows the change in value of residual dye concentration during photocatalytic degradation but after adsorption. In other words this represents change in residual dye concentration excluding initial adsorptive change. Series 3 curve shows the total color removal after 30 minutes of adsorption followed by further 30 minute of photocatalysis (i.e. sum of series 1 and 2).

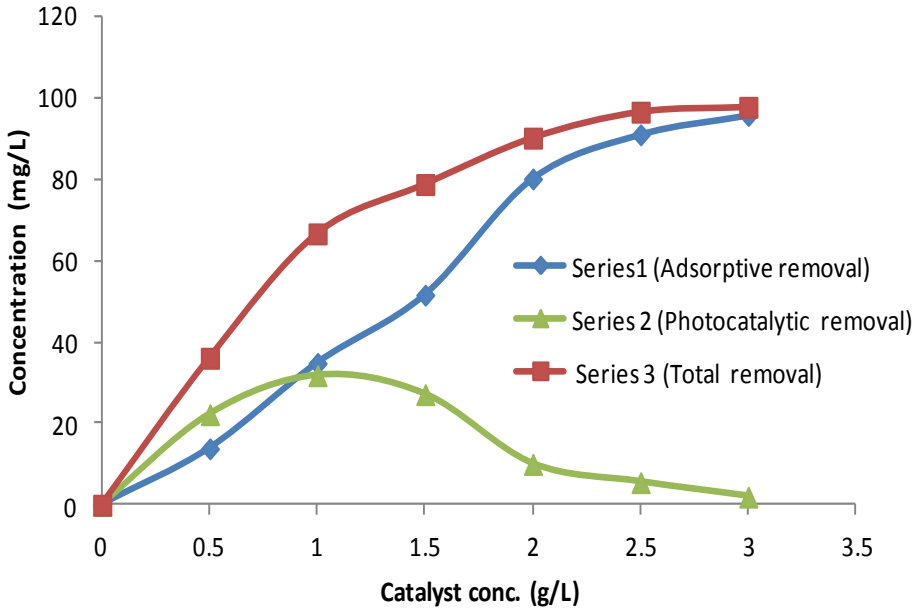

Figure 5.8 Determining optimum catalyst load for RR120 dye solution at pH = 3.0, C_0 = 100 mg/L

(**Note**: Data values are shown in Appendix B)

It has been observed that photocatalytic reaction of anionic dyes in acidic pH condition; mainly occurs by photo-oxidation and photo-reduction reactions over catalyst surface. Thus, most of the decolorization is expected from reaction occurring over catalyst surface [68]. After decolorization the intermediates are probably released to liquid phase. This results in adsorption of dye from liquid phase over the catalyst, which is further, decolorized by photo oxidation and photo reduction

reactions. Thus decrease in residual dye concentration represents the actual decolorization occurring over catalyst surface.

Series 1 and series 2 curves intersect at point 0.9 g/L value of catalyst load. Also series 2 is having its peak near 0.9 g/L of catalyst load. So, with 0.9 g/L is the catalyst load at which amount of color removed by adsorption and photocatalysis are equal. This implies that 0.9 g/L of catalyst load is the optimum value of catalyst load because at this value of catalyst load the dye removed from catalyst surface seems to be compensated equally by further adsorption upon catalyst surface under the experimental investigation conditions. Any higher amount of catalyst load might be causing initial decolorization due to adsorption only. Also higher amount of catalyst load may decrease the photoactivated volume of reactor due to higher amount of suspended catalyst.

5.5.4 Effect of A/V ratio of reactor

The ratio of area to volume (A/V) is critical for the shallow pond reactor as the photocatalytic oxidation reaction depends on area available for the irradiation of light. More area and lesser depth enhance the rate of decolorization as the penetration of UV rays into the solution increases. Hence, the reaction rate increases with increasing area to volume ratio of the shallow pond type reactor as shown in Fig. 5.9. As A/V ratio is increased from 0.1005 to 0.5027 cm^2/mL, the decolorization is increased from 76.3 % to 91.21 % in 1 h. With decreasing A/V value the apparent rate constant of decolorization decreases. It can be seen in Fig 5.9 that, the rate constant shows almost linear variation with A/V ratio between 0.1675 cm^2/mL and 0.5027 cm^2/mL. However, for A/V lesser than 0.1675 cm^2/mL the decrease in rate constant is sharp. This may happen because with increasing depth the photo-activated volume may not be increasing linearly. Another reason for decrease in rate constant can be the lower amount of suspended catalyst concentration in the upper volume of the reactor.

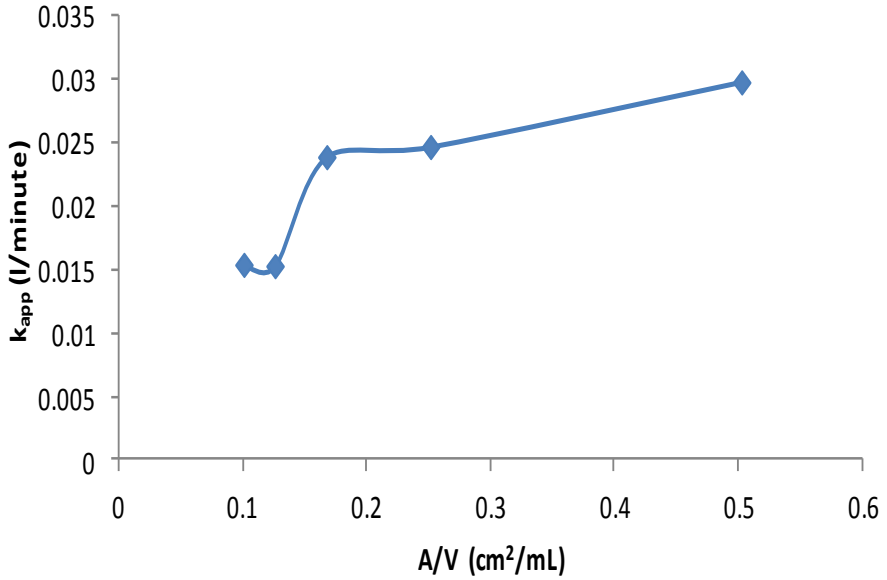

Figure 5.9 Effect of area to volume ratio (A/V) of reactor on decolorization rate constant of RR120 at pH 3, C_0 = 100 mg/L

(**Note**: Data values are shown in Appendix B)

5.5.5 Effect of UV intensity

The effect UV intensity on decolorization kinetics were observed by varying UV intensity from 4.7 W/m^2 to 14.7 W/m^2. The values of apparent decolorization constant were determined. It was found that the there is linear relationship between apparent decolorization rate constant and UV intensity. The linear relationship is shown in Fig 5.10

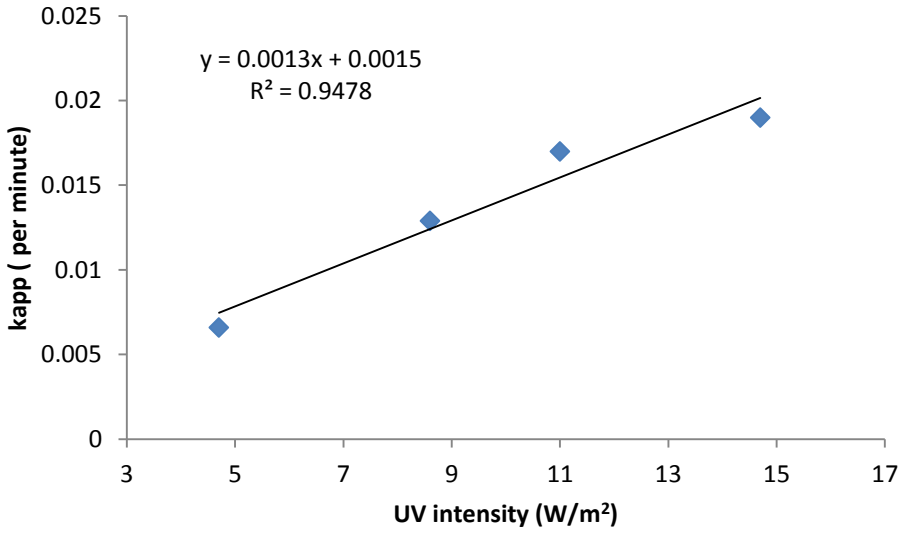

Figure 5.10 Effect of UV intensity on decolorization rate constant of RR120 at pH 3, C_0 = 100 mg/L

5.6 TOC variation vs. decolorization

In order to determine the degree of mineralization during photocatalysis, the TOC of samples was determined along with dye concentration. Area to volume ratio was reduced to 0.10054 cm^2/mL, so that dye volume in reactor should not get reduced appreciably due to increase in number of samples withdrawn. Further, UV intensity was increased to 14.7 W/m^2 from 10.7 W/m^2. TOC variation along with dye concentration is shown in Fig. 5.11. Initial adsorptive removal of TOC is 60.59%. However the color removal by adsorption at same time is 41.84%. This implies that larger amount of adsorption is occurring over catalyst surface than suggested by reduction in color. This can be accounted to the impurities present in dye. As per the supplier (Sigma Aldrich) the dye purity is lies in 50-70% range. This implies that approximately 40% of compounds present in dye do not contribute to color and exist as impurities.

Table: 5.1 Changes in TOC and dye color of RR120 due to adsorption

Parameter	Initial values	After adsorption	Percent change due to adsorption
TOC	20.91	8.239	60.59
Color	99.99	58.16	41.83

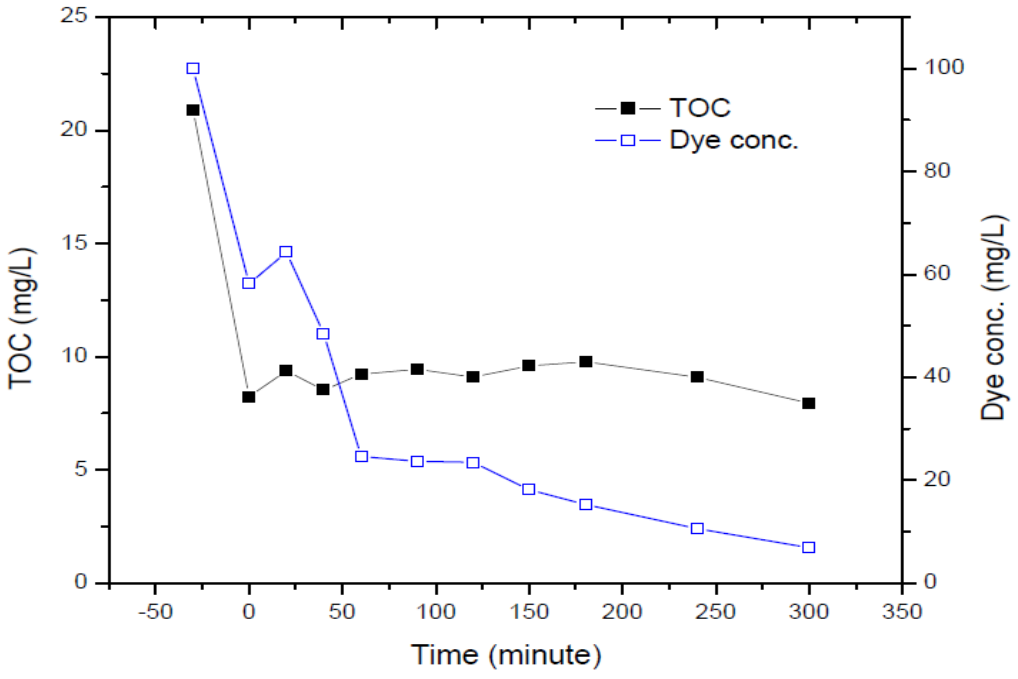

Figure 5.11 Simultanous variation of TOC and dye concentration due to andsorption and during photocatalysis at pH = 3, TiO_2 = 1 g/L, C_0 = 100 mg/L, Area to volume ratio of reactor = 0.10054 cm^2/mL. The time less than zero indicate the time for adsorption equilibrium

(**Note**: Data values are shown in Appendix B)

These impurities might be getting adsorbed over catalyst surface along with dye. So, the higher percent removal of TOC stands justified. There is initial decrease in TOC value due to adsorption which is followed by slight increase on start of photocatalysis. Similar trend is also observed in dye concentration measurements. The RR120 dye under experimental conditions shows almost complete decolorization by the end of 300 minutes. However, the decrease in TOC value is not appreciable. This implies that decolorized product is contributing to TOC due to formation of colorless intermediates.

It may be concluded here that reduction in TOC is very slow at A/V ratio of 0.10054 cm^2/mL and other experimental conditions. Percentage decolorization in 30 minutes is decreased to 48% at A/V ratio of 0.10054 cm^2/mL from 75% at A/V ratio of 0.20108 cm^2/mL. Kusvuran et. al. also observed that fast decolorization of RR120 was accompanied by slower TOC reduction indicating that stable intermediates had been formed [108]. It has been observed that such stable intermediates include strongly recalcitrant chemical like acetic acid [125]. Variations in TOC during photocatalysis may occur by adsorption, desorption, degradation of intermediates, and complete mineralization occurring simultaneously.

5.7 Conclusions

The results presented show that Reactive Red 120, an anionic diazo dye can be successfully decolorized under UV radiation. The dye shows good adsorption at low pH due to catalyst surface charge interactions with dye. The adsorption data fits well with Langmuir isotherm. It is observed that adsorption is prerequisite for efficient photocatalytic degradation. Both adsorption and degradation are highest at pH 3. The maximum adsorption at pH 3 was found to be 49 mg/g. The optimum catalyst load at pH 3 is 0.9 g/L and lower dye concentration improves decolorization rate. Rate constant of decolorization varies linearly with area to volume ratio (A/V) of reactor between 0.1675 cm^2/mL and 0.5027 cm^2/mL. However, there is sharp decrease in decolorization rate constant for A/V value below 0.1675 cm^2/mL. So, A/V ratio should be kept above 0.1675 cm^2/mL. Reduction in TOC was very slow and complete mineralization was not achieved even after 5 hours at pH 3 (under the condition: A/V ratio of 0.10054 cm^2/mL, and 14.7 W/m^2 UV intensity). Impurities present in dye also get adsorbed over catalyst surface. Slow reduction in TOC may also be due to formation of stable intermediates.

Appendix B

B1: Raw data related to equilibrium adsorption studies of reactive red 120 (RR120) dye

Table BT1: Data related to equilibrium adsorption studies of RB5 dye at pH 3

C_o (mg/L)	W(g)	V (mL)	Absorbance	C_e (mg/L)	C_o-C_e (mg/L)	q_e (mg/g)	C_e/q_e
100	0.0625	250	0.943	88.4609	11.53906	46.1562	1.9165550
100	0.125	250	0.808	75.7968	24.2031	48.4062	1.5658479
100	0.1875	250	0.684	64.1646	35.8353	47.7804	1.3429067
100	0.25	250	0.512	48.0297	51.9703	51.9703	0.9241757
100	0.3125	250	0.411	38.5550	61.4449	49.1559	0.7843425
100	0.375	250	0.288	27.0167	72.9833	48.6555	0.5552648
100	0.5	250	0.128	12.0074	87.99258	43.9962	0.2729190

where W = Weight of catalyst used (g)

C_0 = Initial dye concentration (mg/L)

C_e = Dye concentration at equilibrium after adsorption (mg/L)

V = Volume gram of dye used (mL)

q_e = Amount of dye adsorbed in mg per gram of catalyst (mg/g)

B2: Effect of pH on RR120 photocatalytic decolorization

Table BT2: Values of apparent RR120 decolorization rate constant at various pH values

Sr. No.	pH	k_{app} (per min)	R square
1	3	0.0332	0.9714
2	5	0.0108	0.9934
3	7	0.0101	0.9648
4	9	0.0083	0.9297
5	11	0.0059	0.9096

B3: Effect of dye concentration

Table BT3.1: Values of apparent RR120 decolorization rate constant at various initial dye conc.

Sr. No.	C_o (mg/L)	k_{app} (per min)	$1/k_{app}$ (min)
1	100	0.0116	86.2069
2	80	0.0152	65.78947
3	60	0.0186	60.24096
4	40	0.0419	23.86635

Table BT3.2: Raw data and determination of optimum catalyst load for RR120 during 30 minutes of photocatlysis

TiO_2 conc. (g/L)	Weight of TiO_2 actual (g)	Volume dye (mL)	Absorbance after adsorption	Residual dye conc. after adsorption (mg/L)	mg/L removed by adsorption	Absorbance after photocatalysis	Residual dye conc. after 30min photocatlysis (mg/L)	Total color removal (mg/L)	mg/L removed by photocatalysis	Percent color removal after adsorption (%)
0.5	0.125	250	0.946	86.15	13.84	0.702	63.93	36.07	22.22	25.79
1	0.25	250	0.716	65.208	34.79	0.367	33.42	66.57	31.78	48.74
1.5	0.375	250	0.532	48.451	51.55	0.234	21.31	78.68	27.14	56.01
2	0.5	250	0.219	19.94	80.05	0.109	9.92	90.07	10.02	50.22
2.5	0.625	250	0.1	9.1074	90.89	0.039	3.55	96.45	5.55	61
3	0.75	250	0.048	4.371	95.63	0.026	2.36	97.63	2.01	45.83

B4: Effect of area to volume ratio of reactor

Table BT4: Values of apparent RR120 decolorization rate constant at various area to volume ratio of reactor

Sr. No.	A/V (cm^2/ml)	k_{app} (per min)	R square
1	0.5027	0.0298	0.9598
2	0.25136	0.0247	0.9703
3	0.1675	0.0239	0.9622
4	0.12568	0.0153	0.9688
5	0.100544	0.0154	0.9664

B5: Decolorization and mineralization studies

Table BT5: Raw data for variation of dye concentration and TOC of RR120 photocatalysis

Sr. No.	Time (min)	TOC (mg/L)	Dye conc. (mg/L)
1	-30	20.91	99.9966
2	0	8.239	58.16316
3	20	9.373	64.30974
4	40	8.523	48.43872
5	60	9.23	24.58632
6	90	9.44	23.67
7	120	9.098	23.48544
8	150	9.59	18.13
9	180	9.772	15.3
10	240	9.095	10.5501
11	300	7.942	6.8805

CHAPTER – 6

PHOTOCATALYTIC DEGRADATION OF SIMULATED EFFLUENT

Photocatalytic Degradation of Simulated Effluent

6.1 Introduction

This chapter deals with the adsorption and subsequent decolorization kinetics of reactive azo dyes RR120 and RB5 in their mixture. The objective of the study is to compare the adsorption and subsequent photodegradation behavior of the two dyes in their single solution to that of their mixture. These two dyes have been chosen because (1) they have widely varying molecular weight and (2) Different number of sulphonate groups.

A novel methodology to quantify each dye separately in dye solution has been also developed. Further studies compare the adsorption isotherms of two dyes Reactive Red 120 (RR120) and Reactive Black 5 (RB5) in single dye solution to that in their mixture. Photocatalytic treatment of the dye mixture has been done, in order to optimize catalyst load. Individual dyes decolorization kinetics, in case of dye mixture, have been also studied. Decolorization kinetics of single dye solution has been compared with that of dye mixture. Mineralization of dye mixture along with decolorization has been studied. To simulate the industrial dye house effluent degradation characteristics of dye mixture has been studied in presence of salts required for dyeing. Additional the catalyst deactivation has been studied on the basis of its reusability. The amount of carbon irreversibly adsorbed on catalyst has been also determined.

6.2 Calibration of two dyes in mixture

In the absorbance spectra of mix dye, it was observed that the value of absorbance at 524 nm gets affected due to additional absorbance by other dye (Fig. 6.1). Thus, in case of unknown mixture, it is not possible to measure accurately individual dye concentration using a single wavelength.

Table 6.1 Absorbance values and concentration of dye mixtures at λ_{max} of dyes

Sr. No.	λ_{524}	λ_{597}	RR120 concentration (mg/L)	RB5 concentration (mg/L)	Total RR120 and RB5 concentration (mg/L)
1	1.633	1.199	50	50	100
2	1.36	0.623	50	25	75
3	1.09	1.157	25	50	75
4	1.082	0.03	50	0	50
5	0.556	1.17	0	50	50
6	0	0	0	0	0

Various mixtures with varying dye ratios were made for calibration purpose. Absorbance values at 524 and 597 nm were taken. Multiple regression method was used for calibration purpose [126]. The final equations to determine individual dye in mixture of dyes are:

$$\text{RR120 concentration (mg/L)} = 46.937*\lambda_{524} - 22.362*\lambda_{597} \quad (1)$$

$$\text{RB5 concentration (mg/L)} = 43.754*\lambda_{597} - 1.371*\lambda_{524} \quad (2)$$

$$\text{Sum of RB5 and RR120 concentration (mg/L)} = 45.565*\lambda_{524} + 21.391*\lambda_{597} \quad (3)$$

where λ_{524}, and λ_{597} represent absorption values at 524 nm and 597 nm respectively. It may be noted that negative terms in the equations (1) and (2) removes the interference from other dyes in proportion to their concentration.

Statistical parameters related to this calibration are given in Table 6.2, which suggest a good fit of calibration data.

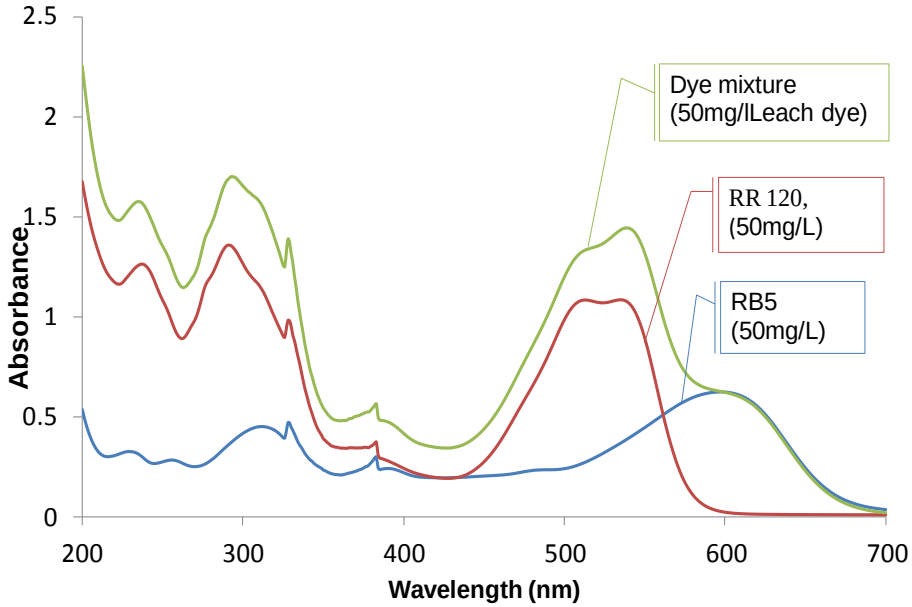

Fig. 6.1 UV-vis spectra of RR120, RB5 and dyes mixture

Table 6.2 Statistical parameters related to calibration of both dyes in mixture.

Parameter	Equation (1)	Equation (2)	Equation(3)
No. of points	5	5	5
Degree of freedom	3	3	3
Residual sum of squares	0.1372	1.774	0.566
Adjusted R square	0.99997	0.99976	0.99997

Previous studies on photocatalytic degradation of dyes mixture have used absorbance at single wavelength to quantify dye concentration [118, 119, 127]. However as explained previously, additional absorbance caused by presence of other dyes cannot be ignored. The calibration made in such case can give actual results only if the dye concentration ratio does not vary to great extent during study. However, in the intended application this ratio cannot be kept constant due to competitive adsorption and preferential degradation of one dye over the other. So the multiple regression based calibration is the option.

Additional techniques to measure dye concentration in case of dye mixture like MCR-ALS [128] and first order derivative of spectrum have been also used [129]. These techniques also attempt to remove interference from other dyes but are mathematically more rigorous.

6.3 Equilibrium adsorption

RR120, and RB5 are both anionic dyes. Sulphonate groups in these dyes are supposed to be negatively charged. The TiO_2 surface can be charged negatively or positively according to pH of its solutions. For pH less than point of zero charge pH (pH_{pzc}), the TiO_2 surface is positively charged and for pH more than pH_{pzc}, it is negatively charged. Point of zero charge pH (pH_{pzc}), for TiO_2 is 6.8. Thus adsorption is favored in acidic pH conditions due to attraction between dye and catalyst surface. So adsorption and further photcatalytic degradation studies were performed at pH 3.

6.3.1 Adsorption isotherms of single dye solutions

Fig. 6.2 shows adsorption equilibrium for RR120 and RB5 when the solutions were made with single dyes. RR120 dye shows maximum adsorption of 50 mg/g while RB5 shows 25 mg/g adsorption. The adsorption equilibrium characteristics of both dyes are of typical L-1 shape [130]. There is clearly seen a difference in maximum adsorption quantity for both dyes. This can be interpreted from the fact that the two dyes have different molecular structure. The molecule of RR120 contains six number of sulphonate groups, while RB5 has four groups per molecule. Thus, RR120 shows higher adsorption per gram of catalyst. Another reason for this difference is the difference in purity of the dyes. The non-dye content might be also getting adsorbed, which cannot be measured by spectrophotometer based study.

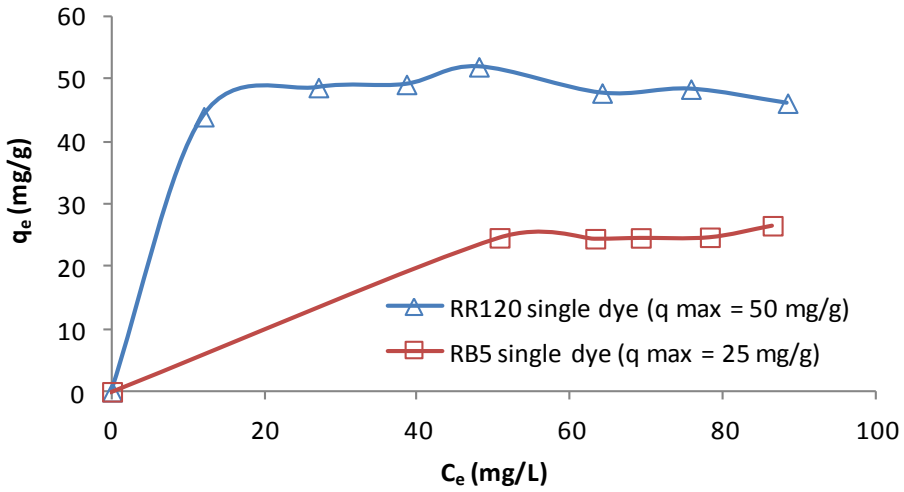

Figure 6.2 Adsorption equilibrium of RR120 and RB5 dyes in case of single dye solutions (at pH 3)

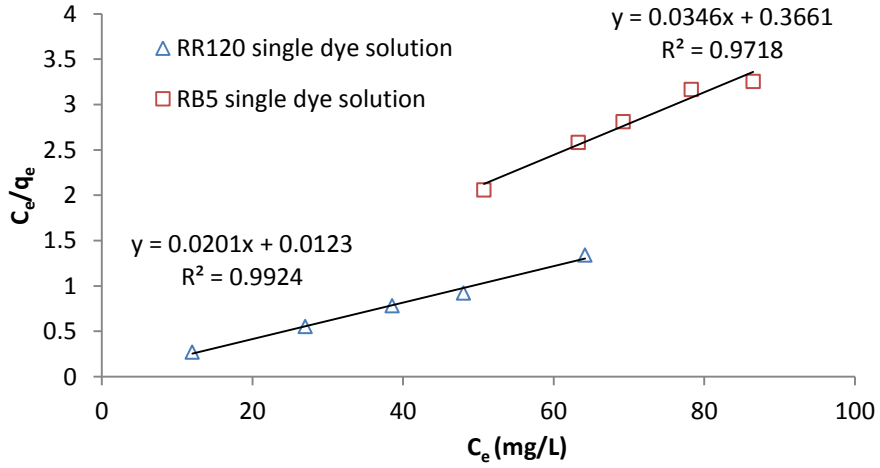

Figure 6.3 Langmuir adsorption isotherms of RB5 and RR120 in case of single dye solutions.

The equilibrium data has been found to fit well in linearized form of Langmuir equation (Eq. (4)).

$$C_e / q_e = 1/b.q_m + C_e / q_m \qquad (4)$$

A plot between C_e/q_e vs. C_e has shown a good fit for both dyes in single dye solution (Fig. 6.3). The equilibrium constants were determined by fitting the experimental data to the Langmuir equation to describe the adsorption of dye. The equilibrium constant for RR120 and RB5 thus obtained were 1.626 L/g and 1.342 L/g respectively.

6.3.2 Adsorption isotherms of dye mixture

Fig. 6.4 shows the combined adsorption equilibrium of total dye (RR120 and RB5) when adsorption study is done with mixed dye solution. Fig. 6.5 shows the adsorption equilibrium of single dyes when in mixed dye solution**.** It has been observed that value of 'q_{max}' (40 mg/g in Fig. 6.6) for RR120 dye in dye mixture is close to q_{max} value of RR120 in single dye solution (49 mg/g in Fig. 6.2). This implies that RR120 dye is largely adsorbing over catalyst surface in case of dye mixture as well. In case of dye mixture there is seen a competition among dyes to occupy the active sites over catalyst surface. RR120 shows higher adsorption, which can be clearly observed in Fig. 6.5. The adsorption equilibrium of RR120 in dye mixture still shows typical L-1 shape [130]. However, RB5 adsorption equilibrium is strongly altered in presence of RR120. This also shows that competitive adsorption is taking place. Sahel et al. observed similar alteration in RB5 adsorption behavior, while studying mixture of Procion Red MX-5B and RB5 [119]. They concluded that this alteration in RB5 adsorption behavior was due to pH change resulting from mixing of dyes. Our studies rule out this reason, because our adsorption studies were made at constant pH. Our observation is that, the amount of RB5 adsorbed per unit catalyst weight was high at higher catalyst load only because under such conditions, residual concentration of RR120 was found limiting to compete with RB5. In other words the adsorption of RB5 was high only when the residual concentration of RR120 in solution was very small. Thus, it may be concluded that adsorption of RR120 occurs preferentially over RB5 (Table 6.3). Competitive adsorption can also be explained based upon free energy change associated with dyes. RR120 dye has higher value of equilibrium constant, so the associated decrease in free energy due to its adsorption is also higher. All chemical systems tend naturally toward states of minimum Gibbs free energy. So adsorption of RR120 occurs preferentially. Competitive adsorption of metanil yellow and reactive blue 15 dyes and remazol black 5 and remazol brilliant orange 3R dyes has also been reported in literature [131, 132].

All the adsorption isotherms show an excellent fit to Langmuir isotherm except of RB5 in dye mixture (Fig. 6.6 & 6.7). RB5 isotherm data was also found not to fit in Freundlich isotherm.

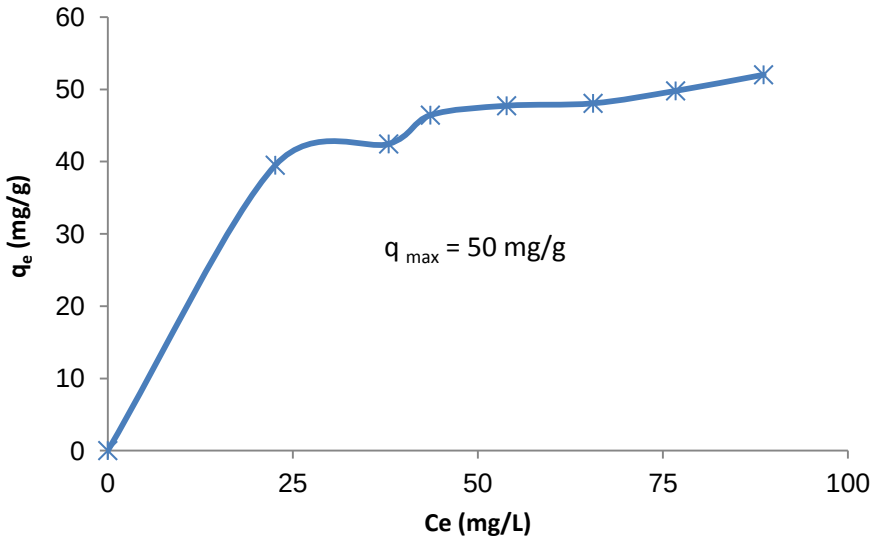

Figure 6.4 Adsorption equilibrium for total adsorption of RR120 and RB5 dyes in dye mixture (at pH 3)

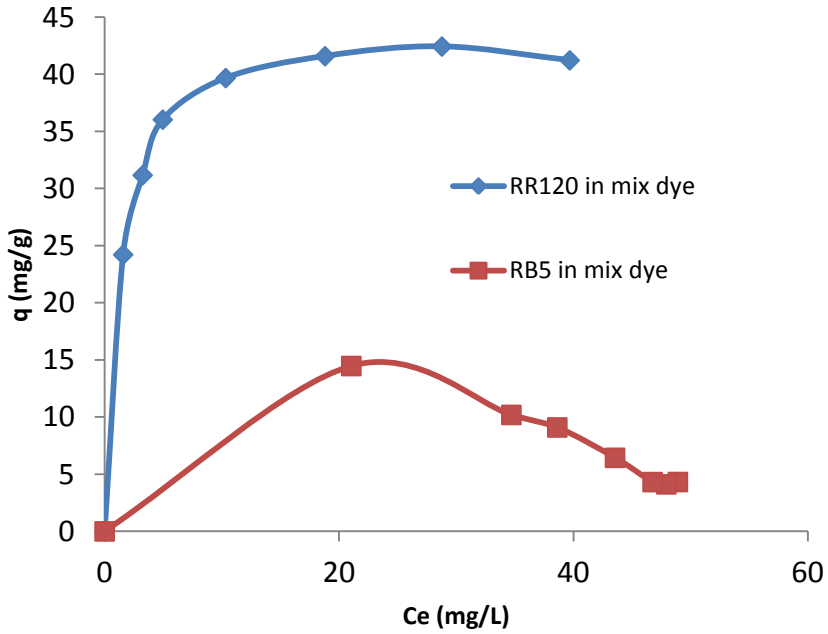

Figure 6.5 Adsorption equilibrium of RR120 and RB5 dyes in dye mixture (at pH 3)

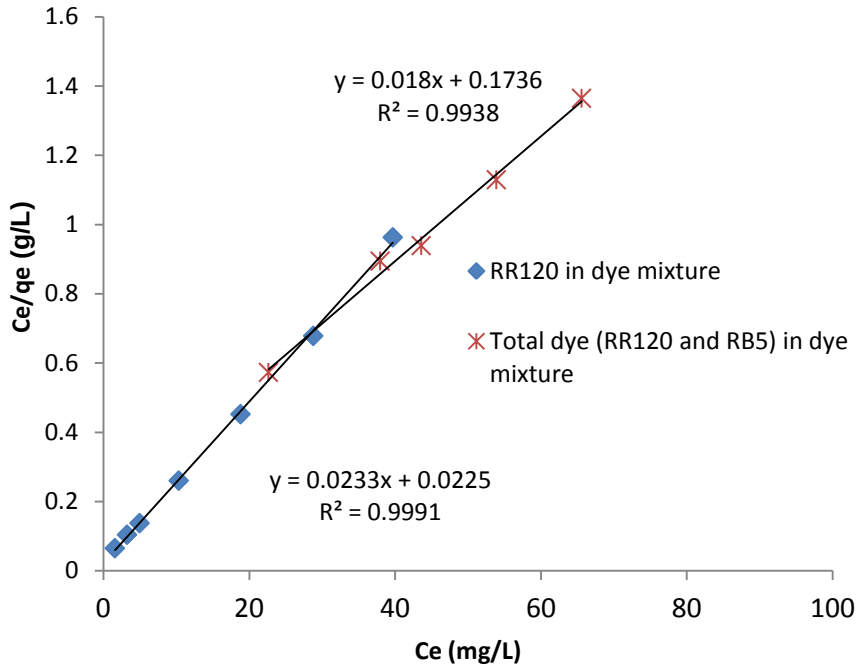

Figure 6.6 Adsorption isotherms of RR120 and total dye (RR120 and RB5) in dye mixture

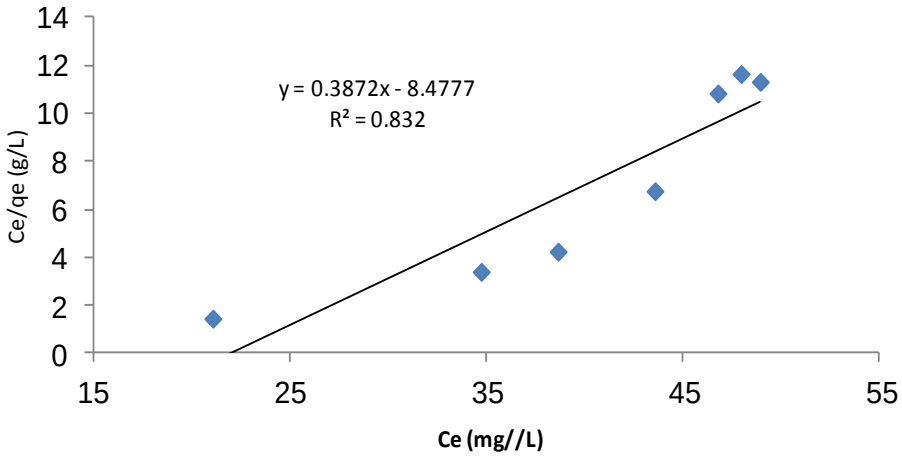

Figure 6.7 Langmuir adsorption isotherm of RB5 dye in dye mixture showing a poor fit

Table 6.3 Adsorption equilibrium data of dye mixture.

Sr. No.	TiO_2	C_o(RR120)	C_o(RB5)	C_e(RR120)	q_e(RR120)	C_e(RB5)	q_e(RB5)
1	0.0625	50	50	39.69	41.22	48.91	4.32
2	0.125	50	50	28.78	42.43	47.94	4.11
3	0.1875	50	50	18.80	41.58	46.76	4.31
4	0.25	50	50	10.33	39.66	43.56	6.43
5	0.3125	50	50	4.95	36.03	38.62	9.09
6	0.375	50	50	3.2	31.16	34.71	10.19
7	0.5	50	50	1.5	24.21	21.05	14.47

The non-applicability of Freundlich isotherm suggests that the adsorption of RB5 does not have wide variation in heat of adsorption. Freundlich isotherm is expected to be applicable in case adsorption sites are distributed exponentially with respect to heat of adsorption.

6.4 Photocatalytic decolorization kinetics

6.4.1 Photocatalytic decolorization kinetics of a dyes mixture

Equal amounts of RR120 and RB5 in equal concentration of 100 mg/L were mixed for dye mixture studies. This makes total concentration to 100 mg/L for dye but each dye concentration is reduced to 50 mg/L. Photocatalytic decolorization studies were performed on dye mixture with various amounts of catalyst.

Fig. 6.8 shows the decolorization characteristics of individual dyes in dye mixture with 0.25 g/L as catalyst load. When the kinetics of the photocatalytic decolorization reactions were studied, it was found that the correlation between ln (C/C_0) and the irradiation time was linear. This is a typical first-order reaction plot. The slopes of the lines give the apparent rate constant (k_{app}). The kinetic expression can be presented as follows:

$$\ln\left(C/C_0\right) = k_{app}t \qquad (5)$$

The data fits well with pseudo first order kinetics. Overall decolorization behavior taking both dyes into consideration is also found to be pseudo first order.

Fig. 6.9 shows decolorization of RR120 and RB5 in a dye mix with.1.5 g/L as catalyst load. It can be observed here that RR120 dye is getting desorbed during photocatalytic exposure with higher amount of catalyst. Desorption of red color from catalyst surface can be also observed with naked eye (Fig. 6.10). Thus pseudo first order nature of RR120 decolorization kinetics is lost. Desorption

of RR120 during photocatalysis suggests a weak attraction between catalyst surface and dye. Table 6.4 shows the decolorization rate constants for individual dye components in dye mixture as well as for combined dye in dye mixture.

It has been observed that pseudo first order decolorization kinetics of RR120 is limited to catalyst load up to 0.25 g/L only. However, pseudo first order decolorization kinetics of RB5 remains retained for higher catalyst loads. For 0.25 g/L catalyst load k_{app} value of RR120 is 2.18 times more than that of RB5. It may be noted that the q_{max} value of RR120 (49 mg/g) is roughly twice to that of RB5 (25 mg/g) in case of single dye solution. This suggests that dye which has higher adsorption has also higher decolorization rate constant. Also the ratio of decolorization rate constant is proportion the ratio of their q_{max} values. Christopher et al. also observed in their study on single dye solution that photocalytic effect was increasing with increasing adsorption [133]. Our studies suggest that the observation is also valid in case of dye mixture.

Table 6.4 Pseudo first order decolorization rate constants for individual dyes RR120, RB5 and for total dye content (RR120 +RB5) in mix dye

Catalyst load (g/L)	**k_{app} for RR120 (per min)**	**k_{app} for RB5 (per min)**	**k_{app} (RR120+RB5) (per min)**
0.25	0.0109	0.005	0.0074
0.5	*	0.0103	0.0105
0.75	*	0.0164	0.0195
1.0	*	0.0251	0.0199
1.25	*	0.0314	*
1.5	*	0.0401	*
2.0	*	0.0503	*

*decolorization rate constant determination could not be done due to excessive desorption from catalyst surface during photocatalysis.

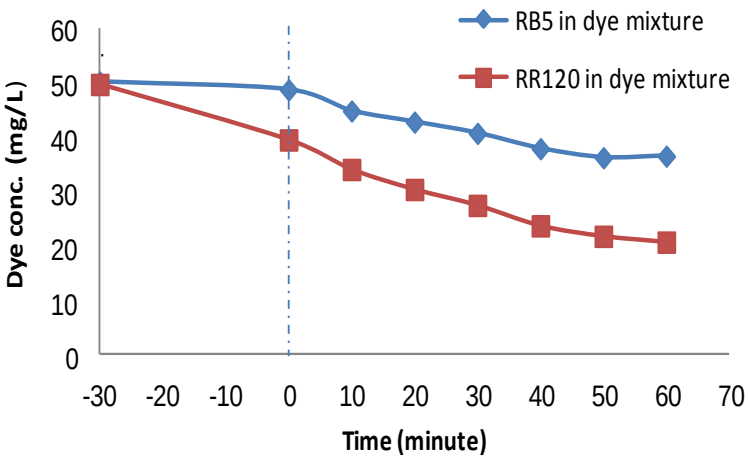

Figure 6.8 Decolorization characteristics of RR120 and RB5 dyes in the mixture with 0.25 g/L as catalyst load

(The time less than zero indicate the time for adsorption equilibrium without UV exposure)

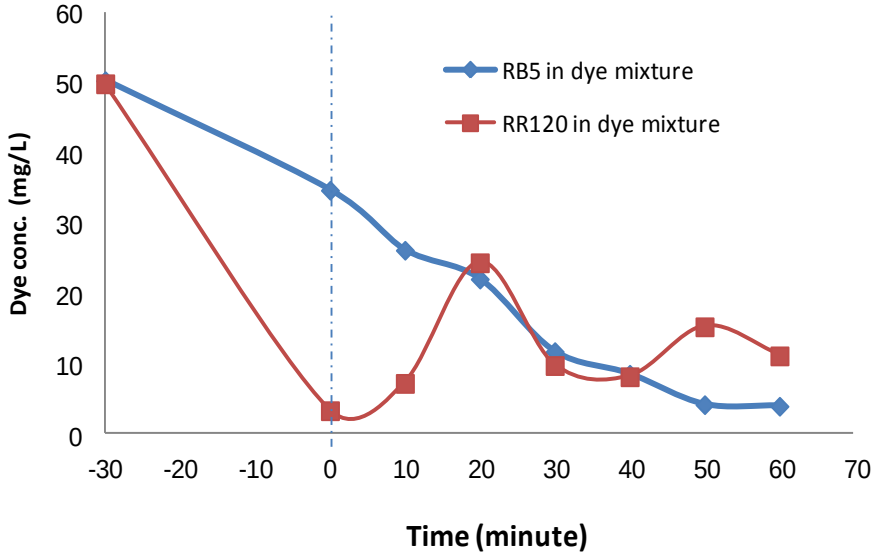

Figure 6.9 Decolorization characteristics of RR120 and RB5 dyes in dye mixture with 1.5 g/L as catalyst load

(The time less than zero indicate the time for adsorption equilibrium without UV exposure)

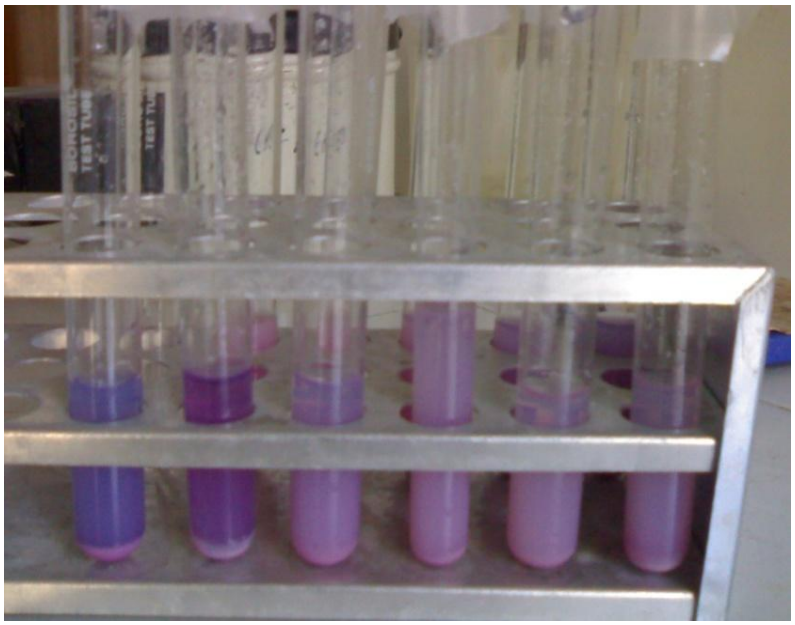

Figure 6.10 Desorption of RR120 Red color during photocatalysis. The figure shows sample withdrawn during photocatalysis from left to right

6.4.2 Photocatalytic decolorization kinetics of a mixture of dyes vs. single dye solutions

In order to compare decolorization characteristics of single dye solution to the mixture of dyes, experiments were performed with 100 mg/L of both RB5 and RR120. The catalyst load was kept at 0.25g/L. Decolorization rate constant of RR120 and RB5 were found to be 0.0083 and 0.0064 per minute in case of single dye solution while for dye mixture the decolorization rate constant was 0.0074 per minute (Table 6.4). The decolorization rate constant for dye mixture is found to be exactly the average of decolorization rate constants for single dyes. Thus, we may conclude that photocatalytic degradation efficiency of dyes is not affected due to presence of multiple dyes in dye solution. However it may be noted in dye mixture degradation rate of RB5 is suppressed, while RR120 shows higher degradation rates. This can be explained again based upon the amount of adsorption in both cases.

6.5 Simultaneous TOC and color removal of mixed dye solution

The dye solution made of dye mixture was studied for decolorization and TOC content simultaneously. Initial pH was fixed at 3. Total dye concentration was kept at 100 mg/L with each dye contributing 50 mg/L. Area by volume ratio was kept 0.10054 cm^2/mL. Fig. 6.11 shows the regime of change in TOC and dye concentration simultaneously with time due to adsorption and during photocatalytic exposure. As observed in case of single dye solutions the final decreasing trend in TOC starts only after complete decolorization. Variations in TOC during photocatalysis may occur by adsorption, desorption, degradation of intermediates, and complete mineralization

occurring simultaneously. The decline in TOC in this case is continuous in contrast to RR120 single dye solution (Fig. 5.11). This implies that the mineralization in case of dye mixture is better than single dye solution. The possible reason may be the formation of such intermediate, which might be reacting with each other.

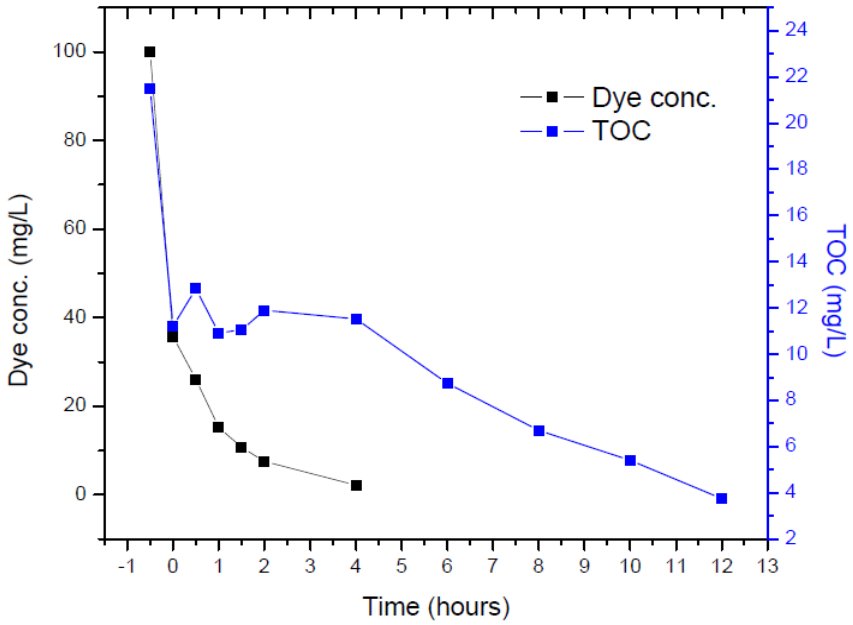

Figure 6.11 Variation in dye concentration and TOC due to adsorption and during photocatalytic exposure at pH= 3, Dye conc. = 100 mg/L (50mg/L of RB5 and 50 mg/L of RR120), Area to volume ratio of reactor = 0.10054 cm^2/mL.

6.6 Effect of salts on photocatalytic degradation of dyes

In textile sector dyeing salts like NaCl and Na_2SO_4 are used. These salts are used for exhaustion of dye on to the fabric. The ionic force is exerted by these salts in dye solution. The absence of salts results in poor exhaustion of dyes and poor color of fabric. Keeping this in mind, the effect of salts at various concentrations was studied on degradation of dye at natural pH values. Figure 6.12 shows the effect of NaCl and Na_2SO_4 at natural pH on dye mixture degradation. The results show final percentage degradation of dye mixture at the end of one hour photocatalytic treatment.

Addition of Cl^- had a detrimental effect on the degradation of the dyes. This can be explained by competitive adsorption and by the positive holes and hydroxyl radical scavenging properties of chloride ions. The chloride radicals can also block the active sites on catalyst surface.

$$Cl^- + h^+_{vVB} \rightarrow Cl^{\cdot} \qquad (6)$$

$$Cl + Cl^- \rightarrow Cl_2^- \qquad (7)$$

$$Cl^- + OH \rightarrow Cl^{\cdot} + OH^- \qquad (8)$$

The inhibiting effect of NaCl on photocatalytic degradation has been reported earlier [134, 135] also.

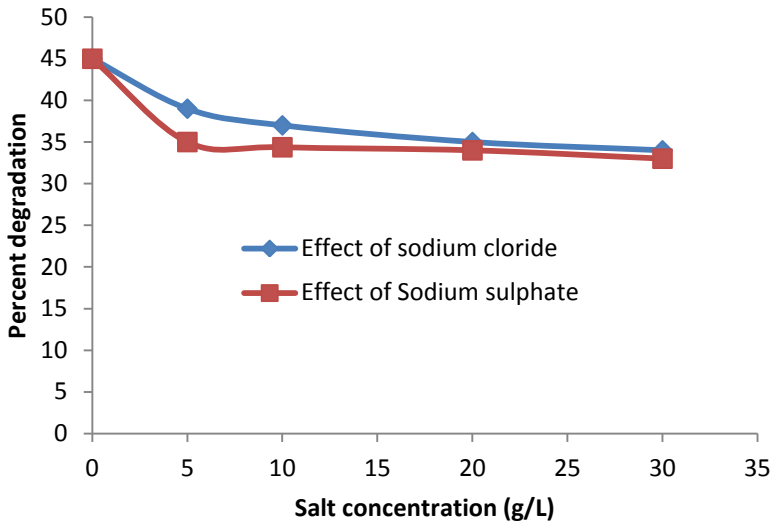

Figure 6.12 Effect of the presence of salts, sodium chloride and $Na_2SO_4.7H_2O$ on percentage degradation at natural pH

Similarly $Na_2SO_4.7H_2O$ shows reduction in percent degradation. Following reactions result in reduction of photocatalytic degradation.

$$SO_4^{2-} + h^+ \rightarrow SO_4^{\cdot -} \qquad (9)$$

$$SO_4^{2-} + {}^{\cdot}OH \rightarrow SO_4^{\cdot -} + OH^- \qquad (10)$$

SO_4^{2-} ions react with holes to form $SO_4^{\cdot -}$ ions which are less reactive. These ions further quench hydroxyl ions. This reduces the degradation due to photocatalysis [136].

Thus photocatalytic degradation is affected due to the presence of salts.

6.7 Catalyst deactivation and reusability studies

The catalyst deactivation was studied based upon the reusability of catalyst after recovery. The catalyst was recovered after centrifugation. The recovered catalyst was washed with distilled water. The washed catalyst was heated to dryness at 150 ^{0}C for 6 hours. The effect of catalyst reuse on percentage decolorization resulting after 60 minute of photocatalytic action is shown by bar graph (Figure 6.13).

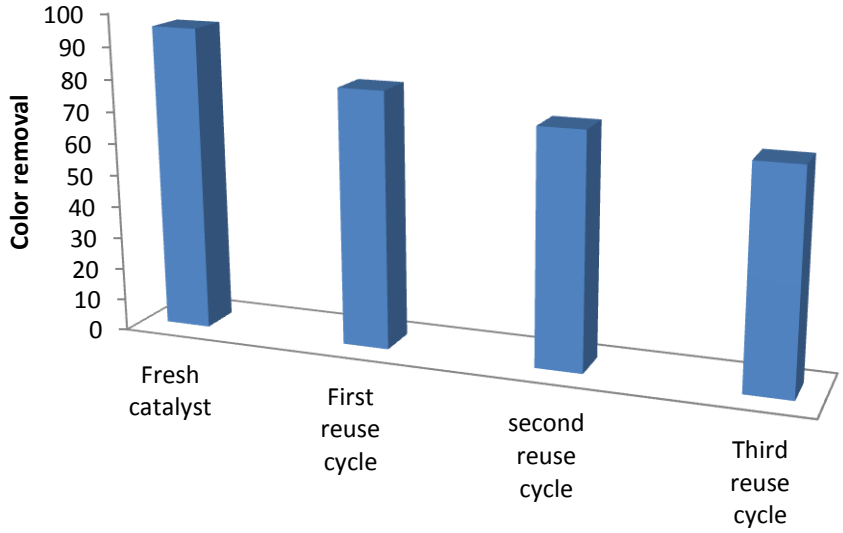

Figure 6.13 Percentage decolorization of dye mixture during reuse cycles

Additionally the catalyst was recovered by making separate runs to determine the amount of carbon content on recovered catalyst. The catalyst recovery for this purpose was done in a manner similar to reuse purpose. The recovered catalyst was grounded using pestle mortar (made of Granite stone). The catalyst samples thus obtained were analyzed for presence of carbon content. This was done by using TOC-SSM module. The value of percent carbon on TiO_2 is shown in Table 6.5. The recovered catalyst shows increasingly larger amount of carbon which is irreversibly adsorbed upon catalyst surface. This carbon is expected to origin from various dye degradation intermediates. The amount of carbon already deposited on catalyst surface can hinder the subsequent photocatalytic degradation. Thus catalyst deactivation may be supposed to result from deactivation resulting from the dye degradation intermediates irreversibly adsorbed upon catalyst surface.

Table 6.5 Amount of carbon content on recovered and washed catalyst

Sr. No.	Description	Amount of carbon on recovered and washed TiO_2 (weight percent)
1	At the end of first use	0.384
2	At the end of 1^{st} reuse cycle	0.410
3	At the end of 2^{nd} reuse cycle	0.449
4	At the end of 3^{rd} reuse cycle	0.477

6.8 Conclusions

Present study was about the adsorption and subsequent photoctalytic decolorization kinetics of reactive RR120 and RB5 in single dye solution as well as in their mixture. Additionally,

quantification of single dyes in solution has been made by a new method. The conclusions drawn are as below.

A novel methodology to quantify the dyes in the dye mixture solution has been used for the first time. The method is based upon the multiple regressions. Statistical results have been used to verify the calibration. It has been observed that this method is a better choice when we study adsorption and photo-degradation. This is because dye concentration ratio varies due to competitive adsorption and preferential photodegradation.

Adsorption studies of single dye solutions show that both dyes RR120 and RB5 show adherence to Langmuir adsorption isotherms, that maximum specific adsorption of RR 120 and RB5 is 50 mg/g and 25 mg/g respectively. Adsorption studies of dye mixture show that RR120 is preferentially adsorbed than RB5, that both RR120 and total dye content follows Langmuir adsorption isotherm, that adsorption characteristics of RB5 are strongly altered.

Ratio of decolorization rate constants of dyes in case of single dye solution is found to be in proportion to their maximum specific adsorption values. Photocatalytic degradation studies of dye mixture suggest that RR120 degrades at higher rate for low catalyst load. However, with increasing catalyst load desorption of RR120 causes loss of pseudo first order decolorization characteristics. Release of dye due to desorption presents a technical problem in optimizing catalyst load in case of mix dye effluent. Primarily, it appears that photocatalytic degradation efficiency of dyes is not affected due to presence of multiple anionic dyes in dye solution.

Mineralization studies show that adsorption results larger percent change in TOC as compared due to change in color. This can be attributed to impurities component in dyes. Mineralization studies also reveal that mere decolorization at experimental conditions does not represent mineralization process.

CHAPTER – 7

CONCLUSION AND RECOMMENDATIONS

Conclusions and Recommendations

7.1 Conclusions

Present study is about photocatalytic decolorization and mineralization of three dyes Reactive Black 5 (RB5), and Reactive Red 120 (RR120). Further photocatalytic studies of dye mixture and simulated effluent are made.

7.1.1 Conclusions related to RB5 degradation

The photocatalytic decolorization and mineralization of Reactive Black 5 (RB5) dye in presence of TiO_2 Degussa P25 has been studied using artificial light radiation (>290 nm) in a shallow pond slurry reactor. From this experimental study, several conclusions can be drawn:

- The reactive black 5 dye can be degraded by TiO_2-P25 assisted photocatalysis in aqueous dispersion under irradiation by UV light.
- The dye shows good adsorption at low pH due to catalyst surface charge interactions with dye. The adsorption data fits well with Langmuir isotherm.
- The optimum catalyst load is 1.5 g/L at pH 3 and lower dye concentration improves decolorization rate.
- Dye decolorization follows modified Langmuir-Hinshelwood kinetics between 20 mg/L and 100 mg/L dye concentration.
- Rate constant of decolorization varies linearly with UV intensity between 4.6 W/m^2 and 14.7 $W/m^{2.}$
- Rate constant of decolorization also varies linearly with area to volume ratio between 0.1 cm^2/mL and 0.5 cm^2/mL.
- The mineralization of the dye was investigated by total organic carbon (TOC) measurements that showed 70% mineralization of 100 mg/L dye at 12 h.

7.1.2 Conclusions related to RR120 degradation

- The results presented show that Reactive Red 120, an anionic diazo dye can be successfully decolorized under UV radiation.
- The dye shows good adsorption at low pH due to catalyst surface charge interactions with dye.
- The adsorption data fits well with Langmuir isotherm. It is observed that adsorption is prerequisite for efficient photocatalytic degradation.

- Both adsorption and degradation are highest at pH 3. Dye decolorization appears to be due to direct reduction mechanism.
- The maximum adsorption at pH 3 was found to be 49 mg/g.
- The optimum catalyst load at pH 3 is 0.9 g/L and lower dye concentration improves decolorization rate.
- Rate constant of decolorization varies linearly with area to volume ratio (A/V) of reactor between 0.1675 cm^2/mL and 0.5027 cm^2/mL. However, there is sharp decrease in decolorization rate constant for A/V value below 0.1675 cm^2/mL. So, A/V ratio should be kept above 0.1675 cm^2/mL.
- Reduction in TOC was very slow and complete mineralization was not achieved even after 5 hours at pH 3 (under the condition: A/V ratio of 0.10054 cm^2/mL, and 14.7 W/m^2 UV intensity). Impurities present in dye also get adsorbed over catalyst surface.
- Slow reduction in TOC may also be due to formation of stable intermediates. Slow reduction in TOC implies that toxicity of effluent may persist even after complete decolorization.

7.1.3 Conclusions related to simulated effluent degradation

Present study was about the adsorption and subsequent photoctalytic decolorization kinetics of reactive RR120 and RB5 in single dye solution as well as in their mixture. Additionally quantification of single dyes in solution has been made by a new method. The conclusions drawn are as below.

- A novel methodology to quantify the dyes in the dye mixture solution has been used for the first time. The method is based upon the multiple regression. Statistical results have been used to verify the calibration. It has been observed that this method is better choice when we study adsorption and photo-degradation. This is because dye concentration ratio varies due to competitive adsorption and preferential photodegaradtion.
- Adsorption studies of single dye solutions show that both dyes RR120 and RB5 show adherence to Langmuir adsorption isotherms, that maximum specific adsorption of RR 120 and RB5 is 50 mg/g and 25 mg/g respectively.
- Adsorption studies of dye mixture show that RR120 is preferentially adsorbed than RB5, that both RR120 and total dye content follows Langmuir adsorption isotherm, that adsorption characteristics of RB5 are strongly altered.
- Ratio of decolorization rate constants of dyes in case of single dye solution is found to be in proportion to their maximum specific adsorption values. Photocatalytic degradation studies

of dye mixture suggest that RR120 degrades at higher rate for low catalyst load. However, with increasing catalyst load the desorption of RR120 causes loss of pseudo first order decolorization characteristics.

- Release of dye due to desorption presents a technical problem in optimizing catalyst load in case of mix dye effluent.
- Primarily, it appears that photocatalytic degradation efficiency of dyes is not affected due to presence of multiple anionic dyes in dye solution.

7.1.4 Generalized conclusions about reactive azo dyes degradation

Based upon photocatalytic degradation studies following generalized conclusion were drawn.

- That photocatalysis is strongly influenced by adsorption.
- The mineralization rates may be too slow under mild solar radiations in slurry type reactors.
- The charge status and pH play significant role in determining adsorption of dyes. This factor may be explored and exploited for other type of dyes also.
- The impurities component (non-dye content) of dye account for significant level of pollution.
- In case of dye mixture, one dye may get preferentially adsorbed over catalyst surface.
- In case of dye mixture, one dye may get preferentially degraded over catalyst surface.
- The extent of decolorization is not an indication of extent of mineralization.
- That it may become difficult to optimize catalyst load in case of dye mixture.

7.2 Recommendations

- Since it has been observed that the initial decolorization does not result any mineralization. So the toxicity of effluent at various stages of treatment needs to be evaluated.
- BOD/COD ratio after initial decolorization needs to be determined. A higher value of BOD/COD ratio may result. This may result in usability of conventional biological treatment methods.
- Since dyes have low purity and significant level of pollution is caused by non dye content, so dye purity is an important parameter. Keeping in view the environmental considerations, there should be some effort to improve the quality of dyes.
- The effect of mixing various streams to partly treated effluent by photocatalytic process may be explored for degradability of dyes by conventional biological processes.
- The removal of pollutant from dye effluent by adsorption on catalyst may be explored. Desorption process may take place after changing the pH of recovered catalyst in a separate

container. The small amount of concentrated effluent generated may be done by other means.

- Photocatalytic decolorizarion and degradation processes are strongly influenced by adsorption. Also, it is well-known that adsorption is influenced by temperature in case of dyes. The different extent of adsorption may also result in different amount of residual dye concentration. Screening effect under conditions will be different. So optimum catalyst load may also differ. The effect of temperature on adsorption of dyes needs to be determined.

List of Publications

The list of papers published in journal/conferences is given below:

In journals

[1] S. K. Sharma, H. Bhunia, P. K. Bajpai, Photocatalytic Decolorization Kinetics and Mineralization of Reactive Black 5 Aqueous Solution by UV/TiO_2 Nanoparticles. *CLEAN - Soil, Air, Water.* 40, 2012, 1290-1296. (DOI: 10.1002/clen.201100557)

[2] S. K. Sharma, H. Bhunia, P. K. Bajpai, Photocatalytic Decolorization Kinetics and Adsorption Isotherms of a Mixture of Two Anionic Azo Dyes: Reactive Red 120 and Reactive Black 5. *Desal. Wat. Treat. 44,* 2012, 261-268. (DOI: 10/5004/dwt.2012.3107)

[3] S. K. Sharma, H. Bhunia, P. K. Bajpai, TiO_2-Assisted Photocatalytic Degradation of Diazo Dye Reactive Red 120: Decolorization Kinetics and Mineralization Investigations. *Journal of Advance Oxidation Processes,* 2012, *Submitted.*

[4] S. K. Sharma, H. Bhunia, P. K. Bajpai, Photocatalytic Decolorization Kinetics of a Triazo Dye Direct Blue 71 Aqueous Solution by UV-A/TiO_2 Nanoparticles, *Desal. Wat. Treat.* 2012, Submitted.

In conferences

[1] Sandeep K. Sharma, Haripada Bhunia, Photocatalytic degradation of reactive black 5 dye., *Advances in Chemical Engineering*, 2009; Macmillan Publishers India Ltd.: Thapar University Patiala, 2009; 152-156.

[2] Sandeep K. Sharma, Haripada Bhunia, Photocatalytic decolorization of a mixture of two anionic dyes: Rective red 120 and reactive black 5., *Advances in Chemical Engineering*, Macmillan Publisher India Ltd.: Thapar University Patiala, 2011; 288-294.

[3] Sandeep K. Sharma, Haripada Bhunia, Application of response surface methodology and experimental design for photocatalytic degradation of textile dyestuff with UV/TiO_2 process. In *Eleventh Punjab Science Congress*, Thapar University Patiala: Patiala, 2008; 52.

References

[1] The United Nations World Water Development Report 3: Water in a Changing World, in United Nations Educational, Scientific and Cultural Organization, 2009.

[2] Ü.D. Buch, International Textile Auxiliaries Buyers´ Guide 2008/09, in Melliand Textilberichte, Frankfurt, Germany, 2008.

[3] Integrated Pollution Prevention and Control (IPPC)**:** Reference Document on Best Available Techniques for the Textiles Industry, in European commission: European IPPC Bureau (EIPPCB), 2003.

[4] A. Al-Kdasi, A. Idris, K. Saed, C.T. Guan, Treatment of Textile Wastewater by Advance Oxidation Processes-A Review, Global nest:The international Journal, 4 (2004) 220-230.

[5] A.P. Toor, Photocatalytic degradation of chlorinated organic compounds in industrial wastewater, in Department of chemical engineering, Thapar Institute of Engineering and Technology, Deemed University, Patiala, 2007.

[6] H. Zollinger, Color Chemistry: Syntheses, Properties, and Applications of Organic Dyes and Pigments, in Wiley-VCH, Weinheim, 2004.

[7] D.S. Brookstein, Factors Associated with Textile Pattern Dermatitis Caused by Contact Allergy to Dyes, Finishes, Foams, and Preservatives, Dermatologic Clinics, 27 (2009) 309-322.

[8] K.L. Hatch, H.I. Maibach, Textile dye dermatitis: A review, Journal of the American Academy of Dermatology, 12 (1985) 1079-1092.

[9] H.S. Rai, Treatment of basic dye bath effluent in anaerobic reactor, in: Department of Chemical Engineering, Thapar University, Patiala, 2006.

[10] S. Ozkurt, B.A. Kargi, M. Kavas, F. Evyapan, G.k. Kiter, S. Baser, Respiratory Symptoms and Pulmonary Functions of Workers Employed in Turkish Textile Dyeing Factories, International Journal of Environmental Research and Public Health, 9 (2012) 1068-1076.

[11] Y. Kim, J. Park, Y. Shin, Dye-manufacturing workers and bladder cancer in South Korea, Archives of Toxicology, 81 (2007) 381-384.

[12] T. Robinson, G. McMullan, R. Marchant, P. Nigam, Remediation of Dyes in Textile Effluent: A Critical Review on Current Treatment Technologies with a Proposed Alternative, Bioresource Technology, 77 (2001) 247-255.

[13] C.E.G. Ilha, A.J.M.G. dos Santos, J.R. SouzaDe, Degradation of Monoazo Pigments Red 53:1 and Red 48:2 by Fenton, Photo-Fenton and UV/Peroxide Reactions, Clean- Soil, Air, Water, 37 (2009) 799-805.

[14] A.R. Khataee, M. Zarei, A.R. Khataee, Electrochemical Treatment of Dye Solution by Oxalate Catalyzed Photoelectro-Fenton Process Using a Carbon Nanotube-PTFE Cathode: Optimization by Central Composite Design, Clean- Soil, Air, Water, 39 (2011) 482-490.

[15] Y. Ku, L.-C. Wang, C.-M. Ma, Y.-C. Chou, Photocatalytic Oxidation of Reactive Red 22 in Aqueous Solution Using $La_2Ti_2O_7$ Photocatalyst, Water, Air & Soil Pollution, 215

(2011) 97-103.

[16] Y.-L. Song, J.-T. Li, B. Bai, TiO_2-Assisted Photodegradation of Direct Blue 78 in Aqueous Solution in Sunlight, Water, Air & Soil Pollution, 213 (2011) 311-317.

[17] P. Chen, X. Zhang, Fabrication of Pt/TiO_2 Nanocomposites in Alginate and Their Applications to the Degradation of Phenol and Methylene Blue in Aqueous Solutions, Clean- Soil, Air, Water, 36 (2008) 507-511.

[18] A.F. Martins, F. Mayer, E.C. Confortin, C.d.S. Frank, A Study of Photocatalytic Processes Involving the Degradation of the Organic Load and Amoxicillin in Hospital Wastewater, Clean- Soil, Air, Water, 37 (2009) 365-371.

[19] N. Sridewi, L.-T. Tan, K. Sudesh, Solar Photocatalytic Decolorization and Detoxification of Industrial Batik Dye Wastewater Using P(3HB)-TiO_2 Nanocomposite Films, Clean-Soil, Air, Water, 39 (2011) 265-273.

[20] R. Andreozzi, V. Caprio, A. Insola, R. Marotta, Advanced Oxidation Processes (AOP) for Water Purification and Recovery, Catalysis Today, 53 (1999) 51-59.

[21] S. Baig, Liechti, Ozone Treatment for Biorefractory COD removal, Water Science and Technology, 43 (2001) 197-204.

[22] H. Zhou, D.W. Smitch, Advanced Technologies in Water and Wastewater Treatment, Journal of Environment Engineering Sciene, (2002) 247-264.

[23] S. Kaur, V. Singh, Visible Light Induced Sonophotocatalytic Degradation of Reactive Red Dye 198 using Dye Sensitized TiO_2, Ultrasonics Sonochemistry, 14 (2007) 531-537.

[24] M. Muruganandham, M. Swaminathan, Photocatalytic Decolorisation and Degradation of Reactive Orange 4 by TiO_2-UV Process, Dyes and Pigments, 68 (2006) 133-142.

[25] M. Muruganandham, M. Swaminathan, Solar Photocatalytic Degradation of a Reactive Azo Dye in TiO_2-Suspension, Solar Energy Materials and Solar Cells, 81 (2004) 439-457.

[26] W.Z. Tang, A. Huren, UV/TiO_2 Photocatalytic Oxidation of Commercial Dyes in Aqueous Solutions, Chemosphere, 31 (1995) 4157-4170.

[27] T. Velegraki, I. Poulios, M. Charalabaki, N. Kalogerakis, P. Samaras, D. Mantzavinos, Photocatalytic and Sonolytic Oxidation of Acid Orange 7 in Aqueous Solution, Applied Catalysis B-Environment, 62 (2006) 159-168.

[28] S. Kaur, V. Singh, TiO_2 Mediated Photocatalytic Degradation Studies of Reactive Red 198 by UV Irradiation, Journal of Hazardous Materials, 141 (2007) 230-236.

[29] K. Ntampegliotis, A. Riga, V. Karayannis, V. Bontozoglou, G. Papapolymerou, Decolorization Kinetics of Procion H-exl dyes from Textile Dyeing using Fenton-like Reactions, Journal of Hazardous Materials, 136 (2006) 75-84.

[30] P. Chowdhury, J. Moreira, H. Gomaa, A.K. Ray, Visible-Solar-Light-Driven Photocatalytic Degradation of Phenol with Dye-Sensitized TiO_2: Parametric and Kinetic Study, Industrial & Engineering Chemistry Research, 51 (2012) 4523-4532.

[31] A.P. Toor, A. Verma, C.K. Jotshi, P.K. Bajpai, V. Singh, Photocatalytic Degradation of

3,4-dichlorophenol using TiO_2 in a Shallow Pond Slurry Reactor, Indian Journal of Chemical Technology, 12 (2005) 75-81.

[32] A.P. Toor, V. Singh, C.K. Jotshi, P.K. Bajpai, A. Verma, Treatment of Bleaching Effluent from the Pulp and Paper Industry by Photocatalytic Oxidation, Tappi Journal, 6 (2007) 9-13.

[33] J.M. Herrmann, Heterogeneous Photocatalysis: State of the Art and Present Applications, Topics in Catalysis, 34 (2005) 49-65.

[34] O.K. Dalrymple, E. Stefanakos, M.A. Trotz, D.Y. Goswami, A Review of the Mechanisms and Modeling of Photocatalytic Disinfection, Applied Catalysis B: Environmental, 98 (2010) 27-38.

[35] V.A. Sakkas, M.A. Islam, C. Stalikas, T.A. Albanis, Photocatalytic Degradation using Design of Experiments: A Review and Example of the Congo Red Degradation, Journal of Hazardous Materials, 175 (2010) 33-44.

[36] M.R. Hoffmann, S.T. Martin, W.Y. Choi, D.W. Bahnemann, Environmental Applications of Semiconductor Photocatalysis, Chemical Reviews, 95 (1995) 69-96.

[37] D.S. Bhatkhande, V.G. Pangarkar, A. Beenackers, Photocatalytic Degradation for Environmental Applications - A Review, Journal of Chemical Technology and Biotechnology, 77 (2002) 102-116.

[38] I. Arslan-Alaton, A Review of the Effects of Dye-Assisting Chemicals on Advanced Oxidation of Reactive Dyes in Wastewater, Coloration Technology, 119 (2003) 345-353.

[39] J. Zhao, X.D. Yang, Photocatalytic Oxidation for Indoor Air Purification: A Literature Review, Building and Environment, 38 (2003) 645-654.

[40] I.K. Konstantinou, T.A. Albanis, TiO_2-Assisted Photocatalytic Degradation of Azo Dyes in Aqueous Solution: Kinetic and Mechanistic Investigations: A Review, Applied Catalysis B: Environmental, 49 (2004) 1-14.

[41] H. Gerischer, F. Willig, Reaction of Excited Dye Molecules at Electrodes, in Physical and Chemical Applications of Dyestuffs, Springer Berlin / Heidelberg, 1976, 31-84.

[42] P.V. Kamat, M.A. Fox, Photosensitization of TiO_2 Colloids by Erythrosin B in Acetonitrile, Chemical Physics Letters, 102 (1983) 379-384.

[43] P.V. Kamat, B. Patrick, Photophysics and Photochemistry of Quantized Zinc Oxide Colloids, Journal of Physical Chemistry, 96 (1992) 6829-6834.

[44] K. Soutsas, V. Karayannis, I. Poulios, A. Riga, K. Ntampegliotis, X. Spiliotis, G. Papapolymerou, Decolorization and Degradation of Reactive Azo Dyes via Heterogeneous Photocatalytic Processes, Desalination, 250 (2010) 345-350.

[45] A. Vohra, D.Y. Goswami, D.A. Deshpande, S.S. Block, Enhanced Photocatalytic Disinfection of Indoor Air, Applied Catalysis B: Environmental, 64 (2006) 57-65.

[46] A. Katsoni, H.T. Gomes, L.M. Pastrana-Martinez, J.L. Faria, J.L. Figueiredo, D. Mantzavinos, A.M.T. Silva, Degradation of Trinitrophenol by Sequential Catalytic Wet

Air Oxidation And Solar TiO_2 Photocatalysis, Chemical Engineering Journal, 172 (2011) 634-640.

[47] R. de Richter, S. Caillol, Fighting Global Warming: The Potential of Photocatalysis Against CO_2, CH_4, N_2O, CFCs, Tropospheric O_3, BC and Other Major Contributors to Climate Change, Journal of Photochemistry and Photobiology C: Photochemistry Reviews, 12 (2011) 1-19.

[48] Y. Paz, Application of TiO_2 Photocatalysis for Air Treatment: Patents' overview, Applied Catalysis B: Environmental, 99 (2010) 448-460.

[49] V. Augugliaro, C. Baiocchi, A.B. Prevot, E. Garcia-Lopez, V. Loddo, S. Malato, G. Marci, L. Palmisano, M. Pazzi, E. Pramauro, Azo-Dyes Photocatalytic Degradation in Aqueous Suspension of TiO_2 Under Solar Irradiation, Chemosphere, 49 (2002) 1223-1230.

[50] A. Chowdhury, A. Kudo, T. Fujita, M.W. Chen, T. Adschiri, Nano-Twinned Structure and Photocatalytic Properties under Visible Light for Undoped Nano-Titania Synthesised by Hydrothermal Reaction in Water-Ethanol Mixture, Journal of Supercritical Fluids, 58 (2011) 136-141.

[51] J. Du, W. Chen, C. Zhang, Y. Liu, C. Zhao, Y. Dai, Hydrothermal Synthesis of Porous TiO_2 Microspheres and Their Photocatalytic Degradation of Gaseous Benzene, Chemical Engineering Journal, 170 (2011) 53-58.

[52] C.-Y. Chen, M.-C. Cheng, A.-H. Chen, Photocatalytic Decolorization of Remazol Black 5 and Remazol Brilliant Orange 3R by Mesoporous TiO_2, Journal of Environmental Management, 102 (2012) 125-133.

[53] S. Sitthisang, S. Komarneni, J. Tantirungrotechai, Y. D. Noh, H. Li, S. Yin, T. Sato, H. Katsuki, Microwave-Hydrothermal Synthesis of Extremely High Specific Surface Area Anatase for Decomposing NOx, Ceramics International, 38 (2012) 6099-6105.

[54] W. Mekprasart, W. Pecharapa, Synthesis and Characterization of Nitrogen-Doped TiO_2 and its Photocatalytic Activity Enhancement Under Visible Light, Energy Procedia, 9 (2011) 509-514.

[55] Y. Liu, X. Chen, J. Li, C. Burda, Photocatalytic Degradation of Azo Dyes by Nitrogen-Doped TiO_2 Nanocatalysts, Chemosphere, 61 (2005) 11-18.

[56] M.S. Nahar, K. Hasegawa, S. Kagaya, Photocatalytic Degradation of Phenol by Visible Light-Responsive Iron-Doped TiO_2 and Spontaneous Sedimentation of the TiO_2 particles, Chemosphere, 65 (2006) 1976-1982.

[57] G. Zhanqi, Y. Shaogui, T. Na, S. Cheng, Microwave Assisted Rapid and Complete Degradation of Atrazine Using TiO_2 Nanotube Photocatalyst Suspensions, Journal of Hazardous Materials, 145 (2007) 424-430.

[58] S. Luo, Y. Xiao, L. Yang, C. Liu, F. Su, Y. Li, Q. Cai, G. Zeng, Simultaneous Detoxification of Hexavalent Chromium and Acid Orange 7 by a Novel Au/TiO_2 Heterojunction Composite Nanotube Arrays, Separation and Purification Technology, 79 (2011) 85-91.

[59] Y. Liu, X. Zhang, R. Liu, R. Yang, C. Liu, Q. Cai, Fabrication and Photocatalytic Activity of High-Efficiency Visible-Light-Responsive Photocatalyst ZnTe/TiO_2 Nanotube Arrays, Journal of Solid State Chemistry, 184 (2011) 684-689.

[60] X. Li, X. Zou, Z. Qu, Q. Zhao, L. Wang, Photocatalytic Degradation of Gaseous Toluene Over Ag-Doping TiO_2 Nanotube Powder Prepared by Anodization Coupled with Impregnation Method, Chemosphere, 83 (2011) 674-679.

[61] L.H. Huang, C. Sun, Y.L. Liu, Pt/N-Codoped TiO_2 Nanotubes and its Photocatalytic Activity Under Visible Light, Applied Surface Science, 253 (2007) 7029-7035.

[62] A.F. Martins, M.L. Wilde, C.D. Silveira, Photocatalytic Degradation of Brilliant Red Dye and Textile Wastewater, Journal of Environmental Science and Health, Part A-Toxic/Hazardous substances and Environmental Engineering, 41 (2006) 675 - 685.

[63] U.G. Akpan, B.H. Hameed, Parameters Affecting the Photocatalytic Degradation of Dyes Using TiO_2-Based Photocatalysts: A Review, Journal of Hazardous Materials, 170 (2009) 520-529.

[64] I. Poulios, I. Tsachpinis, Photodegradation of the Textile Dye Reactive Black 5 in the Presence of Semiconducting Oxides, Journal of Chemical Technology & Biotechnology, 74 (1999) 349-357.

[65] A.B. Prevot, C. Baiocchi, M.C. Brussino, E. Pramauro, P. Savarino, V. Augugliaro, G. Marci, L. Palmisano, Photocatalytic Degradation of Acid Blue 80 in Aqueous Solutions Containing TiO_2 Suspensions, Environmental Science & Technology, 35 (2001) 971-976.

[66] H. Lachheb, E. Puzenat, A. Houas, M. Ksibi, E. Elaloui, C. Guillard, J.M. Herrmann, Photocatalytic Degradation of Various Types of Dyes (Alizarin S, Crocein Orange G, Methyl Red, Congo Red, Methylene Blue) in Water by UV-Irradiated Titania, Applied Catalysis B: Environmental, 39 (2002) 75-90.

[67] M. Stylidi, D.I. Kondarides, X.E. Verykios, Pathways of Solar Light-Induced Photocatalytic Degradation of Azo Dyes in Aqueous TiO_2 Suspensions, Applied Catalysis B: Environmental, 40 (2003) 271-286.

[68] S. Tunesi, M. Anderson, Influence of Chemisorption on the Photodecomposition of Salicylic Acid and Related Compounds Using Suspended Titania Ceramic Membranes, Journal of Physical Chemistry, 95 (1991) 3399-3405.

[69] C. Guillard, J. Disdier, C. Monnet, J. Dussaud, S. Malato, J. Blanco, M.I. Maldonado, J.M. Herrmann, Solar Efficiency of a New Deposited Titania Photocatalyst: Chlorophenol, Pesticide and Dye Removal Applications, Applied Catalysis B: Environmental, 46 (2003) 319-332.

[70] S. Sakthivel, B. Neppolian, M.V. Shankar, B. Arabindoo, M. Palanichamy, V. Murugesan, Solar Photocatalytic Degradation of Azo Dye: Comparison of Photocatalytic Efficiency of ZnO and TiO_2, Solar Energy Materials and Solar Cells, 77 (2003) 65-82.

[71] M. Saquib, M. Muneer, Photocatalytic Degradation of Two Selected Textile Dye Derivatives, Eosine Yellowish and p-Rosaniline in Aqueous Suspensions of Titanium

Dioxide, Journal of Environmental Science and Health, Part A, 38 (2003) 2581-2598.

[72] B. Zielinska, J. Grzechulska, B. Grzmil, A.W. Morawski, Photocatalytic Degradation of Reactive Black 5: A Comparison Between TiO_2-Tytanpol A11 and TiO_2-Degussa P25 Photocatalysts, Applied Catalysis B: Environmental, 35 (2001) L1-L7.

[73] J. Grzechulska, A.W. Morawski, Photocatalytic Decomposition of Azo-Dye Acid Black 1 in Water Over Modified Titanium Dioxide, Applied Catalysis B: Environmental, 36 (2002) 45-51.

[74] S. Chakrabarti, B.K. Dutta, Photocatalytic Degradation of Model Textile Dyes in Wastewater using ZnO as Semiconductor Catalyst, Journal of Hazardous Materials, 112 (2004) 269-278.

[75] A. Assabane, Y. Ait Ichou, H. Tahiri, C. Guillard, J.-M. Herrmann, Photocatalytic Degradation of Polycarboxylic Benzoic Acids in UV-Irradiated Aqueous Suspensions of Titania: Identification of Intermediates and Reaction Pathway of the Photomineralization of Trimellitic Acid (1,2,4-benzene tricarboxylic acid), Applied Catalysis B: Environmental, 24 (2000) 71-87.

[76] M.L. Huang, C.F. Xu, Z.B. Wu, Y.F. Huang, J.M. Lin, J.H. Wu, Photocatalytic Discolorization of Methyl Orange Solution by Pt Modified TiO_2 Loaded on Natural Zeolite, Dyes and Pigments, 77 (2008) 327-334.

[77] C.M. So, M.Y. Cheng, J.C. Yu, P.K. Wong, Degradation of Azo Dye Procion Red MX-5B by Photocatalytic Oxidation, Chemosphere, 46 (2002) 905-912.

[78] I. Michael, E. Hapeshi, C. Michael, D. Fatta-Kassinos, Solar Fenton and Solar TiO_2 Catalytic Treatment of Ofloxacin in Secondary Treated Effluents: Evaluation of Operational and Kinetic Parameters, Water Research, 44 (2010) 5450-5462.

[79] M. Sleiman, D. Vildozo, C. Ferronato, J.-M. Chovelon, Photocatalytic Degradation of Azo Dye Metanil Yellow: Optimization and Kinetic Modeling using a Chemometric Approach, Applied Catalysis B: Environmental, 77 (2007) 1-11.

[80] T.A. McMurray, J.A. Byrne, P.S.M. Dunlop, J.G.M. Winkelman, B.R. Eggins, E.T. McAdams, Intrinsic Kinetics of Photocatalytic Oxidation of Formic and Oxalic Acid on Immobilised TiO_2 Films, Applied Catalysis A- General, 262 (2004) 105-110.

[81] S. Hwang, M.C. Lee, W. Choi, Highly Enhanced Photocatalytic Oxidation of CO on Titania Deposited with Pt Nanoparticles: Kinetics and Mechanism, Applied Catalysis B: Environmental, 46 (2003) 49-63.

[82] G.A. Epling, C. Lin, Photoassisted Bleaching of Dyes Utilizing TiO_2 and Visible Light, Chemosphere, 46 (2002) 561-570.

[83] N. Daneshvar, D. Salari, A.R. Khataee, Photocatalytic Degradation of Azo Dye Acid Red 14 in Water: Investigation of the Effect of Operational Parameters, Journal of Photochemistry and Photobiology A: Chemistry, 157 (2003) 111-116.

[84] D.F. Ollis, E. Pelizzetti, N. Serpone, Photocatalyzed Destruction of Water Contaminants, Environmental Science & Technology, 25 (1991) 1522-1529.

[85] B. Neppolian, H.C. Choi, S. Sakthivel, B. Arabindoo, V. Murugesan, Solar Light Induced and TiO_2 Assisted Degradation of Textile Dye Reactive Blue 4, Chemosphere, 46 (2002) 1173-1181.

[86] T. Sauer, G.C. Neto, H.J. Jose, R.F.P.M. Moreira, Kinetics of Photocatalytic Degradation of Reactive Dyes in a TiO_2 Slurry Reactor, Journal of Photochemistry and Photobiology A: Chemistry, 149 (2002) 147-154.

[87] J. Madhavan, P. Maruthamuthu, S. Murugesan, S. Anandan, Kinetic Studies on Visible Light-Assisted Degradation of Acid Red 88 in Presence of Metal-Ion Coupled Oxone Reagent, Applied Catalysis B: Environmental, 83 (2008) 8-14.

[88] G. Jacques, What Kind of Experimental Design for Finding and Checking Robustness of Analytical Methods?, Analytica Chimica Acta, 544 (2005) 184-190.

[89] T. Lundstedt, E. Seifert, L. Abramo, B. Thelin, A. Nystrom, J. Pettersen, R. Bergman, Experimental Design and Optimization, Chemometrics and Intelligent Laboratory Systems, 42 (1998) 3-40.

[90] S.L.C. Ferreira, R.E. Bruns, H.S. Ferreira, G.D. Matos, J.M. David, G.C. Brandao, E.G. da Silva, L.A. Portugal, P.S. dos Reis, A.S. Souza, W.N. dos Santos, Box-Behnken Design: An Alternative for the Optimization of Analytical Methods, Analytica Chimica Acta, 597 (2007) 179-186.

[91] S.L.C. Ferreira, R.E. Bruns, E.G.o.P. da Silva, W.N.L. dos Santos, C.M. Quintella, J.M. David, J.B. de Andrade, M.C. Breitkreitz, I.C.S.F. Jardim, B.B. Neto, Statistical Designs and Response Surface Techniques for the Optimization of Chromatographic Systems, Journal of Chromatography A, 1158 (2007) 2-14.

[92] S. Wold, M. Sjostrom, R. Carlson, T. Lundstedt, S. Hellberg, B. Skagerberg, C. Wikstrom, J. Ohman, Multivariate design, Analytica Chimica Acta, 191 (1986) 17-32.

[93] J.L. Goupy, Methods for Experimental Design: Principles and Applications for Physicists and Chemists, Elsevier, Amsterdam, 1993.

[94] R.H. Myres, D.C. Montgomery, Response Surface Methodology: Product and Process Optimization using Designed Experiments, Second ed., Wiley, New York, 2002.

[95] P. Chowdhury, H. Gomaa, A.K. Ray, Factorial Design Analysis for Dye-Sensitized Hydrogen Generation from Water, International Journal of Hydrogen Energy, 36 (2011) 13442-13451.

[96] J.F. Fu, Y.Q. Zhao, X.D. Xue, W.C. Li, A.O. Babatunde, Multivariate-Parameter Optimization of Acid Blue-7 Wastewater Treatment by Ti/TiO_2 Photoelectrocatalysis via the Box Behnken Design, Desalination, 243 (2009) 42-51.

[97] C. Lizama, J. Freer, J. Baeza, H.D. Mansilla, Optimized Photodegradation of Reactive Blue 19 on TiO_2 and ZnO Suspensions, Catalysis Today, 76 (2002) 235-246.

[98] M.B. Kasiri, H. Aleboyeh, A. Aleboyeh, Modeling and Optimization of Heterogeneous Photo-Fenton Process with Response Surface Methodology and Artificial Neural Networks, Environmental Science and Technology, 42 (2008) 7970-7975.

[99] B.K. Karbahti, M.A. Rauf, Application of Response Surface Analysis to the Photolytic Degradation of Basic Red 2 Dye, Chemical Engineering Journal, 138 (2008) 166-171.

[100] B.K. Karbahti, M.A. Rauf, Determination of Optimum Operating Conditions of Carmine Decoloration by UV/H_2O_2 using Response Surface Methodology, Journal of Hazardous Materials, 161 (2009) 281-286.

[101] S.-M. Lee, Y.-G. Kim, I.-H. Cho, Treatment of Dyeing Wastewater by TiO_2/H_2O_2/UV Process: Experimental Design Approach for Evaluating Total Organic Carbon (TOC) Removal Efficiency, Journal of Environmental Science and Health, Part A-Toxic/Hazardous substances and Environmental Engineering, 40 (2005) 423-436.

[102] C. Betianu, F.A. Caliman, M. Gavrilescu, I. Cretescu, C. Cojocaru, I. Poulios, Response Surface Methodology Applied for Orange II Photocatalytic Degradation in TiO_2 Aqueous Suspensions, Journal of Chemical Technology and Biotechnology, 83 (2008) 1454-1465.

[103] A. Filiz, E.C. Catalkaya, F. Kargi, Advanced Oxidation of Direct Red (DR 28) by Fenton Treatment, Environmental Engineering Science, 25 (2008) 1455-1462.

[104] I.H. Cho, K.D. Zoh, Photocatalytic Degradation of Azo Dye (Reactive Red 120) in TiO_2/UVsystem: Optimization and Modeling using a Response Surface Methodology (RSM) based on the Central Composite Design, Dyes and Pigments, 75 (2007) 533-543.

[105] C. Tang, V. Chen, The Photocatalytic Degradation of Reactive Black 5 using TiO_2/UV in an Annular Photoreactor, Water Research, 38 (2004) 2775-2781.

[106] C.H. Yu, C.H. Wu, T.H. Ho, P.K.A. Hong, Decolorization of CI Reactive Black 5 in UV/TiO_2, UV/Oxidant and UV/TiO_2/Oxidant Systems: A Comparative Study, Chemical Engineering Journal, 158 (2010) 578-583.

[107] K. Sahel, N. Perol, H. Chermette, C. Bordes, Z. Derriche, C. Guillard, Photocatalytic Decolorization of Remazol Black 5 (RB5) and Procion Red MX-5B--Isotherm of Adsorption, Kinetic of Decolorization and Mineralization, Applied Catalysis B: Environmental, 77 (2007) 100-109.

[108] E. Kusvuran, O. Gulnaz, S. Irmak, O.M. Atanur, H.I. Yavuz, O. Erbatur, Comparison of Several Advanced Oxidation Processes for the Decolorization of Reactive Red 120 Azo Dye in Aqueous Solution, Journal of Hazardous Materials, 109 (2004) 85-93.

[109] J.-H. Park, I.-H. Cho, Y.-G. Kim, Solar Light Induced Degradation of Reactive Dye Using Photocatalysis, Journal of Environmental Science and Health, Part A- Toxic/Hazardous substances and Environmental Engineering, 39 (2005) 159 - 171.

[110] W.S. Kuo, P.H. Ho, Solar Photocatalytic Decolorization of Dyes in Solution with TiO_2 Film, Dyes and Pigments, 71 (2006) 212-217.

[111] M. Muruganandham, M. Swaminathan, TiO_2-UV Photocatalytic Oxidation of Reactive Yellow 14: Effect of Operational Parameters, Journal of Hazardous Materials, 135 (2006) 78-86.

[112] N. Guettai, H.A. Amar, Photocatalytic Oxidation of Methyl Orange in Presence of Titanium Dioxide in Aqueous Suspension. Part II: Kinetics Study, Desalination, 185

(2005) 439-448.

[113] W. Chung-Hsin, Effects of Operational Parameters on the Decolorization of C.I. Reactive Red 198 in UV/TiO_2-Based Systems, Dyes and Pigments, 77 (2008) 31-38.

[114] A.H. Mahvi, M. Ghanbarian, S. Nasseri, A. Khairi, Mineralization and Discoloration of Textile Wastewater by TiO_2 Nanoparticles, Desalination, 239 (2009) 309-316.

[115] C.-H. Wu, H.-W. Chang, J.-M. Chern, Basic Dye Decomposition Kinetics in a Photocatalytic Slurry Reactor, Journal of Hazardous Materials, 137 (2006) 336-343.

[116] H.-L. Liu, Y.-R. Chiou, Optimal Decolorization Efficiency of Reactive Red 239 by UV/TiO_2 Photocatalytic Process Coupled with Response Surface Methodology, Chemical Engineering Journal, 112 (2005) 173-179.

[117] J.M. Monteagudo, A. Durán, Fresnel Lens to Concentrate Solar Energy for the Photocatalytic Decoloration and Mineralization of Orange II in Aqueous Solution, Chemosphere, 65 (2006) 1242-1248.

[118] R.B.M. Bergamini, E.B. Azevedo, L.R.R. de Araujo, Heterogeneous Photocatalytic Degradation of Reactive Dyes in Aqueous TiO_2 Suspensions: Decolorization Kinetics, Chemical Engineering Journal, 149 (2009) 215-220.

[119] K. Sahel, N. Perol, F. Dappozze, M. Bouhent, Z. Derriche, C. Guillard, Photocatalytic Degradation of a Mixture of Two Anionic Dyes: Procion Red MX-5B and Remazol Black 5 (RB5), Journal of Photochemistry and Photobiology A: Chemistry, 212 (2010) 107-112.

[120] A.P. Toor, A. Verma, C.K. Jotshi, P.K. Bajpai, V. Singh, Photocatalytic Degradation of Direct Yellow 12 Dye Using UV/TiO_2 in a Shallow Pond Slurry Reactor, Dyes and Pigments, 68 (2006) 53-60.

[121] K. Hustert, R.G. Zepp, Photocatalytic Degradation of Selected Azo Dyes, Chemosphere, 24 (1992) 335-342.

[122] K. Vinodgopal, D.E. Wynkoop, P.V. Kamat, Environmental Photochemistry on Semiconductor Surfaces: Photosensitized Degradation of a Textile Azo Dye, Acid Orange 7, on TiO_2 Particles Using Visible Light, Environmental Science & Technology, 30 (1996) 1660-1666.

[123] M.S.T. Gonçalves, A.M.F. Oliveira-Campos, E.M.M.S. Pinto, P.M.S. Plasência, M.J.R.P. Queiroz, Photochemical Treatment of Solutions of Azo Dyes Containing TiO_2, Chemosphere, 39 (1999) 781-786.

[124] D. Liao, B. Liao, Effects of Surfactant Composition and Concentration on Shape, Size and Photocatalytic Activity of TiO_2 Nanoparticles, International Journal of Chemical Reactor Engineering, 5 (2007) 1542-6580.

[125] Y. Kaçar, E. Alpay, V.K. Ceylan, Pretreatment of Afyon alcaloide Factory's Wastewater by Wet Air Oxidation (WAO), Water Research, 37 (2003) 1170-1176.

[126] D.C. Montgomery, G.C. Runger, Applied Statistics and Probability for Engineers, 4th ed., John Wiley and Sons, United States of America, 2010.

[127] A.K. Gupta, A. Pal, C. Sahoo, Photocatalytic Degradation of a Mixture of Crystal Violet (Basic Violet 3) and Methyl Red Dye in Aqueous Suspensions using Ag^{+} Doped TiO_2, Dyes and Pigments, 69 (2006) 224-232.

[128] C. Fernández, M.S. Larrechi, M.P. Callao, Study Of The Influential Factors In The Simultaneous Photocatalytic Degradation Process of Three Textile Dyes, Talanta, 79 (2009) 1292-1297.

[129] B. Gozmen, M. Turabik, A. Hesenov, Photocatalytic Degradation of Basic Red 46 and Basic Yellow 28 in Single and Binary Mixture by UV/TiO_2/Periodate System, Journal of Hazardous Materials, 164 (2009) 1487-1495.

[130] C.H. Giles, A.P. D'Silva, I.A. Easton, A General Treatment and Classification of the Solute Adsorption Isotherm Part. II. Experimental Interpretation, Journal of Colloid and Interface Science, 47 (1974) 766-778.

[131] M.-S. Chiou, G.-S. Chuang, Competitive Adsorption of Dye Metanil Yellow and RB15 in Acid Solutions on Chemically Cross-Linked Chitosan Beads, Chemosphere, 62 (2006) 731-740.

[132] C.-Y. Chen, J.-C. Chang, A.-H. Chen, Competitive Biosorption of Azo Dyes from Aqueous Solution on the Templated Crosslinked-Chitosan Nanoparticles, Journal of Hazardous Materials, 185 (2010) 430-441.

[133] C. O'Rourke, A. Mils, Adsorption and Photocatalytic Bleaching of Acid Orange 7 on P25 Titania, Journal of Photochemistry and Photobiology A: Chemistry, (2010) 261-267.

[134] G.A. Epling, C. Lin, Investigation of Retardation Effects on the Titanium Dioxide Photodegradation System, Chemosphere, 46 (2002) 937-944.

[135] G. Li, J. Qu, X. Zhang, H. Liu, H. Liu, Electrochemically Assisted Photocatalytic Degradation of Orange II: Influence of Initial pH Values, Journal of Molecular Catalysis A: Chemical 259 (2006) 238-244.

[136] W. Zhang, T. An, M. Cui, G. Sheng, J. Fu, Effects of Anions on the Photocatalytic and Photoelectrocatalytic Degradation of Reactive Dye in a Packed-Bed Reactor, Journal of Chemical Technology and Biotechnology, 80 (2005) 223-229.